Cape Peninsula
University of Technology

Phenol and COD removal from petroleum refinery wastewater using electrocoagulation and electrochemical oxidation

by

Sharon Chakawa

A thesis submitted in fulfilment of the requirements for the degree
Master of Engineering: Chemical Engineering
in the
Faculty of Engineering and the Built Environment
at the
Cape Peninsula University of Technology

Supervisor: **Dr Mujahid Aziz**

May 2021

Declaration

I, Sharon Chakawa hereby declare that the contents of this dissertation/thesis represent my unaided work and that the dissertation/thesis has not previously been submitted for academic examination towards any qualification. Furthermore, it represents my own opinions and not necessarily those of the Cape Peninsula University of Technology

Signed: *Sharon Chakawa*   Date: *May 2021*

Abstract

The petroleum industry is among the prime consumers of freshwater, through which a large quantity of its discharge enters into the aquatic environment. Immediate disposal of such wastewaters is concerning as it results in odour and the spreading of diseases in local rivers and freshwater sources. Petroleum refinery wastewater (PRW) produced, contains a significant amount of COD, phenol, FOG and BTEX that can lead to environmental deterioration if not properly treated before discharge. Due to the high concentration of organic matter and suspended solids in the wastewater, it is necessary to pre-treat the PRW prior to sequential electrooxidation treatment. Conventional treatment processes are not capable of treating contaminants and pollutants in PRW to sufficient concentrations, and hence advanced treatment processes are necessary.

For this study, a lab-scale integrated treatment process was used to investigate the successful reduction of pollutants, COD, phenol, colour, FOG and BTEX. The integrated treatment process used in this research consisted of two consecutive steps; electrocoagulation (EC) and electrochemical oxidation (EO).

In the electrocoagulation process with aluminium anodes, the experimental runs were conducted in a batch reactor. The effect of the operating parameters, such as the applied current and initial pH of the solution was examined. The efficiency of the pollutant removal was measured through COD, phenol, and colour with 67.5%, 98.7% and 88.5%, respectively. This was achieved at experimental conditions of an initial pH of 5, applied current of 2.5A and electrolysis time of 3 hours. The energy consumption of the EC process was found to be 0.8 kWh/m^3.

The electrocoagulation mechanism was modelled using adsorption isotherms. The adsorption of the pollutants in the wastewater on the surface of flocs was modelled using the Freundlich, Langmuir, Temkin, and Dubinin – Radushkevich isotherms. The Freundlich isotherm model matched satisfactorily with the experimental observations for the electrocoagulation process.

The electrochemical oxidation process with Ti/IrO$_2$ -Ta$_2$O$_5$ electrodes was applied to treat the wastewater effluent from the electrocoagulation process. The experimental runs were also carried out in a batch reactor, and a working volume of 1L. The highest pollutant removal conditions were the current density of 7.5 mA/cm^2, supporting electrolyte (sodium chloride) of 4 g/L, and temperature of 40 °C. The energy consumption of 5.8 kWh/m^3 was estimated at these optimal conditions.

It was observed that the integrated EC-EO treatment system was able to reduce COD, phenol and colour levels by 96%, 100% and 100% respectively. This concludes that the treated PRW effluent complies with local industrial effluent discharge standards, which could be disposed safely without further treatment

Research Outputs

Myburgh D; Aziz M; Roman F; Jardim J; **Chakawa S**; 2019; Removal of COD from industrial biodiesel wastewater using an integrated process: Electrochemical-oxidation with IrO_2-Ta_2O_5/Ti anodes and chitosan powder as an adsorbent, *Environmental Processes an International Journal*, 6, 818-840 [ISSN 2198-7505 / DOI:1007/540710-019-00401-x]

Chakawa S & Aziz M; 2020. Removal of Phenol and COD from industrial petroleum refinery wastewater using an integrated process: Electrocoagulation and Electrochemical-oxidation with IrO_2-Ta_2O_5/Ti anodes, *IWA: Water Science and Technology.* Submitted XX December 2020 [Paper ID.: XX-XX-XX]

Acknowledgements

I thank God for giving me the strength to succeed with this project, for protecting me, and blessing me with my family and friends.

Dedication

To my parents and role models, **Mr Michael Chakawa** and **Mrs Anna Mbedzi**, for their endless love, support, encouragement and inspiration. This achievement would not be possible without you. I am forever grateful for your presence in my life.

I would also like to dedicate this work to the most precious gem in my life, my beautiful and intelligent Goddaughter Mogau Masipa

Table of Contents

List of figures

List of Photographs

List of tables

GLOSSARY

Chemical oxygen demand (COD): Is a calculation of the oxygen absorption potential of water during the degradation of organic matter and the oxidation of inorganic chemicals such as ammonia and nitrite (Pitakpoolsil and Hunsom, 2013).

Electrocoagulation (EC): is a treatment process of applying an electrical current to treat and flocculate contaminants without having to add coagulants. Also, electrocoagulation could reduce residue for waste production (Butler et al., 2011).

Electrochemical oxidation (EO): is a complex phenomenon involving electrical energy to oxidize the pollutant present in the wastewater (Yavuz, Koparal and Bak, 2010a).

Phenol: is an aromatic molecule containing a hydroxyl group attached to the benzene ring structure (Albright, 2009).

Mercaptans: also known as methaniol, is any class of sulphur-containing compounds that have the general R-S-H formula, in which R represents a radical, is a harmless but pungent-smelling gas (Sadeghbeigi, 2000).

ABBREVIATIONS

Abbreviation	Description
BBD	Box Behnken Design
BDD electrodes	Boron Doped Diamond Electrode
BOD_5	Biological Oxygen Demand
BTEX	Benzene, Toluene, Ethylbenzene and Xylene
COD	Chemical Oxygen Demand
D-R	Dubinin – Radushkevich
DSA	Dimensional Stable Anodes
EC	Electrocoagulation
ED	Electrodialysis
EDI	Electrodeionisation
EF	Electro flotation
EFP	Electro Fenton Process
EO	Electrooxidation
FOG	Fats Oil and Grease
MF	Micro-Filtration
MMO	Mixed Metal Oxide
NF	Nano Filtration
O&G	Oil and Grease
Rpm	Rates per minute
PCP	Pentachlorophenol
PRW	Petroleum Refinery Wastewater
RO	Reverse Osmosis
SA	South Africa
SS	Suspended Solids
TOC	Total Organic Carbon
TSS	Total Suspended Solids
TDS	Total Dissolved Solids
WW	Wastewater

LIST OF SYMBOLS

Symbol	Description	Units
A	Area	cm^2
B	Constant related to mean sorption energy	$mol^2 \cdot kJ^2$
°C	Degree Celsius	
Ce	Concentration at equilibrium	mg/l
ΔE_C	Average cell voltage	V
E_S	Sorption energy	kJ/mol
E	Polanyi potential	
F	Faraday constant	C/mole
K_L	Langmuir constant for energy adsorption	
I	Current	A
ICE	Instantaneous current efficiency	%
J	Current density	mA/cm^2
Q	Adsorbed volume	mg/g
q_e	Adsorbed volume at equilibrium	mg/g
q_{max}	Monolayer adsorption capacity for Langmuir constant	
R	Ideal gas constant	kJ/mol.k
T	Time	hours
T	Absolute temperature	K
V	Volume	L
X_m	Maximum sorption capacity	mol/kg

Chemical Formula	Compound Name
Al	Aluminium
C_6H_5OH	Phenol
C_6H_6	Benzene
$C_6H_5CH_2CH_3$	Ethylbenzene
$C_6H_5CH_3$	Toluene
$(CH_3)_2C_6H_4$	Xylene
CO_2	Carbon Dioxide
Fe	Iron
H_2	Hydrogen
H_2O	Water
H_2S	Hydrogen sulphide

H_2SO_4	Sulphuric Acid
IrO_2	Iridium Oxide
O_2	Oxygen
OH^-	Hydroxide
$NaCl$	Sodium Chloride
NH_3	Ammonia
Ni	Nickel
Ta_2O_5	Tantalum Pentoxide
Ti	Titanium

CHAPTER 1

Introduction

Chapter 1: Introduction

1.1. Background

Global demand for petroleum products is increasing rapidly; as a result, our environment is exposed to rising hazardous impact (Martínez-huitle, Moura and Ribeiro, 2014). One of these issues comes from large quantities of wastewater produced during the processing of crude oil, where approximately 0.6 – 1.4 times of wastewater per ton of crude oil generated produces high levels of contaminants (Coelho *et al.*, 2006). It is estimated that the petroleum refinery industry generates an average of 5.34 billion litres per day of wastewater globally (Diya' Uddeen *et al.*, 2010).

Effluents from the petroleum refinery are a significant source of pollution that exhibits high concentrations of organic and inorganic pollutants and are characterised by high concentrations of chemical oxygen demand, phenol, BTEX (benzene, toluene, ethylene and xylene) and fats, oil and grease (FOG) (Gasim *et al.*, 2012). These pollutants have various adverse impacts on the surrounding environment. Therefore, due to the existence of these pollutants, petroleum refinery wastewater (PRW) is categorized as a hazardous waste by many environmental regulations, worldwide (Guo *et al.*, 2011).

 Phenol is, in particular, when present in PRW are dangerous pollutants to the environment (Jing *et al.*, 2017). Accidental ingestion of 1 g/kg body weight of these compounds is known to be toxic to humans and animals, and serious symptoms have been described, such as muscle weakness, tremors, lack of balance, paralysis, convulsions, coma, and respiratory arrest. (Wang *et al.*, 2014). According to El-Naas *et al.* (2013), phenols arising from PRW processes pose a threat specifically to marine environments due to their high environmental toxicity and recalcitrance.

Therefore, before discharging the wastewater into the environment, the amounts of these contaminants must be lowered to acceptable levels (El-Naas, Surkatti and Al-Zuhair, 2016). Several wastewater treatment methods, including ultrafiltration filter membrane (Al-Malack, 2015), biological treatment (Hayder *et al.*, 2014), coagulation, flocculation, flotation (Santo *et al.*, 2012), electrooxidation, electrocoagulation, electro-Fenton (Yavuz, Koparal and Bak, 2010) and adsorption (Wang *et al.*, 2016), have been designed to fulfil the criteria of environmental regulations to accomplish this goal.

Any of these methods, however, may not be successful in handling all kinds of wastewater and may not be able to cope with all forms of pollutants. To treat heavily polluted PRW, a mixture of these approaches is often required (Anglada, Urtiaga and Ortiz, 2009).

While the electrooxidation (EO) process is very effective in completely removing phenolic compounds from PRW, electrooxidation of heavily contaminated wastewater with high COD values above 2000 mg / L, cannot be effectively achieved by using a single process on its own (El-Naas, Surkatti and Al-Zuhair, 2016). Consequently, to ensure successful complete removal of pollutants treatment procedures are usually based on the combination of mechanical or physicochemical processes, such as oil-water isolation and coagulation, with electrooxidation treatment to ensure successful complete removal of pollutants (Hariz *et al.*, 2013; Myburgh *et al.*, 2019). The effectiveness of the EO process has been shown to be improved by the pre-treatment of wastewater using an electrocoagulation (EC) process, which would result in better conditions for the EO process (Keerthi, Vinduja and Balasubramanian, 2013).

In recent years, several studies have been investigated out to remove COD and colour from industrial wastewater by combined EC and EO process (Keerthi, Vinduja and Balasubramanian, 2013; Juárez *et al.*, 2015). However, the integrated method for PRW treatment shows excellent potential to mitigate this problem. Therefore, the research sought to explore the possibility of using combined EC and EO to treat PRW.

1.2. Problem Statement

Petroleum refinery wastewater is classified as industrial wastewater. The "City of Cape Town: Wastewater and Industrial Effluent By-law, 2013" governs the disposal of industrial wastewater in the City of Cape Town. Currently, PRW is discharged into the sewer that does not comply with the industrial discharge standards. Therefore, research studies are being conducted to effectively treat PRW to reduce the adverse effects it has on the environment and biological processes in wastewater treatment facilities, abide by more stringent effluent requirements and avoid fines. Effective treatment of the wastewater may result in the recycling of the water during the production process.

1.3. Research Question

1. Can electrocoagulation (EC) followed by electrochemical oxidation (EO) be used to treat PRW sufficiently so that it meets the required industrial wastewater discharge standards?

2. What effect does current density and NaCl concentration have on the removal of COD, FOG and BTEX during electrochemical oxidation of petroleum refinery wastewater?

3. How will the adsorption rate change when the pH is adjusted?

1.4. Aim and Objectives

The aim of this research is to improve the quality of petroleum refinery wastewater (PRW) in an integrated treatment process using electrocoagulation (EC) followed by electrochemical oxidation (EO), to meet the required industrial effluent discharge standards.

The specific objectives were:
1. Investigate electrochemical cell operating conditions in terms of various current densities and NaCl concentrations on the removal of phenol, colour, COD, FOG and BTEX.
2. Study the effect of initial pH on the adsorption rate during the removal of COD, FOG and BTEX.
3. Determination of electrocoagulation mechanism for organic and inorganic pollutants removal

1.5. Significance of the Study

Effective treatment of petroleum refinery wastewater may result in compliance with industrial wastewater discharge standards, cost savings regarding fines paid as well as reduced freshwater usage through recycling of water in the production process.

1.6. Delineation

During this study, the removal of phenol, COD, FOG and BTEX from petroleum refinery wastewater was observed through an integrated treatment process. This process consists of two consecutive steps:

1. Electrocoagulation
2. Electro-oxidation

Electrocoagulation occurred using Al anodes.
Electrochemical oxidation occurred using IrO_2-Ta_2O_5/Ti anodes.

All other variables are delineated.

1.7. Structure of the thesis

This thesis contains six chapters, with a brief introduction as follows:

Chapter 1: Introduction

This section presents the background and relays the path as to where this study is headed. It outlines some of the current problems faced by industry and provides motivation on how to address it. Specific issues include water scarcity of potable water in South Africa; how water is used in the petrochemical industries. Thereafter presents the problem statement, aim and objectives and delineation.

Chapter 2: Literature Review

This section focuses on previous work that is analogous to what will be carried out—reviewing previous or existing knowledge and technologies with the goal of refining the approach and adapting its application in this study. The literature review focuses on the usage of water, traditional treatment methods, as well as how electrochemical technology can be used to improve the quality of PRW.

Chapter 3: Methodology

This section describes the equipment and chemicals to be used in the experimental runs. It shows the chemical analysis techniques used as well as the design of experiments using Design-Expert software package.

Chapter 4: Results and Discussion

This section displays all the outputs graphically from the experimental runs completed. The graphs are discussed with the intention to optimise the EC and EO processes.

Chapter 5: Optimisation using Response Surface Methodology (RSM)

This section dealt with the optimization of the EC and EO removal process using RSM. This includes the development of the multilevel factorial design, central composite design and Box Behnken design predictive models. The best-fitted models were optimised to identify the optimum condition for COD in petroleum refinery effluent, by evaluation and verification using Design Expert Software.

Chapter 6: Conclusion and Recommendation

This section draws on the outcomes of the results and concludes the thesis based on the findings and outputs. Recommendations are presented based on the experience from the research and findings.

CHAPTER 2

Literature Review

Chapter 2: Literature review

2.1. Introduction

The rapid growth of industries and population in South Africa (SA) has led to the high demand for freshwater (Verlicchi and Grillini, 2020). According to Anderson *et al.* (2010), about one-third of the country's population does not have access to clean drinking water. The scarcity of water resulting from industrialisation and population growth is considered a limitation for sustainable development. Thus, the growth of industries has led to the deterioration of the quality of water in the river (Zhuwakinyu, 2012). Rivers are the most crucial water source in South Africa, so it is imperative to implement waste minimisation and pollution prevention strategies to ensure water quality (Musingafi and Tom, 2014). Various methods of treatment have been used for the treatment of wastewater from industries, and one such sector is the petroleum refinery industry.
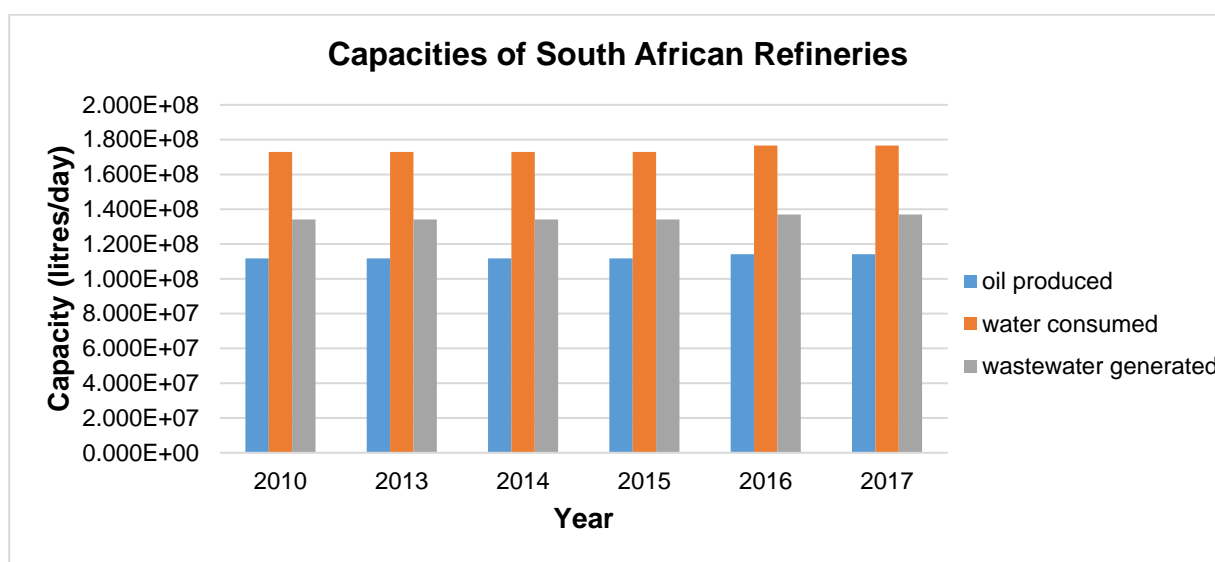
Figure 2-1: the capacity of SA's refineries (Ratshomo and Nembahe, 2018)

Petroleum refineries consume large quantities of water for cooling processes, desalting processes and stripping steam (Coelho, Castro and Jr, 2006) which in turn generates large volumes of wastewater. South Africa (SA) produces about 115 million litres/day of oil through six refineries by consuming 177 million litres of freshwater and generating about 137 million of wastewater as illustrated in Figure 2-1 (Ratshomo and Nembahe, 2018). The South African petroleum refinery industries' high water demands and consumption have resulted in water increasingly becoming a scarce commodity and reducing the groundwater levels, thus increasing water shortages in many areas (Bwapwa, 2018). Globally, petroleum refinery wastewater has been identified as hazardous industrial waste.

2.2. Petroleum Refining Wastewater (PRW)

2.2.1. Petroleum Industry

The main components of our modern industrial society are petroleum and its derivatives. The petroleum refinery industry refines crude oil and converts natural gas into over 2500 refined products including liquified petroleum gas, gasoline, kerosene, aviation fuel, diesel fuel, fuel oil, lubricating oils and petrochemical feedstocks (Santos *et al.*, 2015). Petroleum products are the main components of our modern industrial society; however, the production of these fuels raises inevitable environmental risks (Shabir *et al.*, 2013).

A petroleum refinery is an elaborate process where crude oil and condensates are refined into marketable goods with specified requirements for the petrochemical industry, from gasoline to asphalt (Havard, 2013). Petroleum accounts for the most significant proportion of primary energy production in the world, and at present, it accounts for about 32% of the total energy consumed worldwide as illustrated in Figure 2-2 (Benalcazar, Krawczyk and Kamiński, 2017).
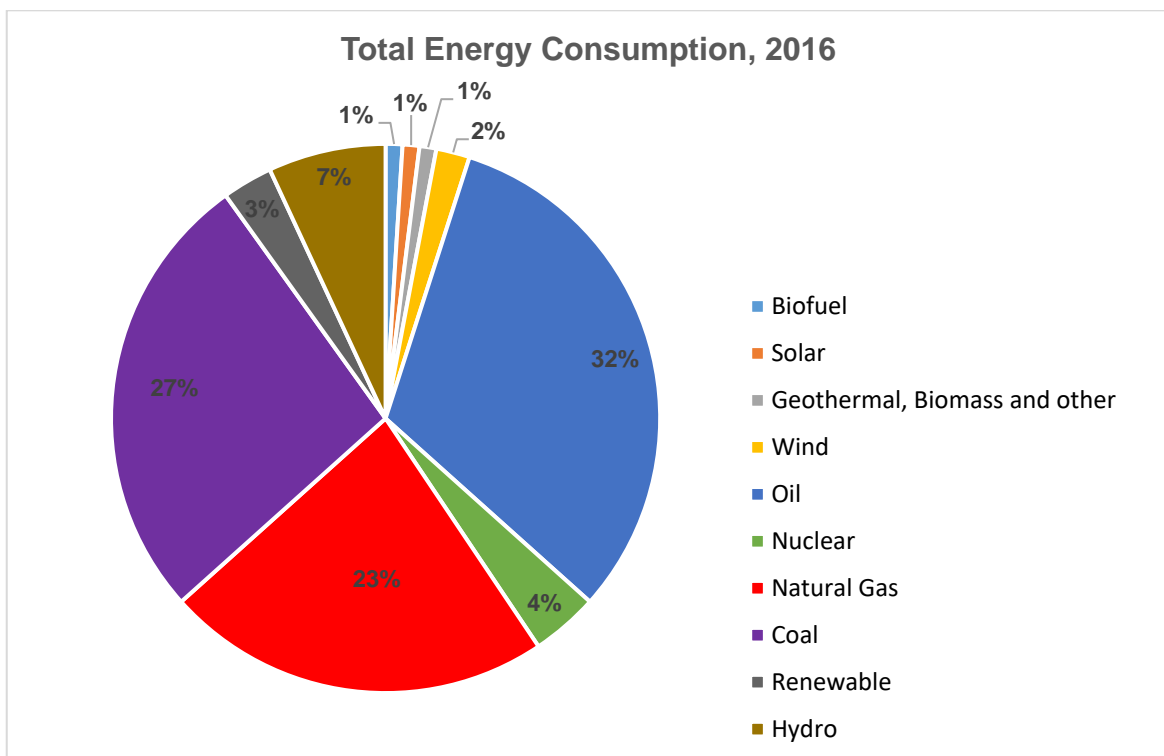
Figure 2-2: World energy consumption by energy source (Benalcazar, Krawczyk and Kamiński, 2017)

The refining process involves three main steps: separation, conversion and treatment:

i. Separation Process

The first separation called the distillation, which is carried out in a sequence of distillation columns. Through fractional distillation, crude oil can be divided into fractions. The fractions at the top are equivalent to those at the bottom. The hard fractions at the bottom are always broken into smaller, more functional items (Demirbas, 2015). Both the products are further stored in other processing systems. An oil refining purifies and extracts the crude oil into specific oils and by-products — the most important of these being gasoline. Certain petroleum goods include diesel, heating oil, and jet fuel (Diya'uddeen, Daud and Abdul Aziz, 2011).

ii. Conversion Process

The conversion methods are concentrated on reducing the hydrocarbons in the long chain. There are three types of conversion units, namely fluidised catalytic cracking (FCC), hydrocracking and coking (Gudde, 2018). Table 2-1 shows the main components of the refinery process. After crude oil is separated and refined, the resulting products are ready for purification. The principal purpose of the conversion processes is to convert low-valued heavy oil into high-valued petrol (Demirbas and Bamufleh, 2017).

iii. Treatment process

Treatment is the final processing process which involves mixing refined goods to produce different levels of octane, vapour pressure properties, and unique properties for materials used in harsh environmental conditions. Another principal procedure is the elimination of sulphur from jet fuel to meet clean air standards (Demirbas and Bamufleh, 2017).

Table 2-1: Unit processes in a petroleum refinery industry (Demirbas and Bamufleh, 2017)

Unit Process	Process Objective
Desalting	Before entering the crude distillation unit (CDU), it washes salt from the crude oil. (CDU). Crude oil is also desalinated before distillation to remove corrosive salts as well as metals and other suspended solids.
Crude Distillation Unit (CDU)	It distils crude oil into fractions or parts of various hydrocarbons that are used to separate the desalted crude (gasoline, naphtha, jet fuel and asphalt).
Vacuum Distillation Units (VDU)	Following the CDU process, it further distils residual bottoms. Heavy crude residue from the CDU column is further isolated by using a low-pressure distillation process at lower

	temperatures, without decomposition and excessive coke formation.
Delayed coking	A method of thermal non-catalytic cracking that transforms low-value oils to gasoline, gas oils, and marketable coke of higher value. Residual fuel oil from vacuum distillation column is a common feedstock
Fluid coking	It is used to convert low-value residue to valuable products (naphtha, diesel, gas oil).
Catalytic Reforming	It is used to convert molecules from the naphtha-boiling range into higher octane reformer products (reformate). To increase their octane numbers, the mechanism by which naphthas are chemically altered. Octane numbers are measurements of the way a fuel knocks in the engine.
Hydrotreating	It desulfurizes distillates (e.g., diesel) after atmospheric distillation.
FCC	FCC upgrades low-value gas oils into lighter, more valuable products (naphtha, diesel fuel and slurry oil).
Hydrocracking	It is used to remove pollutants (nitrogen, sulphur, metals) from the feed and turn low-value gas oils into useful goods (naphtha and middle distillates). Heavier hydrogen fractions are converted into smaller, more productive goods.
Visbreaking	A non-catalytic thermal process used to refine vast volumes of hydrocarbons into lighter products such as natural gas, gasoline, naphtha, and gas oil from heavy feedstocks. Through thermally fracturing, it reduces heavy residual oils to smaller, more useful reduced viscosity materials.
Coking	It transforms very heavy residual oils into gasoline and diesel, leaving petroleum coke as a residual.
Alkylation	A necessary method to upgrade light olefins to components of high-value gasoline. It is used to combine small molecules into large molecules for producing a higher-octane fuel for gasoline mixing. It manufactures high-octane materials for the blending of gasoline.
Dimerisation	It transforms the olefins into components that mix higher-octane gasoline.
Isomerisation	This method is used to produce high-octane compounds to mix into the gasoline reservoir. It converts linear molecules into higher-octane-branched molecules for gasoline

	blending. They are also used to produce isobutene, an essential feedstock for alkylation.
Polymerisation	A process that combines smaller molecules to produce high octane blend-stock.
Solvent refining	It uses a solvent such as cresol or furfural to remove unwanted, mainly asphaltenic materials from lubricating oil stock.
Solvent dewaxing	For removing the heavy waxy constituent's petroleum from vacuum distillation products

2.2.2. Petroleum Refining Wastewater (PRW) Sources

PRW is a significant waste source in the oil sector. It is estimated that in the production of 158.99 litres of oil about 246 – 341 litres of water is consumed (Pal *et al.*, 2016) and roughly 80 – 90 % of the water consumed is discharged as wastewater (Ibrahim, Devi and Balasubramanian, 2013). Figure 2-3 shows the comparison between global oil production, the estimated water usage and water discharged over ten years.   More than 19 billion litres is discharged daily ('BP Statistical Review of World Energy', 2019), PRW levels have risen significantly over the years and are projected to rise in the future, which means that the risk of discharging PRW into the environment has become a significant concern (Diya'uddeen, Daud and Abdul Aziz, 2011).
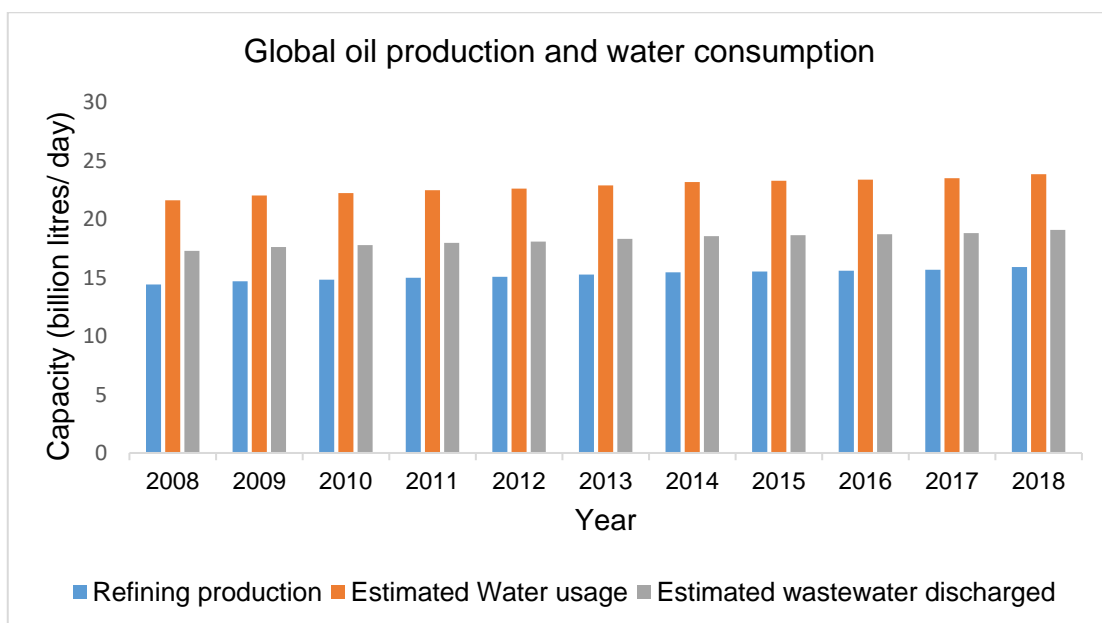
Figure 2-3: Global oil production and water consumption ('BP Statistical Review of World Energy', 2019)

PRW can be defined by their significant variations in several parameters, such as COD, colour, BTEX. Table 2-2 shows the most significant pollutants from the refining industry. In terms of wastewater production and environmental effects, the most crucial refining activities are alkylation and hydrocracking processes. PRW almost always contains impurities, and these impurities may have a detrimental effect on the environment if present in sufficient concentration.

Table 2-2: Major water sources in petroleum refining sources (El-Naas et al., 2014a; Shokrollahzadeh et al., 2008).

Unit	Wastewater main pollutants
Crude desalting	Free oil, ammonia, sulphides, and suspended solids
Crude oil distillation	Oil, ammonia, chloride, sulphides, phenols and mercaptan
Thermal cracking	Ammonia, sulphides and phenols
Catalytic cracking	Oil, cyanide, ammonia, sulphides and phenol
Hydrocracking	High in sulphides
Polymerisation	Sulphides, ammonia and mercaptans
Alkylation	Oil, spent caustic, sulphides
Isomerisation	Low levels of phenols
Reforming	Sulphides
Hydrotreating	Ammonia, sulphides, phenol

2.2.3. Petroleum Refining Wastewater (PRW) Characteristics

In general, investigating and better understanding the constituent of PRW increases the ability to select the proper methods of treating PRW (Bhagawan et al., 2014). Table 2-3 and 2-4 outlines the Industrial wastewater discharge standards from various countries and the characteristics of PRW, respectively.

a) **Oil and Grease**

One of the most critical constituents of PRW is oil and grease. According to Hu (2016), oil and grease in PRW may appear as free oil, dispersed oil or as a suspended matter. Oily waste discharges have a distinct odour, an undesirable appearance, burn on the surface of receiving water, thus causing potential safety hazards and limiting oxygen transfer.

b) **Phenol**

Phenols are called priority pollutants because they are toxic to low concentration species, and all of them are listed as dangerous pollutants owing to their possible damage to human health. Accidental consumption of 1 g per kilogram of these compounds is considered dangerous to humans and animals, and extreme symptoms such as muscle weakness, tremors, lack of control,

paralysis, seizures, coma and respiratory arrest have been reported (Rocha *et al.*, 2007). Due to their high environmental toxicity and recalcitrance, phenols arising from petroleum refining industry pose a threat primarily to the aquatic ecosystem (Abdelwahab, Amin and El-ashtoukhy, 2008).

c) BTEX

Monoaromatic hydrocarbons - benzene, toluene, ethylbenzene and xylene (BTEX) are volatile organic compounds (VOCs) that exist naturally in crude oil and are thus usually found in PRW (Fayemiwo, Daramola and Moothi, 2017). BTEX, are among PW's key pollutants. Human exposure to these substances can lead to health problems ranging from eye inflammation, mucous membranes and skin, to damaged nervous systems, reduced activity of the bone marrow and cancers. In particular, benzene is extremely toxic and is listed as a potential carcinogen by the World Health Organisation, placing sixth in the list of hazardous substances (Costa *et al.*, 2012). Owing to their toxicity to various species, BTEX constitutes a significant class of environmental pollutants (Mazzeo *et al.*, 2010).

Table 2-3: Industrial wastewater discharge standards from various countries

Standards	pH	Colour (TCU)	COD (mg/l)	Oil and grease (mg/l)	Benzene (mg/l)	Toluene (mg/l)	Ethylbenzene (mg/l)	Xylene (mg/l)	Phenol (mg/l)	References
WHO	30	5	150	5					0.2	(Verlicchi and Grillini, 2020)
USA-EPA	5-9	15	300	5	0.005	0.2	0.7	10	0.3	(EPA, 2012)
UGANDA	6 – 8	300	100	10	0.2				0.2	(National Environmental Regulations, 1999)
South Africa	5.5 – 9.5		75	2.5					0.5	(Department of Water and Environmental Affairs, 2013)

Table 2-4: Typical characteristics of PRW

Parameter	Ye & Li (2016)	Diya'Uddeen et al (2014)	El-Naas et al (2014)	Shabir et al (2013)	Abdelwahab et al (2009)
pH	9.1	9.4	8.3 - 8.9	8.13	8
BOD_5 (mg/l)	-	173	3600 - 5300	685	40.25
COD (mg/l)	**593**	**1259**	**3600 - 5300**	**1965**	**80-120**
Conductivity (mS/cm)	1.652		5.2-6.8	9.43	
Chloride (mg/l)	108		-		
Phenol (mg/l)	**140**	**14.7**	**11-14**	**18.32**	**13**
Total Phenol	-		160-185		
TOC (mg/l)		186	-		
Turbidity (NTU)		194		1057	
TDS (mg/l)			3800 – 6200	6267	
TSS (mg/l)		124	380 - 620	315	315
Total iron (mg/l)		6.9			
Oil and grease (mg/l)		233			
Sulphides (mg/l)			14.5 – 16	137	
σ – Cresol (mg/l)			14 – 16.5		
m, p cresol (mg/l)			72.75		

2.3. Stripped sour water

Petroleum refinery stripped sour water (SSW) is a high-strength waste stream that can constitute a large portion of chemical oxygen (COD) and ammonia in wastewater refinery (Merlo *et al.*, 2011). SSW is created when steam is pumped into some of the refinery processing units to reduce partial hydrocarbon vapour pressure, allowing less dramatic temperature activity. SSW may be fed to a rectification tower after separation at the top of the refinery towers to extract ammonia and hydrogen sulphide. SSW is a corrosive substance, in addition to its toxicity. The amount of SSW produced at a refinery depends on many factors, including plant configuration and plant size and processed oil characteristics. Typical SSW output in large refineries contains 200 – 500 L per 1000 litres of refined crude oil (Coelho *et al.*, 2006). Table 2-5 shows the typical characteristics of SSW.

Table 2-5: Typical characteristics of SSW (Coelho et al., 2006)

Parameter	Range
COD (mg/l)	850 – 1020
Dissolved organic content (DOC) (mg/l)	300 – 400
BOD_5 (mg/l)	570
Phenol (mg/l)	98 – 128
Ammonia (mg/l)	5.1 – 21.1
pH	8.0 – 8.2
Turbidity (NTU)	22 – 52
Sulphide (mg/l)	15 – 23
Toluene (µg/l)	1.1
Ethylbenzene (µg/l)	3.7
m,p – Xylene (µg/l)	15.4
o -Xylene (µg/l)	3.7
Oil and grease (mg/l)	12.7

2.4. Petroleum Refinery Wastewater Treatment Technologies

PRW treatment process requires multiple treatment steps due to the complex characteristics of the effluent. In each stage, several treatment technologies can be used. Technologies tested for the treatment of PRW are classified according to the treatment principle: biological, physical and chemical (Aljuboury *et al.*, 2017).

2.4.1. Biological Treatment

Biological treatment is defined by Pintor et al. (2016), as the most critical and essential part of any wastewater treatment plant that treats wastewater from either municipalities or industries with soluble organic impurities or a combination of the two types of wastewater sources. The biological treatment process takes place within a body of water where the organic and inorganic matter is converted biologically to inert mineralised materials.

There are two types of biological treatment, namely the aerobic and the anaerobic treatment (Pal *et al.*, 2016). In the presence of air, aerobic treatment processes take place using microorganisms (also known as aerobes) that use molecular or free oxygen to assimilate organic impurities, such as converting them into carbon dioxide, water, and biomass. In the other hand, in the absence of oxygen, anaerobic treatment processes are carried out by certain microorganisms (also called anaerobes) that do not need oxygen to assimilate organic impurities. (Mittal, 2011).

Rastegar *et al.* (2011), treated PRW to remove COD by an upflow anaerobic sludge blanket (UASB), by operating the process for 48 hours at a constant organic loading rate of 0.4 kg/m$^3\cdot$d, the COD removal was 81%.

Wenyu, Li and Jianjun (2007), investigated the treatment of oil refinery wastewater using an aerated biological filter process their results revealed that the removal efficiency of suspended solids (SS), COD, and oil pollutants was 83.4%, 84.% and 94.0%, respectively. When hydraulic retention time was 1 hour, the air/water volume flow ratio was about 5:1, and the backwashing cycle was at every 4-7 days.

Although biological treatment has been widely used, its major disadvantage of this method is the amount of sludge produced, and the biodegradation of heavy metals is not achievable, which causes the sludge to retain these pollutants (Diya'Uddeen *et al.*, 2014)

2.4.2. Chemical Treatment

In early wastewater treatment technology, chemical treatment followed biological treatment. Biological treatment has recently been followed by chemical treatment in the treatment process. Chemical treatment is now considered to be a tertiary treatment that can be described more generally as wastewater treatment by a chemical treatment process (Samer, 2015). Chemical treatment allows for the reduction of dissolved and suspended contaminants as well as the high concentration of fat, oil and grease from PRW (El-Shamy, El Boraey and El-Awdan, 2017). The most widely applied methods for chemical treatment are chemical precipitation, coagulation, adsorption, disinfection, and ion exchange (chlorine, ozone, ultraviolet light).

Adsorption is a method that has been used for the treatment of PRW for the removal of dissolved components. The process uses adsorbents such as activated carbon and chitosan flakes which can either be regenerated or disposed of after the adsorption capacity is exhausted. One of the most efficient adsorbent materials is activated carbon, which has been widely used in the treatment of PRW (Yu *et al.*, 2013; El-Naas *et al.*, 2010). Adsorption has been found to be effective in removing heavy metals; however, this method is not so efficient in removing phenols, COD, FOG and BTEX (Diya'Uddeen *et al.*, 2014).

2.4.3. Advanced Treatment

i. **Membrane process**

Membrane technology has been explored for wastewater treatment and is considered to be a promising technology for PRW treatment (Zheng *et al.*, 2015). Membranes such as micro-filtration (MF), ultra-filtration (UF), Nano-filtration and reverse osmosis (RO) can remove different sized components. Membrane processes have many advantages such as being widely applicable across various industries, no extra chemicals are required and concentrate up to 40−70% oil and solids can be obtained with UF or MF (Jamaly, Giwa and Hasan, 2015). However, frequent fouling of the membrane renders the method unattractive (Diya'Uddeen *et al.*, 2014).

Table 2-6: Literature review of treatment processes for PRW treatment

REMOVAL TECHNIQUE	REMOVAL PARAMETERS	REMOVAL %	SOURCES	COMMENTS
Adsorption–Coagulation	pH = 9	89.27% COD	(Wang *et al.*, 2016)	Less efficient at higher feed concentration, high retention time (García *et al.*, 2014; Pitakpoolsil and Hunsom, 2014)
	$65 \cdot s^{-1}$ and $20 \cdot s^{-1}$ shear rates	85.18% total organic carbon (TOC)	(Wang *et al.*, 2016)	
Adsorption	Date-pit activated carbon 80 g/l Adsorbent dosage	89% COD	(El-Naas *et al.*, 2010)	Less efficient at higher feed concentrations, high retention time (García *et al.*, 2014; Pitakpoolsil and Hunsom, 2014)
	BDH activated carbon 80 g/l Adsorbent dosage	90% COD	(El-Naas *et al.*, 2010)	
Electro-Fenton	Iron Electrode	67.3% COD	(Davarnejad, Mohammadi and Fauzi, 2014)	Ferrous ions are used more rapidly than they are regenerated, It is limited by a narrow pH range (pH < 3), and water pollution caused by the homogenous catalyst added as an iron salt cannot be retained in the process (Ye and Li, 2016).
	Aluminum Electrode	71.58% Colour	(Davarnejad, Mohammadi and Fauzi, 2014)	
Electrocoagulation	Fixed bed Anode (Aluminum raschig rings) 8.59 mA/cm^2 current density	100% phenol	(Abdelwahab *et al.*, 2013)	More effective and rapid organic matter separation than in coagulation and operating costs are much lower than in the coagulation process (Dos Santos *et al.*, 2014a)

	pH = 7 1 g/l NaCl Time = 2hrs			
	13 mA/cm^2 current density at a pH level of 9.5			
	Al anode and Al cathode	34% Sulfate 40% COD	El-Naas *et al.*, 2009)	
	Stainless steel anode and Fe cathode	4% Sulfate 23% COD	(El-Naas *et al.*, 2009)	
	Stainless steel anode and Aluminum Cathode	17% Sulfate 38% COD	El-Naas *et al.*, 2009)	
Three-dimensional Electrode reactor (granular activated carbon, porous ceramic particle	30 mA/cm^2 current density 100 minutes of treatment time	45.5% COD 43.3% TOC 67.2% of Toxicity units	(Wei *et al.*, 2010)	Easy to operate and control (Wei *et al.*, 2010).

and DSA type Anodes)				
Electro-catalytic oxidation	Electrodes = Ti/IrO$_2$-Ta$_2$O$_5$ 2 hrs electrolysis time	50.96% COD 94.77% Phenol 41.2% TOC	(Jing *et al.*, 2017).	Bubbles adhere to the surface of the electrode in the process of electrocatalytic oxidation, resulting in a small surface area between the electrolyte and electrode and limit the generation of active particles (Jing *et al.*, 2017).

2.5. Electrochemical methods

An electrochemical process has proven to be one of the most effective technologies in the treatment of PRW from various sources. These technologies include electro flotation, electrocoagulation, electro filtration, electrodialysis, Electrodeionisation, electro-Fenton and electrooxidation (Jamaly, Giwa and Hasan, 2015; Martínez-huitle and Rodrigo, 2018). The advantages of these types of electrochemical techniques are summarised in table 2-7.

According to (Martínez-Huitle *et al.*, 2014; Hashemi *et al.*, 2015) the electrochemical performance is determined by the following principal parameters: electrode potential, current density, current distribution, mass transport regime, cell design, electrolysis medium, and the electrode materials.

2.5.1. Electro flotation

Among the methods used to treat wastewater effectively, electro flotation (EF) has emerged as one of the most innovative modern technologies. EF is an electrochemical version of the traditionally applied flotation, highly effective in treating wastewater (Kolesnikov, Il'in and Kolesnikov, 2019). In EF even the smallest particles can be isolated from a liquid due to uniform and tiny bubbles of hydrogen and oxygen formed on the surfaces of the electrode during electrolysis of the wastewater. EF has several benefits, such as the operating conditions can be quickly checked and are monitored relatively easily; the equipment is reliable and safe to use (Martínez-huitle and Rodrigo, 2018). This process is based on water electrolysis performed on insoluble electrodes and flotation effect. During water electrolysis, gas bubbles of oxygen and hydrogen are produced at the anode and cathode, respectively (Sillanpaa and Shestakova, 2017). The Equation 2-1 to 2-3 below simulate the development of hydrogen and oxygen bubbles (Tien *et al.*, 2017):

At anode: $2\text{H}_2\text{O} = \text{O}_2 + 4\text{H}^+ + 4\text{e}^-$ **Equation 2-1**

At cathode: $2\text{H}^+ + 2\text{e}^- = \text{H}_2$ **Equation 2-2**
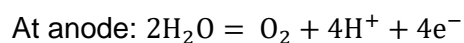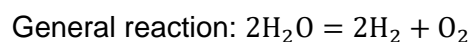
General reaction: $2\text{H}_2\text{O} = 2\text{H}_2 + \text{O}_2$ **Equation 2-3**

2.5.2. Electrocoagulation

Electrocoagulation (EC) is an electrochemical technique for the treatment of polluted water by which sacrificial anodes dissolve due to the potential current applied, thereby creating active precursors to coagulants(Islam, 2019). Electrocoagulation is a complicated process with a multitude of processes acting synergistically to eliminate wastewater pollutants (Wang, Chou and Kuo, 2009). EC is very effective in removing pollutants from water and is characterised by reduced sludge production, no chemical requirements and ease of use (Chen, 2003).

In the study carried out by Wijeyekoon *et al.* (2007), an electrocoagulation reactor using aluminium electrodes was used to degrade an initial concentration of COD (400-500 mg/l). 51.9% COD removal efficiency was achieved at an optimum current density and electrode surface area to volume ratio of 46.9 A/m^2 and 8.5 m^2/m^{3,} respectively.

2.5.3. Electro filtration

Electro filtration is a mechanism that minimizes membrane fouling by using electric fields of direct current (DC) across the filtration system. Exceptions, almost all colloids and suspended solids (SS), including microorganisms, mostly have negative or positive electrical charge; thus, they deviate in the presence of an electrical field (Mostafazadeh, Zolfaghari and Drogui, 2016). According to Li *et al.* (2009), electro filtration for particle removal is commonly used in air–particle systems, such as electrostatic precipitators. However, it has received much less attention in the application of water and wastewater treatment, possibly due to the higher viscosity of water and limitation of high voltage application in water media.

Yang and Li (2007), investigated the use of electro filtration for the treatment of silica nanoparticle-containing wastewater using tubular ceramic membranes The tested wastewater was characterised by high total suspended solids content of 1333 mg/L with a majority of particles greater than 100 nm, a conductivity of 86.3 µS/cm. Their investigation resulted in about 90% of total suspended solids and silica removal efficiency with turbidity reduced to 0.75 NTU.

2.5.4. Electrodialysis

In recent years, the use of electrodialysis (ED) or in wastewater treatment has increased, offering the potential for enhanced water recovery and membrane life expectancy and minimising energy consumption (Pilat, 2001). However, its requirement for high capital cost and energy loss as compared to other electrochemical technologies renders it not to be widely used (Al-Amshawee *et al.*, 2020). In this process, ions are moved from a less concentrated solution to a more

concentrated one due to the passage of a direct current through a series of anion and cation exchange membranes (Lopez *et al.*, 2017). The efficiency of an electrodialysis process depends on current density, pH, flow rate, the structure of the cells, ionic water concentration and ion exchange membrane characteristics (Akhter, Habib and Qamar, 2018). Figure 2-4 illustrates the principle mechanism of ED.

Bi *et al.* (2011) investigated the degradation of Nitrate from groundwater using ED. The results illustrated over 99% Nitrate removal efficiency, and the conductivity was reduced to less than 10 µS/cm when the initial concentration and the voltage were 100 mg/l and 30 V, respectively. The current efficiency of this process ranged from 17-34 % and 0 – 1.7 W·h/l, respectively.
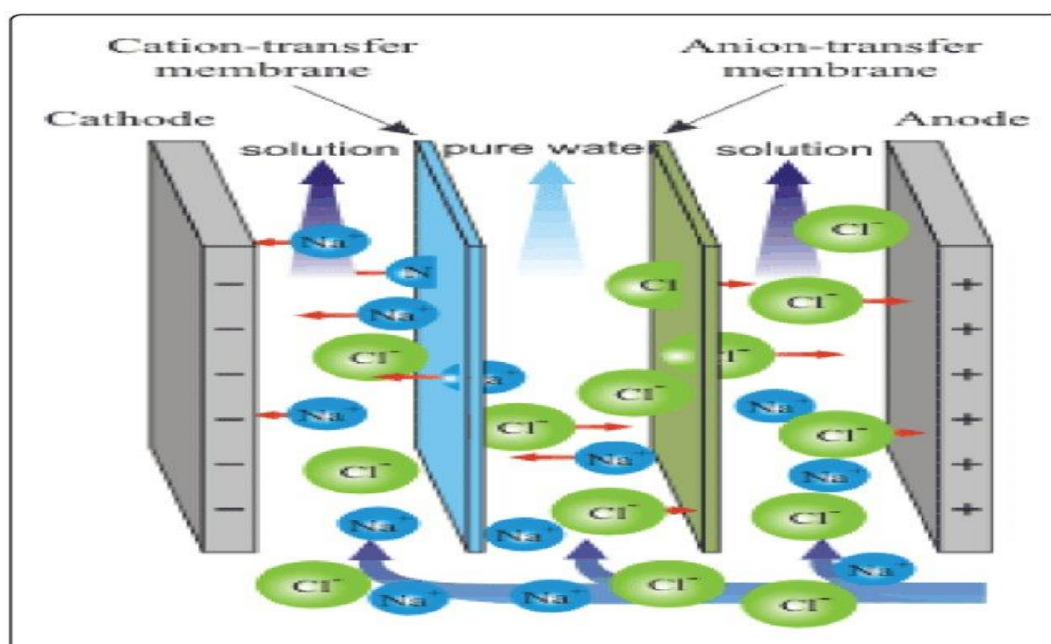
Figure 2-4:Schematic diagram illustrating the principle of electrodialysis (Vasudevan, 2016) - *Reproduced by permission author*.

2.5.5. Electrodeionisation

Electrodeionisation (EDI) is a hybrid technology incorporating the properties of ion-exchange resins and electrodialysis to deionise water. In this process, each compartment is filled with ion-exchange resins, thereby providing a synergistic effect of electrodialysis and processes of ion-exchange for even deeper water demineralisation (Sillanpaa and Shestakova, 2017), Figure 2-5, illustrates this process. Several studies have investigated EDI for the treatment of a dilute solution concerning the exchange of ions, which has the advantages of continuous production and no emission, the resins in the compartments do not require acid and alkali regeneration (Alvarado and Chen, 2014).

Shang, Zhang and Gao (2014) studied the performance of an EDI process with a bipolar membrane (EDI-BP) for the treatment of simulated Ni^{2+} - containing wastewater. In this study, an initial concentration of 30 mg/l Ni^{2+} - containing wastewater, at an electrolysis time of 98.5 hours and a current density of 16.5 mA/cm^2 gave the optimum results. The results showed that the process allows for nearly complete removal of nickel and sulphate anions from the diluted solution.
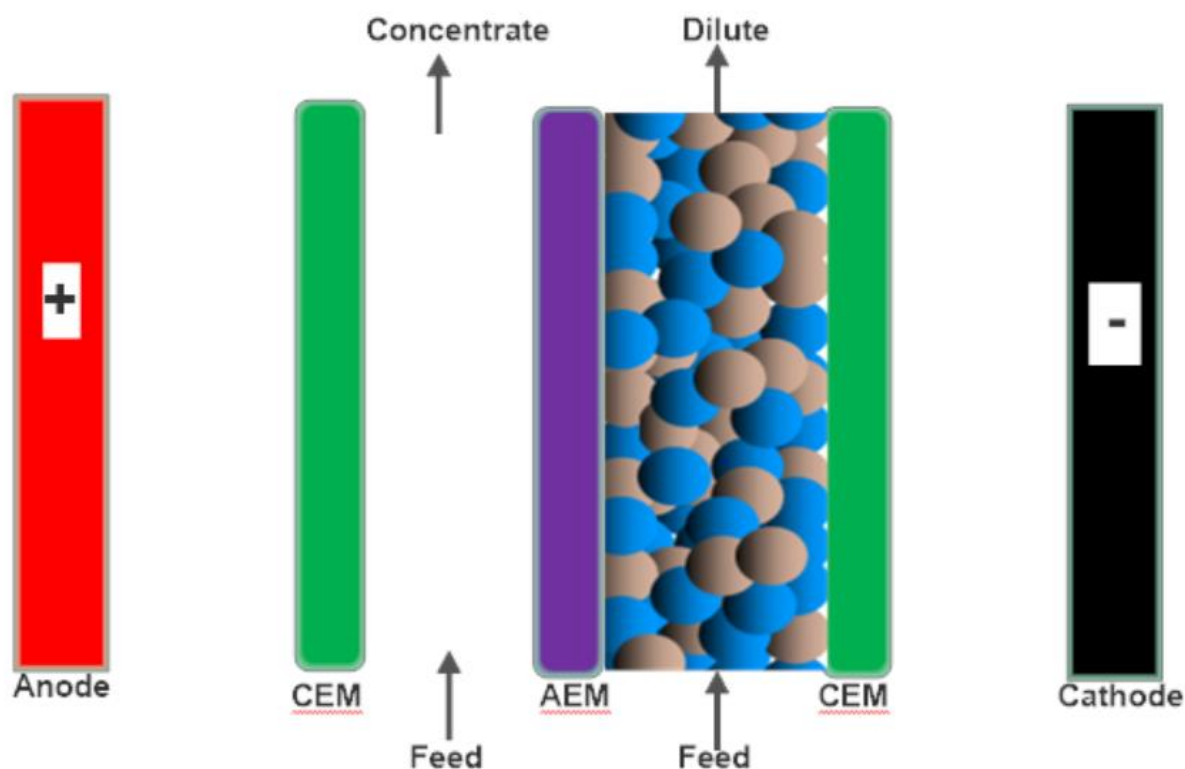
Figure 2-5: Schematic diagram of an EDI cell. The spheres represent the ion exchange resin, AEM: Anionic Exchange Membrane and CEM: Cationic Exchange Membrane (Adapted from Shang, Zhang and Gao, 2014)

2.5.6. Electro-Fenton Process

One of the advanced oxidation methods used in wastewater treatment technology is electro-Fenton. It is a modified process of the traditional Fenton process and consists of an electrolysis cell that, by an electrochemical reaction between the anode and cathode, regenerates the Fenton reagent (H_2O_2 and Fe^{2+}). The electro-Fenton process is a combination of the Fenton and EO reaction, an electrochemical reaction (Tony *et al.*, 2015). In a single reaction chamber, all reactions occur. Fenton is a chemical reaction, whereas EO is an electrochemical reaction that electrochemically oxidizes the contaminant. Figure 2-6 demonstrates the pathway for the oxidation of the Fenton reaction. The electro-Fenton method is commonly used in different forms of wastewater treatment, relying on this principle.

According to various studies, electro-Fenton is dependent on the type of electrode. The electrode of the process may sacrifice (active) like mild steel, iron or Aluminium or neutral like platinum, stainless steel, titanium oxide (Can, 2014; El-Ghenymy *et al.*, 2014; Heidari, Motevasel and Jaafarzadeh, 2015). For commercial process titanium and stainless steel is economically suitable for plant and pilot-scale projects.

Heidari *et al.* (2015) studied the performance of an electro-Fenton process (EFP) for the elimination of pentachlorophenol (PCP) from an aquatic environment. The effects of critical operational variables such as reaction time, pH, the applied voltage, and the distance between the electrodes were investigated on solution degradation. The maximum PCP removal was obtained at 3 cm, a pH of 3, a voltage of 24 volts, and a treatment time of 40 min. This study demonstrated that the distance between the electrodes, pH, applied voltage, and the treatment time have significant effects on the electron-Fenton process, and this process is suitable for the treatment of PCP-polluted wastewaters.
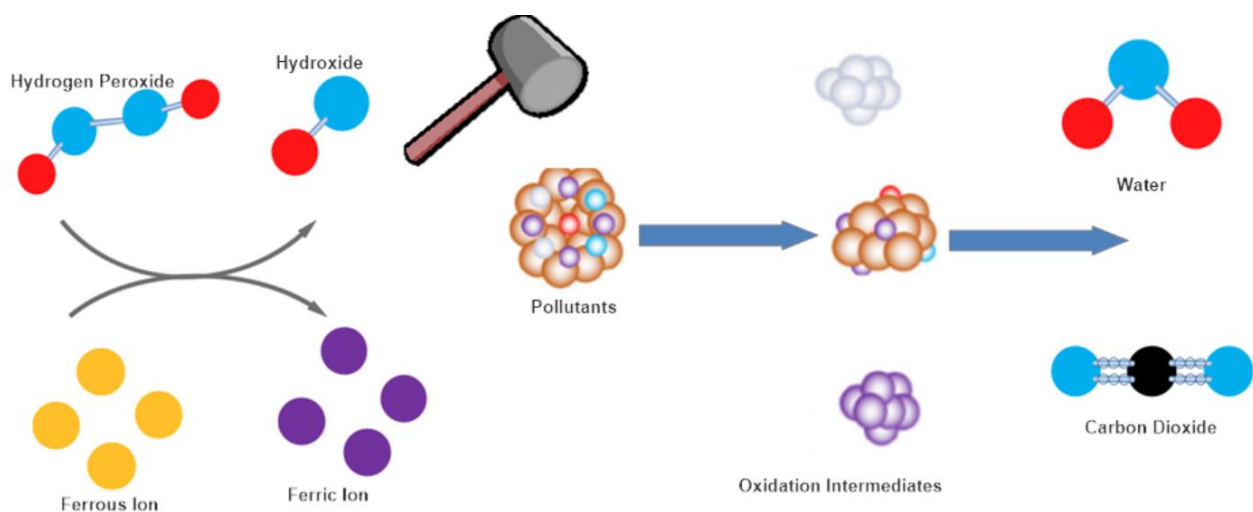
Figure 2-6: The reaction mechanism for electro-Fenton (Adapted from Zhang et al., 2019)

2.5.7. Electrooxidation

Electrooxidation (EO) is a chemical reaction involving the loss of one or more electrons on the anode surface by an atom or molecule formed from catalyst product during the passage through the anode, cathode, and electrolyte solution of direct electrical current (Sillanpaa and Shestakova, 2017). In order to break down even the most resistant organic compounds, EO is considered a very effective method. Organic pollutant anodic oxidation can occur in different ways, including direct and indirect oxidation (Feng *et al.*, 2016).

Table 2-7: Summary of electrochemical processes for water and water and wastewater treatment

Treatment process	Advantages	Disadvantages	References
Electrodialysis	• High removal rates of salt; • Able to generate high brine concentration; • Less susceptible to scaling; • High segregation of metals	• Requires high capital costs; • Clogging • energy loss.	(Al-Amshawee *et al.*, 2020)
Electrodeionisation	• continuous operation, • constant water quality, • modular design,' • small space requirements • elimination of the regenerant waste stream	• Relatively high capital cost • High EDI stack replacement • High energy consumption • Difficulty in removing weakly ionised contaminants • Susceptible to fouling	(Smith and Hyde, 2000)
Electro filtration	• minimisation of the chemical additives dosage, • reduction in residuals generation, • a decrease in the cost of chemicals and waste disposal.	• limitation of the process stream for relatively low conductivity of feed stream, • a high-energy requirement, • substantial heat production, • changes in the process feed due to reaction at the electrode	(Permadi and Wenten, 2010; Mostafazadeh, Zolfaghari and Drogui, 2016)
Electroflotation	• Highly versatile • Competitive with other flotation	• Limitation of separation efficiency by the oil concentration in the emulsion	(Moulai Mostefa and Tir, 2004)

Electro-Fenton	• The on-site production of H_2O_2; • no risks associated with handling, transportation and storage of H_2O_2; • the continuous regeneration of Fe^{2+} on the cathode; • the low iron sludge production.	• The low H_2O_2 yield; • the low unit cell body throughput; • the low current density; • the low conductivity	(Zhang *et al.*, 2019)
Electrocoagulation	• Ability to treat drinking water and wastewater • Combination of oxidation and coagulation processes • Reduced demand for chemicals (replaced by Aluminium and iron electrodes) • Reduce operating costs • Reduce the risk of secondary pollutions • Less generated sludge and Low energy requirements.	• Maintenance required regularly • The electrode breaks down over time • Wastewater must have high conductivity	(Tien *et al.*, 2017)
Electrooxidation	• Ambient temperatures and pressure requirements, • robustness, versatility to treat large volumes, • ease of automation, • addition of nontoxic reagents for increasing conductivity, • attractive compact technology, • application as a pre-treatment or posttreatment of effluents in combination with	• Potential formation of halogenated byproducts, • electrode fouling, and corrosion phenomena, • high operating costs due to the high energy consumption (but coupling with renewable energy sources is possible),	(Martínez-huitle and Rodrigo, 2018)

	other depuration technologies: biological treatment, Fenton oxidation, ion exchange, membrane filtration, membrane bioreactors, electrochemical technologies	• low conductivity of the effluent, optimization of reactor hydrodynamic conditions,	

2.6. Electrocoagulation (EC)

EC technology is a process for the operation of an electrical current to treat and flocculate pollutants without the need to apply coagulants and to eliminate waste generation residues (Butler et al., 2011). The progress of this technology is minimal, despite some encouraging outcomes. However, owing to the need for alternative water treatment methods, there has been growing research, economic and environmental interest in this technology in recent years. EC has some similarities but also essential distinctions with chemical coagulation, such as side reactions. Many electrochemical reactions on the anodes and cathodes co-occur in the EC system. These mechanisms can be divided into critical mechanisms that induce pollutant destabilisation and side reactions, such as the production of hydrogen (Azadi and Kariminia, 2016).

Electrocoagulation consists of pairs of electrodes that are arranged in pairs of two, the anodes and cathodes, called metal sheets. The cathode is oxidised (loses electrons) by applying the principles of electrochemistry, while the water is reduced (gains electrons), thus treating the wastewater. (Chavalparit & Ongwandee, 2009).

According to Emamjomeh and Sivakumar (2009), when the sacrificial anode electrode makes contact with the wastewater, it corrodes to release active coagulant precursors usually aluminium or iron cations into solution. At the cathode gas evolves, usually as hydrogen bubbles accompanying the electrolytic reactions.

Pitakpoolsil and Hunsom (2014) stated that the EC method for biodiesel wastewater treatment, using an aluminium anode and graphite cathode is potentially ideal because it can eliminate oil and grease (O&G) and total suspended solids (TSS) by more than 95 %. However, due to the insufficient elimination of residual glycerol and methanol, it can only produce a 55 % reduction in COD.

2.6.1. Mechanism of electrocoagulation

Generally, during electrocoagulation, Emamjomeh and Sivakumar (2009) state that four mechanisms co-occur:

- Electrolytic reactions at the electrode surfaces,
- Formation of coagulant agents in the aqueous phase,
- Adsorption of soluble pollutants by these agents, and
- Removal by flotation

Figure 2-7: illustrates the mechanism during the EC process. In the process, Aluminium is removed from the anode, and hydrogen gas is formed at the cathode, as shown in Equation 2-4 and 2-5.

$$Al \rightarrow Al^{3+} + 3\bar{e} \qquad \text{(Anode)} \qquad \textbf{Equation 2-4}$$

$$3H_2O + 3\bar{e} \rightarrow \frac{3}{2}H_2 + 3OH^- \qquad \text{(Cathode)} \qquad \textbf{Equation 2-5}$$
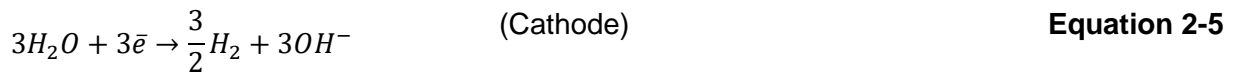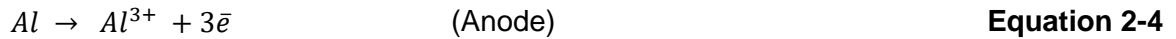
According to Daud *et al.* (2014), the advantage of using the electrocoagulation process include high-efficiency removal of waste particulates, relatively low treatment costs and better operability conditions.
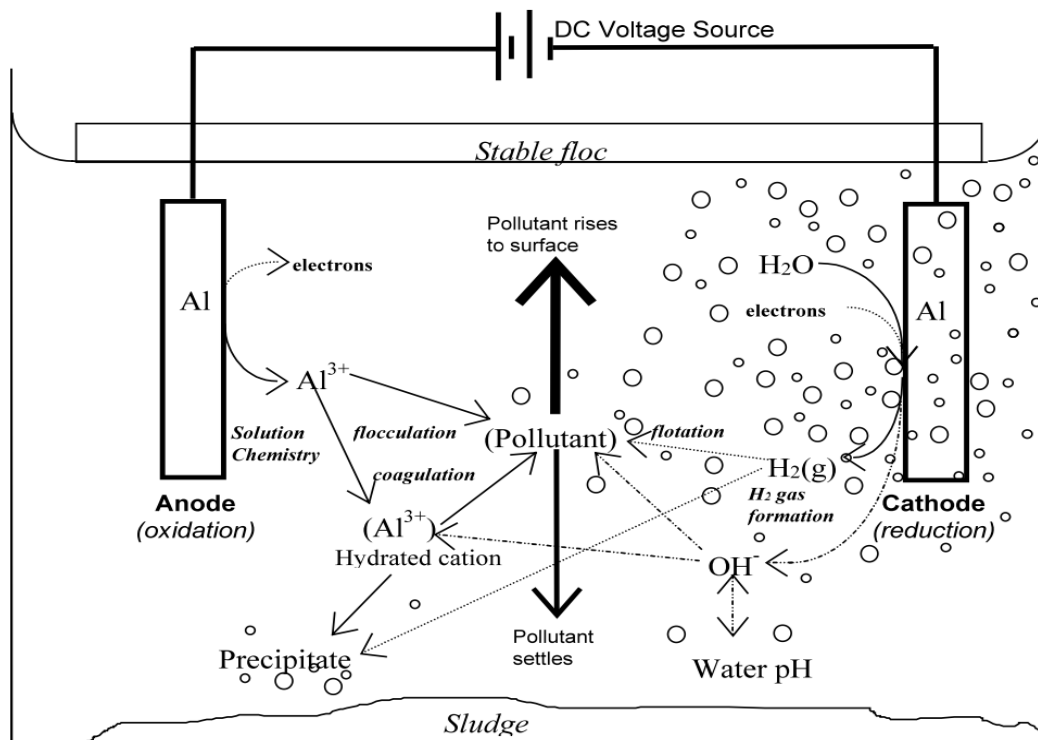
Figure 2-7: Mechanisms during electrochemical coagulation (Holt et al., 2002)- Reproduced by permission author

2.6.2. Factors affecting the electrocoagulation process

The efficiency of the electrocoagulation depends significantly on the initial pH of the wastewater before treatment, the conductivity, the current density and the electrolysis time for the batch processes (Butler *et al.*, 2011).

i.   Effect of initial pH

The initial pH of a solution has been identified as one of the key factors influencing the efficiency of electrochemical processes (Abbas and Ali, 2018). According to Feng *et al.* (2016), the highest efficiency of pollutant elimination is achieved for the EC process at an optimal solution pH based

on the composition of the contaminants. The effectiveness of pollutant removal reduces either by increasing or decreasing the pH of the solution from the optimal pH.

Several investigators found that for a system that uses the aluminium anodes, a decrease in the removal efficiency at a more acidic and alkaline pH were due to an amphoteric activity of $Al(OH)_3$ which leads to soluble Al^{3+} cations at acidic pH and monomeric anions $Al(OH)^{-4}$ at alkaline pH (Ganesan *et al.*, 2013).

Abdelwahab, Amin and El-ashtoukhy (2008) observed a remarkable removal of 97% of phenol from the oil refinery wastewater after 2 hours using a cell with a horizontal aluminium cathode and a horizontal aluminium screen anode at an initial pH of 7.

Ganesan *et al.* (2013) studied the effect of the initial pH on the removal of Manganese. The initial pH on the removal of Manganese. The initial pH was adjusted, ranging from 3 to 11. The authors observed that maximum removal efficiency of 97.2% was achieved at a pH of 7.

One of the benefits of adjusting the initial pH is that after electrocoagulation treatment, the pH of the effluent will increase for acidic wastewater solution but decrease for alkaline wastewater solution.

ii. Effect of conductivity

Another critical factor affecting the electrocoagulation process is the conductivity of the wastewater. The higher the conductivity of the wastewater, the higher the current that passes through for a given potential drop. Usually, the conductivity of the wastewater is adjusted by adding sodium chloride (NaCl) solution to the wastewater. By adding NaCl to the wastewater, it gives an additional positive effect on the anode; however, it has been found to have a negative impact on the process efficiency (Koutsaftis *et al.*, 2012).

iii. Effect of current density

Current density in the EC process defines the number of Al^{3+} or Fe^{2+} ions produced from the respective electrodes and thus influences the dosage rate of coagulants in the electrochemical cells (Vasudevan, Lakshmi and Sozhan, 2012). The rate of dissolution of the anode increases with an increase in the current density. This leads to an increase in the number of flocs of metal hydroxide resulting in an improvement in the capacity of eliminating contaminants. However, The increase in current density above the optimum current density does not contribute to an improvement in the performance of pollutant removal, because there is a large number of metal hydroxide flocs required for the sedimentation of pollutants (Khandegar and Saroha, 2013).

Butler *et al.* (2011) describe the current density to have the following effects on the electrocoagulation process: at higher current densities the rate of the electro dissolution of electrode material increases and thus the removal of waste pollutants from the wastewater is also higher. The rate of water electrolysis at the cathode increases at higher current density; therefore, the amount of hydrogen production at the cathode also increases, which enhances the flotation effect. Moreover, increased rate of water electrolysis at the cathode leads to the production of more hydroxyl ions which increases the pH.

The treatment of oily wastewater by electrocoagulation was studied (Tir and Moulai-Mostefa, 2008). The current density ranging from 5 to 35 mA·cm^{-2} showed a significant effect on turbidity and COD removal when the current density increased from 5 to 25 mA·cm^{-2}. The removal efficiencies increased rapidly from 70% to 99% for turbidity and 54% to 89% for COD after 20 minutes of reaction time.

iv.   Effect of electrolysis time

The efficiency of removing pollutant is also a function of the time of electrolysis. The efficiency of pollutant removal increases with the electrolysis time increasing. However, after the optimal electrolysis time, the efficiency of pollutant removal is constant and does not increase with an increase in electrolysis time. The metal hydroxides are formed by the dissolution of the anode (Khandegar and Saroha, 2013).

Electrolysis time also influences the efficiency of treatment of the EC process, as it can increase or decrease with current density or pH of the wastewater (Sahu, Mazumdar and Chaudhari, 2014). Maha Lakshmi and Sivashanmugam (2013) state that when the electrolysis time increases for batch mode process at a fixed current density, there is higher removal of pollutants and an increased amount of sludge production.

Ugurlu *et al.* (2007) studied the effect of the reaction time on the treatment of paper mill wastewater. Over 80% of lignin and 99% phenol were removed within 7 minutes of electrolysis time.

v.   Effect of electrode material

Removing metals, suspended particles, organic pollutants and oil and greases from PRW highly depends on the electrode material (Bagastyo *et al.*, 2014). In a study done by Hashemi *et al.* (2015), Two different reactions are caused by the voltage applied to metal anodes, usually made of either iron or aluminium: Fe/Al was dissolved from the anode, thereby producing corresponding metal ions that were hydrolyzed to polymeric iron or aluminium hydroxide. They are excellent coagulating agents for these polymeric hydroxides. Consumable (sacrificial) metal anodes are

used in the vicinity of the anode to produce polymeric hydroxides continuously. (Nasution *et al.*, 2013). Coagulation occurs when these metal cations combine with the harmful particles carried toward the anode by electrophoretic motion. Pollutants found in the drainage system are either treated by chemical reactions and precipitation, or by electrode degradation, physical and chemical binding to colloidal compounds and then eliminated by electroflotation or sedimentation and filtration. These coagulating agents are therefore created in situ rather than adding coagulating chemicals as in conventional coagulation processes, and pollutants present in the wastewater stream are treated by chemical reactions (Mollah *et al.*, 2004).

Iron and Aluminium have been widely used as electrode materials in electrocoagulation systems according to the literature (Abdelwahab, Amin and El-ashtoukhy, 2008; Emamjomeh and Sivakumar, 2009; Tezcan, Koparal and Bakir, 2009) because they are cheap and have been demonstrated to be very effective on the electrocoagulation process. Depending on the use, one of them is preferred over the other. Table 2-8 outlines the performance of different types of electrode material. Thus, for applications that are not continuous in time, aluminium electrodes are the best choice, because iron can be easily oxidized and corrosion problems of the electrodes are reported when the cell is not connected. Furthermore, the use of iron as the electrode material has another additional problem because of the colour of Fe(III) salts (Martı, Sa and Rodrigo, 2007).

Dohare & Sisodia (2014) investigated the use of iron and Aluminium as sacrificial electrode materials in the treatment of industrial wastewater by electrocoagulation, which was found to be pH-dependent. The results indicate that in acidic medium, pH<6, COD and turbidity removal efficiencies of Aluminium are higher than those of iron, while in neutral and alkaline mediums iron is preferable. High conductivity favours excellent process performances. On the other hand, for the same turbidity and COD removal efficiencies, iron requires a current density of 80-100 A/m^2, while Aluminium requires 150 A/m^2 for an operating time of 10 minutes. The highest removal efficiencies obtained were98% for turbidity and between 65-61% for COD using an aluminium electrode for pH<6. On the other hand for iron electrodes, the turbidity and COD removals reached 75- 98% and 47-77% respectively for pH in the range of 3-7.

Table 2-8: Summary of reported electrode performance

Type of wastewater	Electrode	Initial pollutant level (mg/l)	Optimum removal efficiency (%)	References
Industrial oil-in-water emulsion	Al (Anode) and Stainless steel (Cathode)	62300	90 % COD	(Kuokkanen *et al.*, 2013)
Car Wash	Fe	572	75 % COD	(Kuokkanen *et al.*, 2013)
Oily wastewater	Al (Anode) / Fe (Cathode)	7960	98 % COD	(Yavuz, Koparal and Bak, 2010b)
Oil Refinery	Al	13 mg/l of phenol	97 % Phenol	(Abdelwahab, Amin and El-ashtoukhy, 2008)
Oily wastewater	Al	305.9	51.9 % COD	(Wijeyekoon *et al.*, 2007)
Oily wastewater	Graphite	305.9	48.7 % COD	(Wijeyekoon *et al.*, 2007)
Oily wastewater	Al (Anode)/ graphite (Cathode)	305.9	51.9 % COD	(Wijeyekoon *et al.*, 2007)
Oily wastewater	Graphite (Anode) and Al (Cathode)	305.9	42.3 % COD	(Wijeyekoon *et al.*, 2007)

2.6.3. Modelling electrocoagulation through adsorption kinetics

i. Kinetics

In the EC process, the pollutant is commonly adsorbed at the surface of the coagulant produced electrochemically (Chatterjee, Rai and Sar, 2014). Critical analysis of the EC of pollutants displays that there are two consecutive separate processes taking place, the electrochemical process through which the metal coagulants are generated and physio-chemical method via which the wastewater is adsorbed on the surface of the coagulants (Chithra and Balasubramanian, 2010)

The pollutant removal is equivalent to traditional adsorption, except for the production of coagulants. The electrodes consumption can be estimated according to Faraday's law, and the amount of flocs produced can be stoichiometrically estimated. The created aluminium floc traps

the contaminant present in the solution by adsorption mechanism: From this, it is possible to obtain a pollutant removal model by the phenomenon of adsorption, and the amount of the adsorbed contaminant is shown in Equation 2-6 (Ouaissa *et al.*, 2014a):

$$q_t = \frac{V(C_i - C_t)}{M}$$ **Equation 2-6**

Where q_t is the amount of pollutant adsorbed (mg/g), V is the volume of the effluent (L), M is the weight of electrode dissolved (g); C_0 and C_t are the initial concentration and the concentration of the pollutant at any time t (mg/L), respectively.

According to Ghanim and Ajjam (2013), in order to investigate the mechanisms of the adsorption process, the kinetic equation is extended further with the pseudo-first or second kinetic order models. The pseudo-first-order kinetic model is given in Equation 2-7 as:

$$\frac{dq_t}{dt} = k_1(q_e - q_t)$$ **Equation 2-7**

Where K_1 (min^{-1}) is adsorption rate constant, q_t, and q_e are the adsorbed amounts at a given time t and equilibrium (mg/g), respectively. After integrating between 0 and a given time t, it results:

$$\ln(q_e - q_t) = \ln q_e - k_1 t$$ **Equation 2-8**

The pseudo-second-order kinetic equation can be given as (Simonin, 2016) :

$$\frac{dq_t}{dt} = k_2(q_e - q_t)^2$$ **Equation 2-9**

Where K_2 is the constant rate of the pseudo-second-order equation (g/mg/min), integration leads to Equation 2-10 (Ouaissa *et al.*, 2014b):

$$\frac{t}{q_t} = \frac{1}{k_2 q_e} + \frac{1}{q_e} t$$ **Equation 2-10**

ii. Adsorption Isotherm

During EC, the insoluble metal hydroxides eliminate contaminants through surface adsorption. In adsorption, it is assumed that the pollutant may act as a ligand to bind a gelatinous precipitate produced in situ by hydrous Al. An adsorption isotherm study had predicted and evaluated the adsorption capacity of the adsorbent (Seader, Henley and Roper, 2011).

- **Freundlich Isotherm**

The Freundlich isotherm states that the degree of adsorption varies directly with pressure. The multilayer adsorption of heterogeneous structures is characterised by this empirical relationship and implies that various sites have many adsorption energies involved (Kumara *et al.*, 2014). The linear model of the isotherm can be expressed logarithmically, as shown in Equation 2-11 (Vafajoo, Ghanaat and Ghalebi, 2014):

$$\ln q = \ln K_F + \frac{1}{n}\ln C_e$$

Equation 2-11

Where C_e is the concentration of equilibrium (mg / l), q is the adsorbed volume (mg / g) and K_F, and n are constants that integrate all parameters affecting the adsorption process, such as adsorption capacity and intensity respectively.

- **Langmuir Isotherm**

The Langmuir isotherm model was developed to reflect chemisorptions in a collection of well-defined localized adsorption sites with the same adsorption energy, independent of the surface coverage, and without interaction between adsorbed molecules. This model assumes a single-layer deposition with a finite number of similar sites on the soil. The linearised form of the Langmuir adsorption isotherm model is presented by Equation 2-12 (Myburgh *et al.*, 2019).

$$\frac{C_e}{q_e} = \frac{1}{q_{max}K_L} + \frac{C_e}{q_{max}}$$

Equation 2-12

Where q_e (mg/g) is the amount adsorbed at equilibrium, Ce (mg/L) equilibrium concentration, q_{max} is the Langmuir constant representing maximum monolayer adsorption capacity, and K_L is the Langmuir constant related to the energy of adsorption

- **Temkin Isotherm**

The Temkin isotherm contains a factor which explicitly takes into account the interactions between adsorbent adsorbents. The linearised form of Temkin model is shown in Equation 2-13 (Chithra and Balasubramanian, 2010).

$$q = B \ln K_T + B \ln C_e$$

Equation 2-13

Where, B =RT/b is the Temkin constant related to the heat of adsorption (J/mol), K_T is the Temkin isotherm equilibrium binding constant (L /g), R is the gas constant (8.3145 J·mol^{-1}·K [-1])

In this equation, the heat of adsorption of all molecules in the layer is assumed to decrease linearly with the coverage due to these interactions and ignoring very low and very large concentration values (Araújo *et al.*, 2017).

- **Dubinin-Radushkevich Isotherm**

In order to assess the nature of adsorption, the experimental data were also fitted to the Dubinin–Radushkevich isotherm. This model is based on surface energy heterogeneity and can be written in the following linear form (Ayawei, Ebelegi and Wankasi, 2017):

$$\ln q_e = \ln X_m + \beta E^2$$ **Equation 2-14**

where: Xm is the maximum sorption capacity of the sorbent (mol·kg^{-1}), β a constant (mol^2·kJ^2) related to the mean sorption energy, E is the Polanyi potential, R the gas law constant (kJ·mol^{-1}·K^{-1}) and T the absolute temperature (K).

With the following relation, the values of the sorption energy E$_s$ (kJ·mol^{-1}) can be compared to β (Cozmuta *et al.*, 2012):

$$E_s = \frac{1}{\sqrt{-2\beta}}$$ **Equation 2-15**

Several researchers have modelled the EC process through adsorption isotherm. Ouaissa *et al.* (2014b), modelled the EC process using adsorption and observed that the Sips isotherm model matched satisfactorily with the experimental observations for the removal of tetracycline. Ghanim and Ajjam, (2013b), modelled the EC process via adsorption isotherm kinetics, and observed that the Langmuir isotherm was the best fit for COD removal experimental data than the Freundlich and Temkin Isotherm model. Chithra and Balasubramanian (2010), also modelled the EC process using various adsorption isotherms and observed that the Langmuir isotherm model match satisfactory with

2.7. Electro-oxidation (EO)

Although EO is effective in removing most of the organic pollutants, such as turbidity (Abdelwahab, Amin and El-ashtoukhy, 2008), Yavuz *et al.*, (2010) states that electrocoagulation is ineffective in treating PRW due to its low removal percentage of COD. Therefore, there is a need to treat the water after the electrocoagulation process further, and EO process is a suitable and attractive technique for such wastewater as a secondary treatment (Da Costa *et al.*, 2016).

Electro-oxidation (EO) is a sustainable technique to abate or convert pollutants to non-toxic material (Palma-Goyes *et al.*, 2018). EO has proven to be very useful for pollutant removal due to its versatility, environmental compatibility and potential cost-effectiveness (Tavares *et al.*, 2012). The electrochemical oxidation process is a complex phenomenon. Electrical energy is used to generate an oxidant, which oxidises the pollutant present in the wastewater. In the electrochemical oxidation process, there are two principal pathways for oxidizing the pollutants: direct oxidation and indirect oxidation (Yavuz, Koparal and Bak, 2010b). Direct oxidation occurs when the pollutants directly oxidize on the surface of the electrode. Indirect oxidation occurs with the help of oxidizing agents generated electrochemically. In direct electrolysis, the rate of oxidation depends on the electrode activity, pollutant diffusion rate and current density. On the other hand, temperature, pH and the diffusion rate of the generating oxidants determine the rate of oxidation in indirect electrolysis (Vasudevan and Oturan, 2014).

i. Indirect electrolysis

According to Gherardini *et al.* (2001), on the metal oxide electrode, oxidation occurs via the surface arbitrator on the anodic surface, where they are produced continuously, this is called indirect electrolysis. In indirect electrolysis, the temperature, the pH and the diffusion rate of the generated oxidants determine the rate of oxidation. For an effective conductivity and production of hypochlorite ions, chloride salts of sodium or potassium are added to the wastewater. The reaction of anodic oxidation of chloride ions to form chlorine is given in Equation 2-16, 2-17 and 2-18 as:

$$2Cl^- \rightarrow Cl_2 + 2e^-$$

Equation 2-16

The free chlorine form hypochlorous acid:

$$Cl_2 + H_2O \rightarrow H^+ + Cl^- + HOCl$$

Equation 2-17

Moreover, further, dissociate to give hypochlorite ion:

$$HOCl \rightarrow 3H^+ + OCl^-$$

Equation 2-18

The generated hypochlorite ions act as the principal oxidising agent in pollutant degradation (Jaruwat *et al.*, 2010).
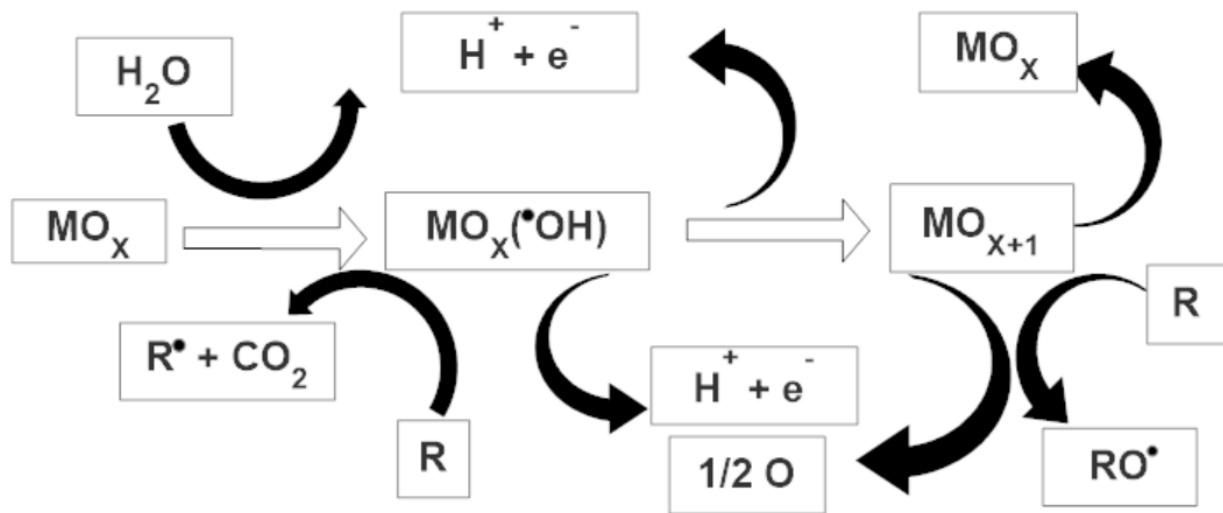
Figure 2-8: Representation of indirect oxidation of pollutant (Adapted from Babu et al., 2014).

ii. Direct oxidation

Electrooxidation of pollutants can also occur directly on anodes through the generation of physically adsorbed "active oxygen" (adsorbed hydroxyl radicals, •OH) or chemisorbed "active oxygen" (oxygen in the oxide lattice, MO_{x+1}),. This process is usually called anodic oxidation or direct oxidation. The physically adsorbed "active oxygen causes organic compounds (R) to be completely combusted, and the chemisorbed "active oxygen (Babu *et al.*, 2014).

Direct oxidation is used to remove the pollutants from the surface of the electrode. The direct oxidation rate of organic pollutants depends on the catalytic activity of the anode, on the diffusion rate of organic compounds on the active points of the anode and the applied current density (Gherardini *et al.*, 2001).

In general, •OH is more effective than oxygen in MO_{x+1} for pollutant oxidation. Since the reaction of oxygen evolution can also take place at the anode, for the reaction to proceed with higher current efficiency, high overpotentials for oxygen (O_2) evolution are necessary. Otherwise, most of the supplied current will be wasted in order to separate water (Vasudevan & Oturan, 2014).

Direct oxidation does not require the addition of a significant amount of chemicals to wastewater or to feed the cathodes with O_2; it does not aim to produce secondary contaminants and requires fewer accessories. These benefits make direct oxidation more desirable than other processes of electro-oxidation. Anode material is the critical component of a direct oxidation phase. (Linares-Hernández & Barrera-Díaz,2009).

2.7.1. Chemical Reaction of the EO process

In Figure 2-9, a generic diagram of the electrochemical conversion and combustion of organics on metal oxide anode (MO_x) is shown. In the first stage, H_2O in acidic or OH^- in basic solution is discharged at the anode to generate adsorbed hydroxyl radical according to the Equation 2-19.

$$MO_x + H_2O \xrightarrow{k_1} MO_x(\bullet OH) + H^+ + e^-$$
<div align="right">**Equation 2-19**</div>
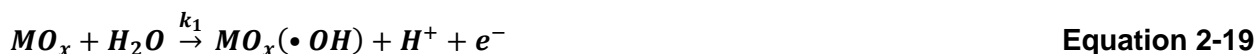
In the second stage, the adsorbed hydroxyl radicals might interact with the oxygen present in the metal oxide anode with the formation of oxygen from the hydroxyl radical which is adsorbed to metal oxide anode lattice, thus forming the so-called higher oxide (MO_{X+1}) as shown in Equation 2-20:

$$MO_x(\bullet OH) \xrightarrow{k_2} MO_{x+1} + H^+ + e^-$$
<div align="right">**Equation 2-20**</div>

Thus, we can consider that the two active oxygen states in physisorbed and chemisorbed active oxygen may be present at the anode surface (Babu *et al.*, 2011)
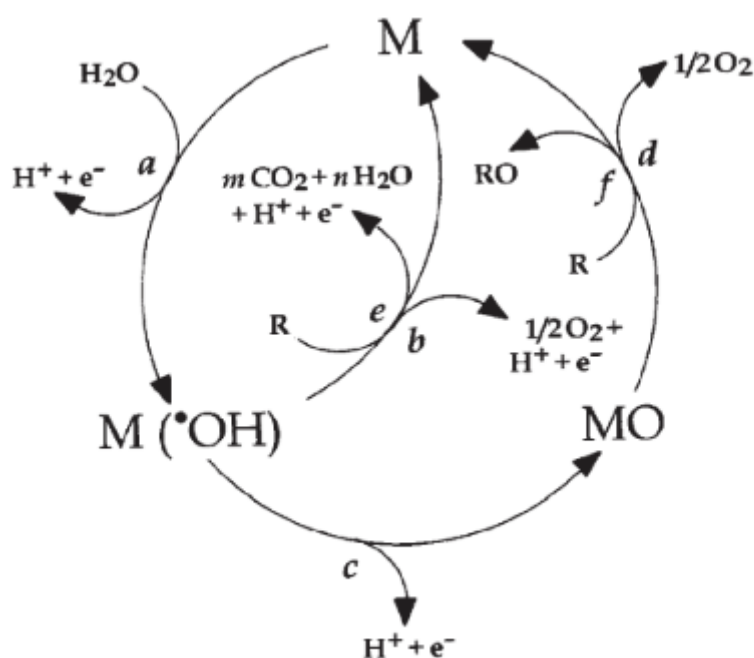
Figure 2-9:Anodic oxidation mechanism scheme for organic compounds (Martınez-Huitle and Ferro, 2006) - Reproduced by permission of The Royal Society of Chemistry

In the absence of any oxidisable pollutants, the physisorbed and chemisorbed active oxygen produce dioxygen as shown in Equation 2-21 and 2-22

$$\text{MO}_x(\bullet\,\text{OH}) \xrightarrow{k_0} \tfrac{1}{2}O_2 + H^+ + e^- + \text{MO}_x \qquad\qquad \textbf{Equation 2-21}$$

$$MO_{x+1} \xrightarrow{k_d} MO_x + \tfrac{1}{2}O_2 \qquad\qquad \textbf{Equation 2-22}$$
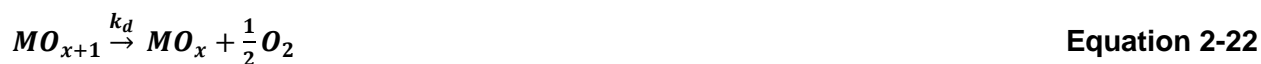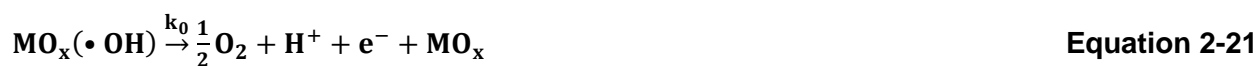
In the presence of oxidisable pollutants, it is proposed that the physisorbed active oxygen (•OH) will primarily cause the complete combustion of pollutants according to Equation 2-23, and chemically adsorbed active oxygen (MO_{x+1}) is involved in the formation of selective oxidation products as described in Equation 2-24

Complete combustion:

$$R + MO_x(\bullet\,OH) \xrightarrow{k_c} CO_2 + zH^+ + ze^- + MO_x \qquad\qquad \textbf{Equation 2-23}$$

Selective oxidation:

$$R + MO_{x+1} \xrightarrow{k_s} RO + MO_x \qquad\qquad \textbf{Equation 2-24}$$

2.7.2. Advantages and disadvantages of the electro-oxidation process

Like any process, EO has its advantages and disadvantages (Anglada, Urtiaga and Ortiz, 2009). These are summarised in Table 2-9.

Table 2-9: Advantages and disadvantages of EO

Advantages of EO	Disadvantages of EO
Environmental compatibility as it uses a clean reagent, the electron, and there is little or no need for the addition of chemicals.	High operating cost is incurred due to high energy consumption.
Robustness: the reaction can be terminated quickly in seconds by cutting off the power, and it can also be restarted quickly after an operation problem.	Potential for the formation of chlorinated organics during indirect oxidation by active chlorine needs to be considered.
Versatility: these processes can deal with many pollutants and treat quantities from microlitres to millions of litres.	
Amenability to automation: the electrical variables used in electrochemical processes are particularly suited to facilitating data acquisition, process automation and control	

2.8. Factors influencing the efficiency of EO

Different parameters affect the efficiency of EO and its ability to remove pollutants from wastewater; the most important parameters are discussed in this section.

2.8.1. Initial pH

Typically the efficacy of organic oxidation in alkaline solution appears to be superior. That also includes the traditional electrode materials used for anodic treatment. Until treatment, the wastewater accessible to the treatment process will be too costly to change pH and adjusting the pH before treatment to the more favourable value above seven will be too expensive (Linares-hernández and Barrera-díaz, 2009).

In addition, Zheng et al. (2015), notes that the removal efficiency decreased with increasing pH for anodic oxidation, likely due to the enhancement of the oxygen evolution side reaction. For indirect oxidation, the efficiency of elimination improves with increasing pH, attributing hydrogen peroxide (H_2O_2) to electrochemical output in a more alkaline solution.

Canizares et al. (2005) indicated the pH does not influence the rate of global oxidation, even when the initial oxidation rate in alkaline media was higher than 7. Nevertheless, the oxidation rate in acidic media exceeds those in the alkaline media after the galvanostatic formed. Thanks to its lower oxidisability, the concentration of oxalic acid in alkaline media were higher than in acidic media.

2.8.2. Current Density

One of the most critical operating parameters in EO is current density; it has an intrinsic impact on the efficiency of the operation (Kabdash *et al.*, 2012). The applied current density in the EO process affects the rate of electrochemical reactions produced by the coagulant and the size and amount of bubbles of hydrogen. It also affects the electrode potential, which defines the reactions that take place on the surface of the electrode. Indeed the dissolution rate of the anode has been reported to be lower than the theoretical value determined by the law of Faraday, suggesting the existence of other anode reactions and the occurrence of the negative difference effect (Taylor *et al.*, 2010).

2.8.3. Effect of electrolyte

According to Babu *et al.* (2009), sodium chloride (NaCl) can increase the efficiency of degradation and shorten the reaction time due to the reaction between the chlorine or hypochlorite produced and the organic molecule. When the NaCl concentration increases, the conductivity of the solution is increased, which leads to less power consumption. Increasing the concentration of NaCl accelerates the rate of removal, allowing organics to be completely mineralized in 2 hours to minimize productivity by 85.56 % COD. However, increasing the concentration of NaCl above the highest concentration of 5 g/L does not contribute to an increase in the performance of COD reduction. The optimum concentration of NaCl used in consecutive studies must therefore be less than 5g/L.

2.8.4. Temperature

The effect of temperature on the elimination of pollutants by EO is not widely reported in the literature. Santos *et al.* (2006), noted that high COD removal efficiency is attributed to an increase in temperature, due to the reactions in the EO process involving the evolution of gaseous products can be favoured to increase effectively.

In a study conducted by Da Silva *et al.* (2013), the influence of temperature on the removal of COD from produced water by EO with $Ti/IrO_2 – Ta_2O_5$ was investigated in the range of 25°C - 40°C. The authors observed that an increase in temperature from 25°C - 40°C reduced the time needed for electrolysis to remove 90% COD from 90 minutes to 15 minutes. These findings are because an increase in temperature favours organic oxidation. Therefore, this behaviour is attributed to an increase in the generation of active chlorine at the anode surface (Körbahti and Artut, 2010).

(i) Reaction temperature

In chemical kinetics and kinetics, temperature plays a fundamental role. The activation energy is used to characterise the change in the temperature reaction rate, and it enables one to equate the intrinsic behaviour of catalysts in an elementary chemical process (Mao and Campbell, 2019). According to Calderón-Cárdenas *et al.* (2020), the experimental versus T^{-1} plots, Therefore, the activation energy (E_a) is a well-known empirical parameter in a chemical reaction that characterises the exponential dependency of the chemical rate coefficient on the temperature (Calderón-cárdenas, Paredes-salazar and Varela, 2020). The dependence of rate constant on temperature over a limited range can usually be represented by an empirical equation (equation 2-25), proposed by Arrhenius as (Arslan, Yazici and Erbil, 2003):

$$k = Ae^{-E_aRT}$$

<div align="right">**Equation 2-25**</div>

Where k is the rate coefficient, A is the frequency factor, R is the gas constant, T is the temperature, and E_a is the activation energy. The equation can be expressed in the logarithmic form, as shown in Equation 2-26:

$$\ln k = \ln A - \frac{E_a}{RT}$$

<div align="right">**Equation 2-26**</div>

Therefore, the free energy change (ΔG) is obtained using the relationship from equation (Eslami, Zare and Namazian, 2012):

$$\ln k = constant - \frac{\Delta G}{RT}$$

<div align="right">**Equation 2-27**</div>

The following equation can express the relationship between ΔG, enthalpy (ΔH) and entropy (ΔS) (Ganesan *et al.*, 2013):

$$\Delta G = \Delta H - T\Delta S$$

<div align="right">**Equation 2-28**</div>

Combining Equation 2-27 and Equation 2-28 results in:

$$\ln k = \frac{\Delta S}{R} - \frac{\Delta H}{RT}$$

<div align="right">**Equation 2-29**</div>

2.8.5. Electrode Material

The electrode material is one of the most critical factors in EO. Ideal material for electrodes that can be used for the degradation of organic pollutants in EO process must be chemical and physical stable; cheap; highly resistant to corrosion and formation of passivation layers and exhibit high catalytic activity and selectivity (Anglada, Urtiaga and Ortiz, 2009).
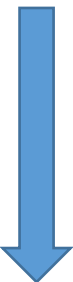
Gargouri *et al.* (2017), states that in order to assess the efficiency of the anode, the following Equation 2-30 must be used:

$$Anode\ efficiency = \frac{COD\ removed\ (kg)}{Time\ (h) \times Current\ (A) \times Surface\ Area\ (m^2)\ of\ Anode}$$

<div align="right">**Equation 2-30**</div>

Electrode material can significantly influence the mechanism and consequently, the products of the anodic reaction. The electrode material is one of the most significant factors in electrochemical studies and applications (Dos Santos *et al.*, 2014). A broad range of electrode materials has been

commonly used, including dimensionally stable anodes (DSA), noble metals, such as platinum, carbon-based anodes, PbO_2 and Boron doped diamond (Yavuz *et al.,* 2010; Ye & Li, 2016). Table 2-10 summarises the oxidation power of different anode materials.

Table 2-10: Oxidation power of various anode materials used in electrochemical mineralisation (EM) process in acid media (Comninellis et al., 2008)

Electrode	Oxidation Potential (V)	Over-potential of O_2 evolution (V)	Adsorption enthalpy of M-OH	Oxidation power of Anode
$RuO_2 – TiO_2$ (DSA – Cl_2)	1.4 – 1.7	0.18	Chermisorption of OH radical	
IrO_2-Ta_2O_5 (DSA – O_2)	1.5 – 1.8	0.25		
Ti/Pt	1.7 – 1.9	0.3		
Ti/PbO_2	1.8 – 2.0	0.5		
Ti/ $SnO_2 – Sb_2O_2$	1.9 – 2.2	0.7		
p –Si/BDD	2.2 – 2.6	1.3	Physisorption of OH radical	

There are some general recommendations to aid in electrode material selection (Anglada, Urtiaga and Ortiz, 2009):

i.   Physical stability
The electrode material must have adequate mechanical strength, must not be prone to erosion by the electrolyte, reactants, or products, and must be resistant to cracking.

ii.   Chemical stability
The electrode substrate must be resistant to degradation, the development of undesirable oxides or hydrides and the deposition of organic film inhibitors under all conditions (potential and temperature) of the electrode.

iii.   Suitable physical form
In order to promote sound electrical connections, and to enable simple installation and replacement on a variety of scales, it must be possible to manufacture the material in the form

needed by the reactor design. Separation of materials, including disengagement of gases or solids, can be considered in the form and design of an electrode.

iv. Rate and product selectivity

The material of the electrode must support the desired reaction, and in certain situations substantial electrocatalytic properties are essential. The material of the electrode must facilitate the desired chemical change while preventing all opposing chemical changes.

v. Electrical conductivity

Throughout the electrode device, including the current feeder, electrode contacts and the whole electrode surface exposed to the electrolyte, the electrical conductivity must be relatively high. It is only in this manner that a uniform current and potential distribution can be achieved and voltage losses leading to energy inefficiencies can be avoided.

vi. Cost/lifetime

For an appropriate initial investment, a continuous and reproducible output, including a lifespan which is likely to stretch over many years, must be obtained. It is important to note that choosing of working and counter electrodes should not be made separately because the chemistry affects the structure of the solution in the cell. Indeed, within the cell and process design context, the choice of electrode material and its shape must be an integrated decision.

2.9. Why Ti/IrO$_2$ – Ta$_2$O$_5$ electrode?

Electrode material can significantly influence the mechanism and consequently, the products of the anodic reaction. The electrode material is one of the most significant parameters in the electrochemical studies and applications (Dos Santos *et al.*, 2014b). In the removal of organic pollutants in wastewater treatment, the ideal electrode material needs to consist of the following characteristics: chemical and physical stability, high resistance to corrosion, low cost and must exhibit high catalytic activity (Anglada, Urtiaga and Ortiz, 2009). Iron, steel and graphite and lead-based electrodes are preferred due to their low cost of fabrication, and they are readily available (Méndez *et al.*, 2012). However, their utilisation is restricted by their rapid loss of activity (graphite), the release of toxins to the environment (lead-based) and their poor stability (Da Costa *et al.*, 2016). Therefore, this compelled researchers to investigate alternative material, and they found a replacement with dimensional stable anodes (DSA). Compared with traditional electrodes, DSAs exhibit both high corrosion resistance and electrochemical activity for oxygen evolution (Yan and Meng, 2011) .

Ti/IrO$_2$ – Ta$_2$O$_5$ is one type of DSA electrodes that is effective in promoting hypochlorite mediated chemistry in the presence of chloride. It is an active anode that mostly depends on the higher oxide mechanism. Ti/IrO$_2$ – Ta$_2$O$_5$ is an essential catalyst for the industry because it is widely used for Cl$_2$ and O$_2$ production. Excellent current efficiency, high oxygen evolution overpotential and high availability make it more attractive (Pérez-Corona *et al.*, 2013).

Da Silva *et al.* (2013) studied the effect of using Ti/IrO$_2$ – Ta$_2$O$_5$ for petrochemical wastewater. Ti/IrO$_2$ – Ta$_2$O$_5$ is effective in promoting hypochlorite mediated chemistry in the presence of chloride. It is an active anode that mostly depends on the higher oxide mechanism. Ti/IrO$_2$ – Ta$_2$O$_5$ is an essential catalyst for the industry because it is widely used for Cl$_2$ and O$_2$ production. Excellent current efficiency, high oxygen evolution overpotential and high availability make it more attractive. Table 2-11 shows a comparative study of different electrodes.

Table 2-11: Comparison of electrodes performance in Electro-oxidation (Sillanpaa and Shestakova, 2017)

Electrode Material	Advantages	Drawbacks
Noble Metal electrodes (Pt, Au)	High stability in a wide range of potentials and pH; Excellent repeatability properties; Intensive use in laboratory scale for new process investigations.	Expensive; Low mineralisation; Low overpotential toward OER; Poor use in industrial wastewater treatment applications.
PbO_2	Cheap; Relatively high overpotential towards OER; Relatively high ability to mineralise organics.	Potential leaching of toxic Pb; It has a lower efficiency in the treatment of industrial wastewater.
Carbon and graphite electrodes	Cheap; Intensive use in laboratory scale for new process investigation	High electrode corrosion rates; Low mineralisation efficiency; Low overpotential toward OER
MMO ($Ti/TiO_2 – RuO_2$, **$Ti/IrO_2 – Ta_2O_5$,** $Ti/TiO_2 – RuO_2 – IrO_2$, $Ti/IrO_2 – RuO_2$, $Ti/SnO_2 – Sb_2O_5$)	High stability; Good Conductivity properties; Acceptable Price; Possibility to regenerate; Catalytic oxide Coating	Sometimes it is difficult to reproduce the quality of the catalyst layer; Potential leaching of toxic compounds such as Sb.
BDD	High overpotential toward OER; High ability to mineralise organics; Excellent conducting properties even at low temperatures; Has high electrochemical stability and corrosion resistance.	Expensive; It has a reduced efficiency in diluted solutions and at increasing current density higher than a limiting current.

2.10. Combination of Electrocoagulation and Electro-oxidation process

As discussed above, the EC and EO processes are applied to various wastewaters; however, they have significant drawbacks such as low performance and high costs. The problem gets extreme because of the tremendous variety of PRW characteristics, which makes one treatment method ineffective (Bhagawan *et al.*, 2014). The EC combined methods have indicated promising exhibitions in which the removal of pollutants from industrial wastewater was enormously improved. EC integrated with the EO process has been considered as one of the new combinations that show synergy and improvement in the removal efficiency (Linares-Hernández *et al.*, 2010).

Juárez *et al.* (2015), treated carwash wastewater by a combined EC and EO process. The combined process was very effective in reducing 100% oils, 99.3% colour, 98.4% turbidity, 96% COD, 93% BOD and 92% methylene blue active substances.

Sharma and Simsek (2019) carried out studies on combined EC and EO process for canola-oil refinery effluent wastewater. The authors found out that the EC process had a low removal efficiency of soluble chemical oxygen demand (sCOD) and dissolved organic compound (DOC), obtaining 75% and 74%, respectively. On the other hand, EC and EO process increased the removal of sCOD and DOC to 99 and 95%, respectively.

2.11. Design of Experiments

2.11.1. Introduction

In many fields of science and industry, experimental design plays an important role. Experimentation is the implementation of experimental unit treatments which is then part of a research process based on one or more response measurements. Therefore, the process and the system's function must be well observed (Czitrom, 1999). For this purpose, an experimenter must plan and design experiments and evaluate the findings in order to achieve an outcome.

Wahid and Nadir (2013), defined the DOE as a method for systematically applying statistical methods to develop the best factors and level settings to optimise a process. DOE can be used for a broad range of experiments, across almost all areas of engineering and science, and even marketing research. In DOE, the use of statistics is relevant but not completely necessary. In particular, by using DOE, we can (Lye, 2005):

- Know the mechanism that we are investigating;
- Screen key variables;
- assess if variables interact;
- Building a predictive mathematical model; and
- If necessary, optimise the response(s).

2.11.2. One-Factor-At-a-Time

At the start of an investigation, there may be several significant factors. It is fair to assume that only a few of them would prove significant, but their identities are not known. Therefore, there is a need for factor screening. For this reason, several screening designs are available, including the one-factor-at-a-time (OFAT) (Abou-Taleb and Galal, 2018).

One factor at a time (OFAT) approach is the most used method and a popular approach in practice. Researchers have historically carried out OFAT experiments by modifying one factor at a time and leaving others unchanged (Delgarm *et al.*, 2018). This factor is varied until it is found in its best setting. At this level, it is then kept constant. Next, the other factor is changed until the optimal setting is identified and at this setting kept constant. The whole procedure is replicated for another factor (Wahid and Nadir, 2013). OFAT is probably the most dominant method used in the industries due to its mathematical simplicity, but overall it may not be the best method.

The OFAT approach was once considered the standardised, systematic and acknowledged method of scientific experimentation (Ahmed *et al.*, 2019). However, it has been proven that this method is inefficient and can potentially be catastrophic. The main pitfalls of this approach are that more runs are needed for the same accuracy in effect estimation; do not predict interactions between the process's operational factors, and they skip optimum factor settings (Frey and Sudarsanam, 2008). Moreover, the OFAT method is time-consuming and costly (Nor *et al.*, 2017). This method of experimentation has become impractical since the discovery of much more successful methods of experimentation based on factorial designs. This group of experimental designs include the two-level factorial, fractional factorial designs and response surface methodology among others. These statistically based methods of experimental design are known as design of experiment (DOE) techniques (Nor *et al.*, 2017).

2.11.3. Factorial Design

Factorial designs are commonly used as experiment plans to investigate the influence of several factors on a process (Bingham *et al.*, 2008). In general factorial designs are usually the most effective approach for this form of experiment (Montgomery, 2013). In a factorial design, the effects on the response or responses of all experimental variables and interaction effects are studied. A factorial design will be composed of 2^k experiments if the combinations of k factors are investigated at two levels (Anderson and Whitcomb, 2016).

The 2^k factorial designs are fundamental in response surface work. They find applications primarily in three areas (Myers, Montgomery and Anderson-Cook, 2016):
- At the start of a response surface analysis, a 2^k design is helpful where **screening experiments** should be performed to classify the significant process or system variables
- A 2^k design is often used to fit the first-order surface response model and to generate the estimation of the factor effect needed to perform the **steepest ascent** process.
- The 2^k design is a simple building block used to create additional surface response designs. For example, if the 2^2 design is increased with axial runs and centre points, the result would be a **central composite design**. Historically, the central composite design is one of the most important designs for fitting second-order response surface models.

2.11.4. Response Surface methodology

Response surface methodology (RSM) is defined as a set of quantitative and statistical methods for the modelling and analysis of problems in which several factors influence a response (Ahmed *et al.*, 2019). RSM has been successfully applied to multiple processes using experimental designs to achieve optimisation, including (Vaez, Zarringhalam Moghaddam and Alijani, 2012). RSM is one of the most widely used experimental designs for optimisation. It is a useful tool since it allows the estimation of the effects of several factors and their interactions on one or more response variables (Bas and Boyaci, 2007). For example, the removal of COD from Baker's yeast wastewater is affected by initial pH (x_1), current density (x_2) and operating time (x_3) (Gengec *et al.*, 2011). The removal efficiency of COD can occur under any condition of treatment x_1, x_2 and x_3. Therefore, initial pH, current density and operating time can vary continuously.

Hence, RSM is designed to enable experiments to predict interactions. Therefore, this gives them an understanding of the design of the response surface they are investigating. This method is also used where basic linear and interaction models are insufficient (Karlsson, 2009). RSM usually contains three steps: (i) design and experiments; (ii) response surface modelling through regression; and (iii) optimisation (Asghar, Abdul Raman and Daud, 2014). In order to implement this method correctly, the steps that must be taken are shown in Figure 2-11. Furthermore, RSM makes it possible to represent independent process parameters in a quantitative form, as shown in Equation 2-31 (Gengec *et al.*, 2012):

$$y = f(x_1, x_2, x_3, \dots, x_n) \pm \varepsilon \qquad \textbf{Equation 2-31}$$

Where y is the response, f is the response function, ε is the experimental error and x_1, x_2, x_3,…,x_n are the independent variables.
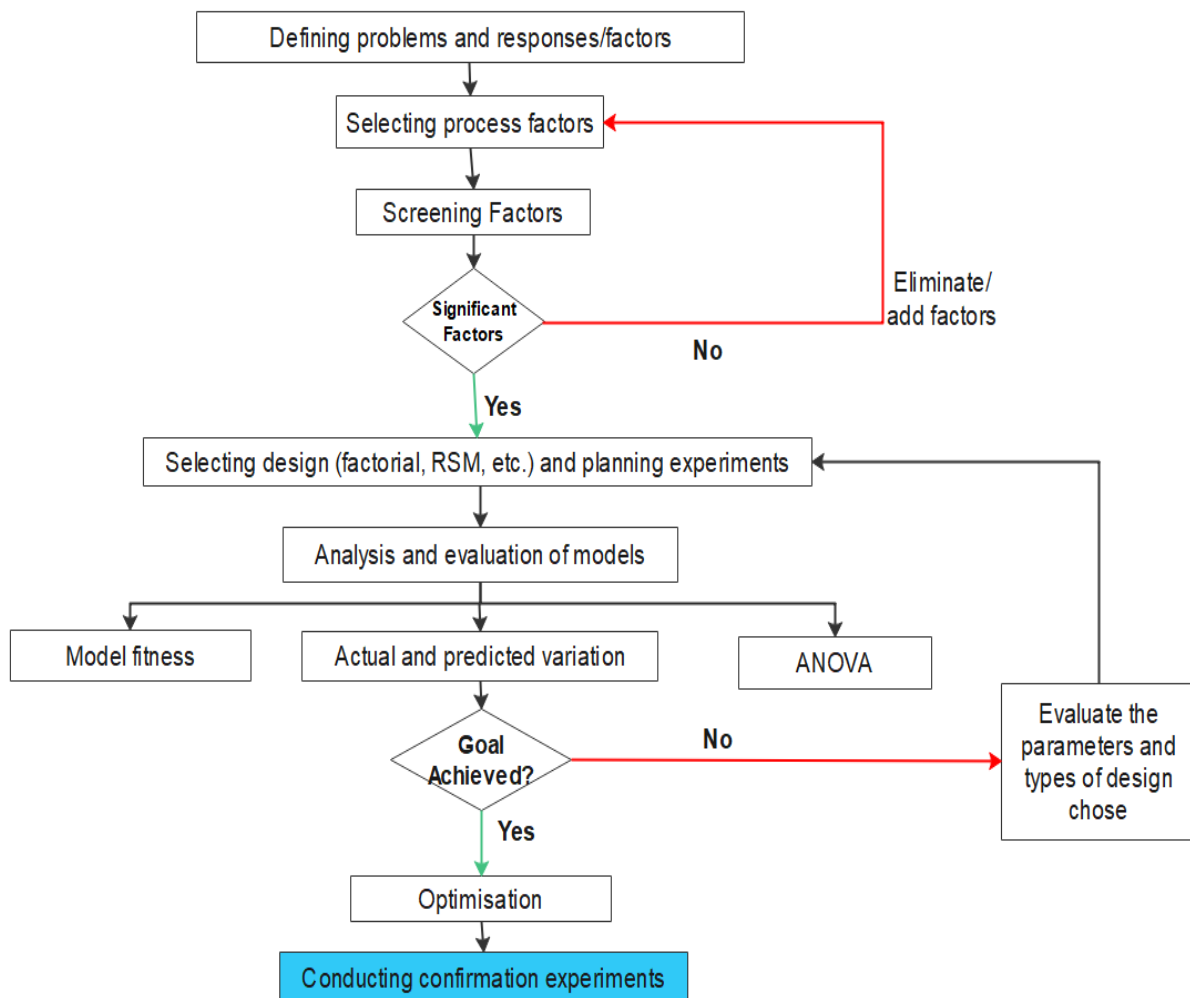
Figure 2-10: Mathematical modelling steps in RSM (Asghar, Abdul Raman and Daud, 2014)

i. Three-level factorial design

This experiment offers more details than a two-level factorial design about a dependent or response factor. A three-level factorial design has a centre point used for each independent variable, along with the high and low values, involving three trials for each independent variable. Because of the third factor level, this is called a three-level factorial design (Hinkelmann and Kempthorne, 2005).

The addition of the third factor raises the number of experiments considerably. For instance, for the two-level factorial design, there are 2^k experiments. In comparison, the three-level factorial design has 3^K experiments. For example, an experiment with four factors will result in $2^4 = 16$ experiments for the two-level factorial design while for the same independent factors using a three-level factorial design has $3^4 = 81$ experiments. In a three-level factorial design, qualitative variables with only two levels can not be used (high/low, on / off, yes / no)

Due to large treatment combinations or experimental points created by three-level factorial designs; alternative response surface designs have been developed to reduce the number of experiments needed while providing similar details. Response surface methodology (RSM) produces models that are used in one or two dimensions to plot contours, depending on the variables used in the experimental space to characterise the response variable. The experiments in RSM are exceptional cases of factorial design that include centre points in the experimental space plus edge centre points or face centre point. The experimental multilevel points allow fitting the responses to quadratic or cubic equations, providing an efficient model design of the response variable in the experimental space. Models that are more practical than the three-level factorial designs are the Central Composite and Box Behnken designs.

ii. **Central Composite Design (CCD)**

Central composite design (CCD) is an appropriate approach for fitting second-order polynomial equations and has been frequently discussed for optimising several research problems. It is based on a two-level factorial design with the addition of 2k (k is the number of independent variables) points between the axes plus repeat points at the centroid. A CCD has three groups of design points (Montgomery, 2013):

1. two-level factorial or fractional factorial design points (2^k), consisting of possible combinations of +1 and −1 levels of factor;
2. $2k$ axial points fixed axially at a distance say α from the centre to generate quadratic terms;
3. Centre points which represent replicate terms; centre points provide a reasonable and independent estimate of the experimental error.

The number of experiments for the CCD method, given these points, would be (Asghar, Abdul Raman and Daud, 2014):

$$N = k^2 + 2k + n$$
<div align="right">**Equation 2-32**</div>

Where N is the complete number of experiments, k is the number of variables studied, and n is the number of replicates.

iii. **Box Behnken Design**

In specific experimental experiments that require RSM, researchers are prone to require three equally distributed levels. Therefore, the Box-Behnken design (BBD) is a practical choice and an effective alternative to the central composite design (Anderson and Whitcomb, 2016). Box-Behnken design is a particular type of three-level incomplete factorial designs, which allows modelling first and second-order response surfaces. These designs are more efficient and cost-

effective than three-level full factorial designs, particularly for a large number of input factors (Fukuda *et al.*, 2018). But, marginally more effective than the CCD

The number of experiments (N) required for the development of BBD is defined as (Ferreira *et al.*, 2007):

$$N = 2k(k-1) + C_0$$

<div align="right">**Equation 2-33**</div>

Where k is the number of factors, and C_0 is the number of central points.

Another benefit of the BBD is that it does not contain combinations in which all variables are at their peak or lowest values at the same time. These designs are thus useful in preventing experiments carried out under severe conditions, for which harmful effects can occur.

The three-factor BBD is shown in Figure 2-11. The figure indicates that BBD does not contain any points at the extremes of the cubic region created by the two-level factorial. All of the design points are either on a sphere or at the centre of a sphere. This design is desirable when the points on one or more corners of the cube represent variations of factor-level that are prohibitively costly or difficult to examine because of experimental physical constraints.
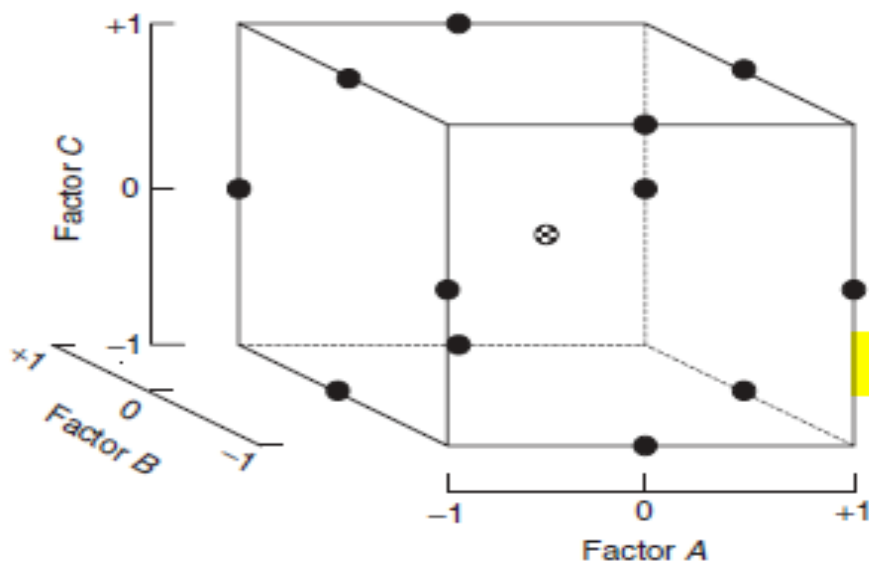
Figure 2-11: Three factor Box–Behnken design (Mason, Gunst and Hess, 2003)

2.11.5. Evaluation of the design model

An essential step in the research is evaluating the model predictions. One of the most common alternatives for evaluating model predictions is the scatter plots of predicted versus observed values (Piñeiro *et al.*, 2008). Another plot that helps to evaluate the model is the normal probability plot of residuals, which is developed in order to verify the assumption of normality. If the residuals are normally distributed, a straight line with some slight scatter will follow the residual plot, suggesting that the model is well fitted (Nair, Makwana and Ahammed, 2014).

i.   Predicted vs actual values plot

Usually, the fitted model must be tested to ensure that it gives an appropriate approximation to the actual system. If the model does not demonstrate good fit, the investigation and optimisation of the fitted response surface is likely to yield poor or misleading results (Thangam, Suresh and Kannan, 2014).

In order to determine the validity of the CCD model for arsenic removal from drinking water; Kobya *et al.* (2013), used the predicted vs actual plot to evaluate the effect of three independent variables (current density, operating time and arsenic concentration. As shown in Figure 2-12, the data points lie close to the diagonal line, and the produced model is efficient for the prediction of arsenic removal. Therefore, this suggests that the response model was adequate for reflecting the expected optimisation.
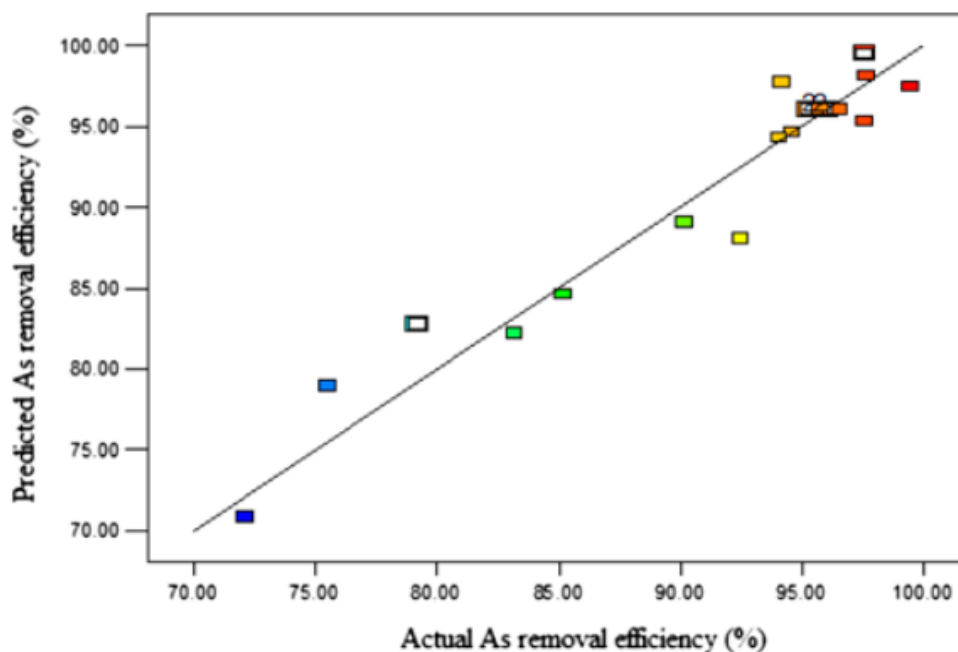
Figure 2-12: Predicted vs actual values for arsenic removal (Kobya et al., 2013)

ii.   Residuals vs Predicted Plot

If the model is right and the assumptions are satisfied, the residuals should be structureless; they should be unrelated to every other factor, including the predicted response, in particular. Figure 2-14 shows the plot of the residuals versus the fitted values. No abnormal structure is evident. Nonconstant variation is a flaw that often appears in this plot (Montgomery, 2013). The variation of the findings also increases as the observation's amplitude increases. If the error or background noise in the experiment were a constant proportion of the observation size, this would be the case (Selvamuthu and Das, 2018).

In cases where the data follows an irregular, distorted distribution, nonconstant variance often exists since the variance appears to be a function of the mean in skewed distributions. The F test is only marginally affected in the balanced fixed effects model if the principle of homogeneity of the variances is violated. However, the issue is more severe in unbalanced compositions or in situations where one deviation is much more significant than the other. In particular, if the factor levels with larger variances also have smaller sample sizes, the real error rate of type I is more significant than predicted (Mason, Gunst and Hess, 2003). Conversely, if the greater sample sizes are often the factor ratios for larger variances, the significance levels are lower than expected. This is an excellent reason to choose identical sample sizes, wherever possible (Hinkelman and Kempthorne, 2005). Unequal error variances will significantly affect inferences on variance components for random-effects models, even though balanced designs are used. In the plot of residuals vs run order, inequality of variance often exists periodically. An outward-opening funnel trend reveals that over time, uncertainty is rising. This could result from the fatigue of the operator/subject, accumulated equipment stress, changes in material properties, or any of several causes (Dehlert, 2010).

Residuals

25.6

12.85

0.1

−12.65

−25.4

551.20   500.15   629.10   668.05   707.00
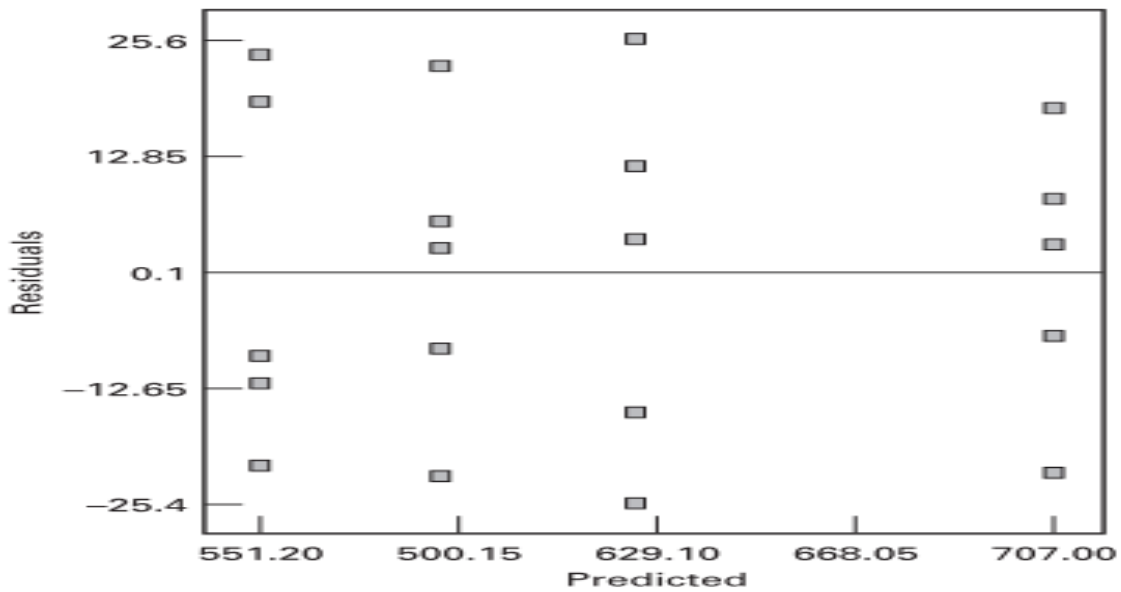
Predicted

Figure 2-13: Residuals vs predicted plot

iii.   3D and contour plot

Figure 2-14 shows the relationship between the yield of the response variable (y) in a chemical phase and the reaction time ($ﺉ_1$) and reaction temperature ($ﺉ_2$) of the two process variables (or independent variables) graphically. Note that for every value of the $ﺉ_1$ and the $ﺉ_2$ there is a corresponding yield y value and we can interpret these response yield values as a surface above the time-temperature plane, as shown in Figure 2-14. It is this graphical viewpoint of the problem area that contributed to the phrase response surface methodology (Goupy and Creighton, 2008). In the two-dimensional time-temperature plane, it is also useful to see the response line, as in Figure 2-15. We look down at the time-temperature plane in this presentation and connect all points that have the same yield to create constant response contour lines. A contour plot is called this type of display (Mason, Gunst and Hess, 2003).

Myers, Montgomery and Anderson-Cook (2016), noted that yield is maximised in the vicinity of time by observing the plot $ﺉ_1 = 4$ hours and $ﺉ_2 = 525°C$. In most practical situations, unfortunately, the actual response function in Figure 2-15 remains unknown.
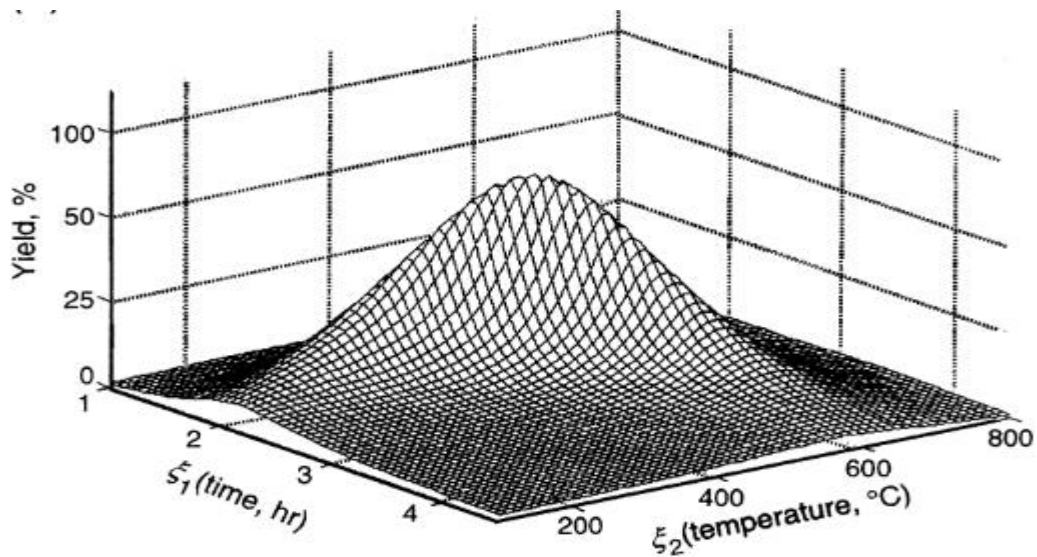
Figure 2-14: A theoretical response surface showing the relationship between the yield of a chemical process and the process variables reaction time (ξ_1) and reaction temperature (ξ_2) (Myers, Montgomery and Anderson-Cook, 2016).
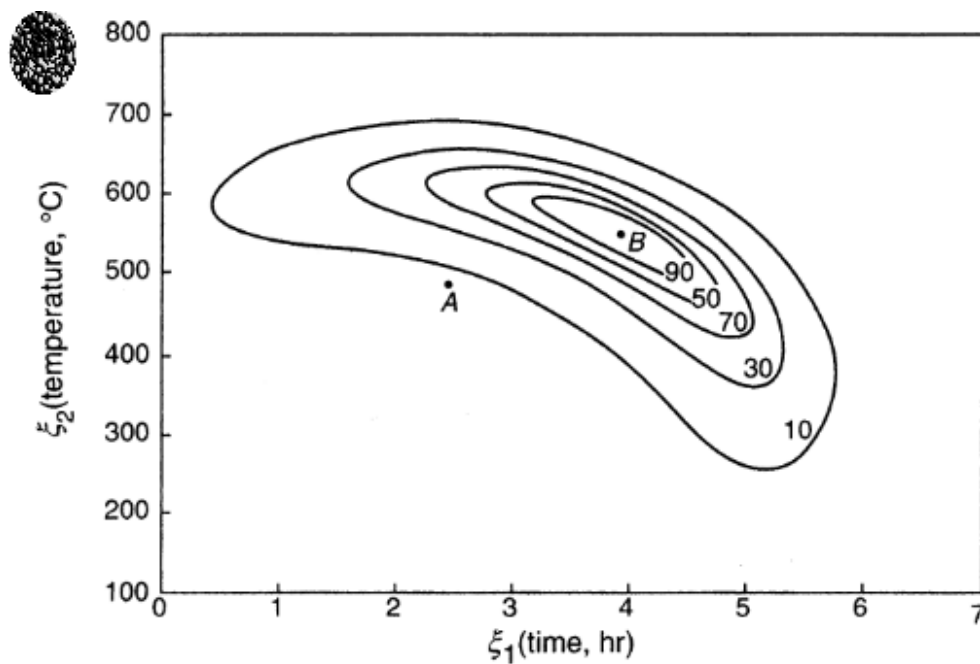
Figure 2-15: A contour plot of the theoretical response surface (Myers, Montgomery and Anderson-Cook, 2016).

The area of the response surface methodology consists of experimental techniques to investigate the process space or independent variables (here the variables ξ_1 and ξ_2), statistical modelling to develop a significant estimated relationship between the variables of yield and process, and methods of optimisation to find the levels or values of the variables of the process ξ_1 and the ξ_2 that produces favourable response values

CHAPTER 3

Research Methodology

Chapter 3: Research Methodology

3.1. Introduction

In this chapter, the details are given regarding the use of equipment and materials as well as experimental procedures followed during experimental runs conducted. Description of instruments used is also included.

3.2. Research Design

During this research, a quantitative experimental approach was used. This study consists of two parts. The first entails the investigation of electrocoagulation, and the second the electrochemical oxidation of petroleum refinery wastewater. The third combines the previous two processes into one integrated treatment process to evaluate Phenol, colour COD, FOG and BTEX removal.

3.2.1. Electrocoagulation

The EC process aimed to effectively reduce the organic pollutants from PRW before the EO process. A laboratory-scale EC reactor was used to treat PRW. A schematic diagram and photo of the EC system are shown in Figure 3.1 and Photograph 3.1, respectively. The EC system consisted of a 4L rectangular shape plexiglass reactor, magnetic stirrer hot plate and magnetic stirrer bar and a direct current (DC) power supply. Six rectangular aluminium plate electrodes (Euro Steel) with a dimension of 100 x 100 x 6 mm thickness and a working area of 1344 cm^2 were used in this system as the anode and cathode. The aluminium electrodes were connected in a monopolar configuration and were partially immersed in the reactor. The distance between the two neighbouring electrode plates was maintained throughout the experiment at 3 cm. The aluminium plates were connected to the positive and negative terminals of the power supply, while the cell voltage was reorded to derive the energy consumption. Direct current (DC) from the DC power supply was passed through the solution via the six aluminium plates during the electrolysis run.

The magnetic stirrer hot plate (Freed electric) and magnetic stirrer bar were used to maintain homogeneity within the EC reactor. The agitation was performed at a constant rate of 300 revolutions per minute (rpm). This rate was chosen because the higher tested rotation speed

rates of up to 600 rpm consume more energy than the one at 300 rpm and at the same time does not increase the removal efficiency (Bayar *et al.*, 2014).

The initial pH of the wastewater was adjusted to the desired value of pH by adding either 1M H_2SO_4 and NaOH ranging from 2 to 8. The solution was continuously stirred at 300 rpm to make a uniform mixing. After Acidification the effluent was added in an EC reactor. The electrolysis of the effluent was initiated by setting an electric current by applying the determined current density. The current was adjusted between 1.5 A and 2.5 A before the EC process started. The monopolar Al plate electrodes were used in the EC treatment configuration, and the spacing between each pair of electrodes was 3 cm. Electrodes were put in 3L wastewater and attached to a DC power supply terminal. A process diagram of the combined EC and EO process is shown in Figure 3.3.

Keeping constant the 3L volume of the solution, electrolysis time at 3 hours, the temperature at 25°C and the stirring speed at 300 rpm. Only the studied parameter (pH and current) was varied in order to assess its effect on the removal efficiency and the treatment constant. Each experiment was repeated twice to assess the reproducibility of data. During EC, samples were taken out at different time intervals and filtered by 0.45 µm filters; the filtered sample was then stored in a fridge at 4 °C and used for chemical analysis.
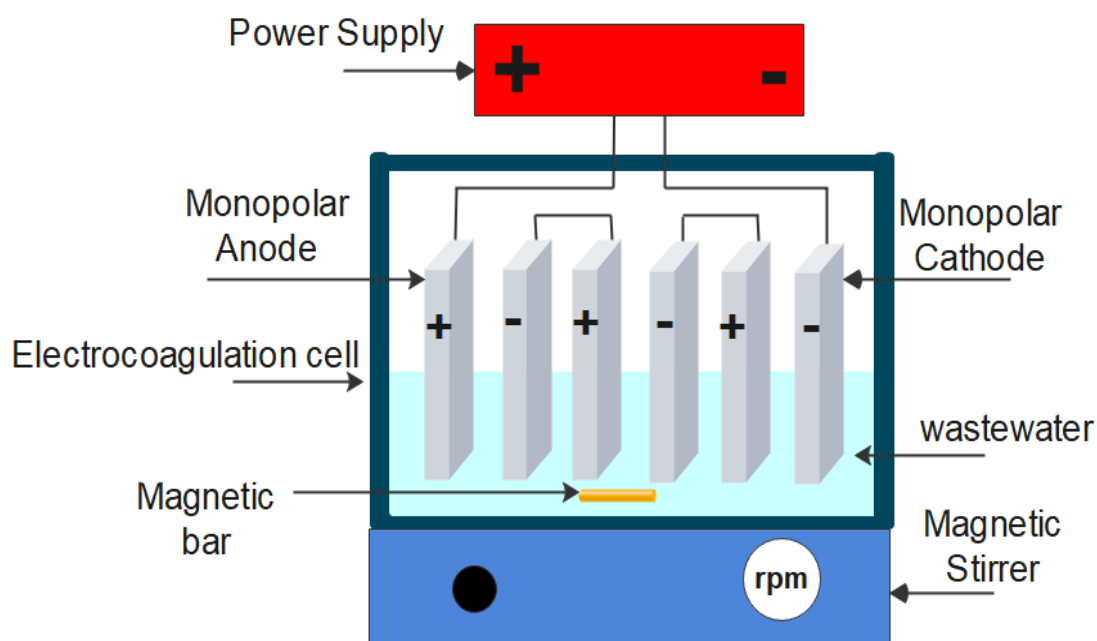
Figure 3-1: Schematic diagram for an EC process

Photograph 3-1: An experimental setup for an EC process

3.2.2. Electrooxidation

A laboratory-scale EO system used in this study is shown in Figure 3.2 and Photograph 3.2. The system consisted of a glass reactor, water bath (FMH instrument), DC power supply and two $Ti/IrO_2 - Ta_2O_5$ electrodes (NMT electrodes). The EO reactor had a total working volume of 1L and was submerged in a water bath (FMH instruments) equipped with an immersion heating unit to keep the temperature at the desired temperature.

The two $Ti/IrO_2 - Ta_2O_5$ electrodes used were immersed in the wastewater and served as anode and cathode with a total effective area of 200 cm^2. The DC power supply was used to supply current to the EO system.

All the EO experiments were conducted at an electrolysis time of 12 hours. In order to study the effect of temperature, the EO reactor was placed in the water bath, and the temperature of the treated wastewater was maintained constant at the desired range of 20 to 60 °C. The parameters used for the study were temperature (20, 40 and 60 °C), current density (5, 7.5 and 10 mA/cm^2) and NaCl concentration as a supporting electrolyte (2, 4 and 6 g/l). Samples were taken after 12 hours, and each run was duplicated.
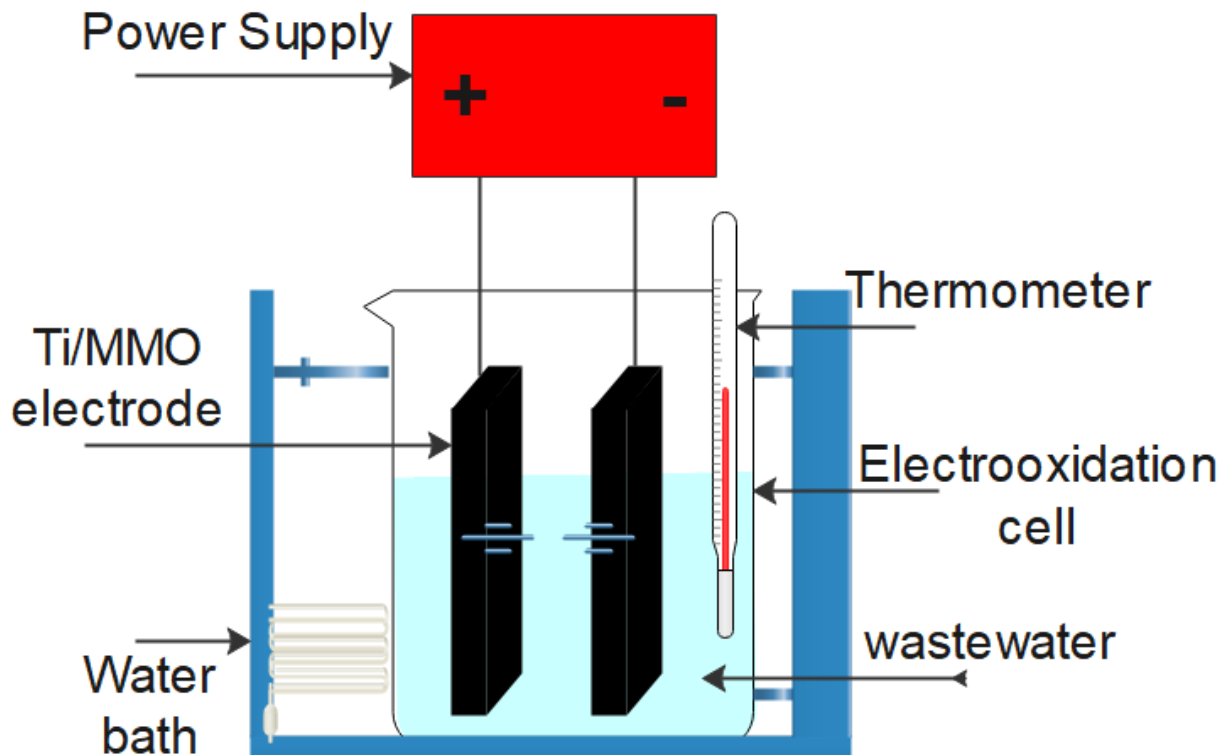
Figure 3-2: A schematic diagram for an EO process
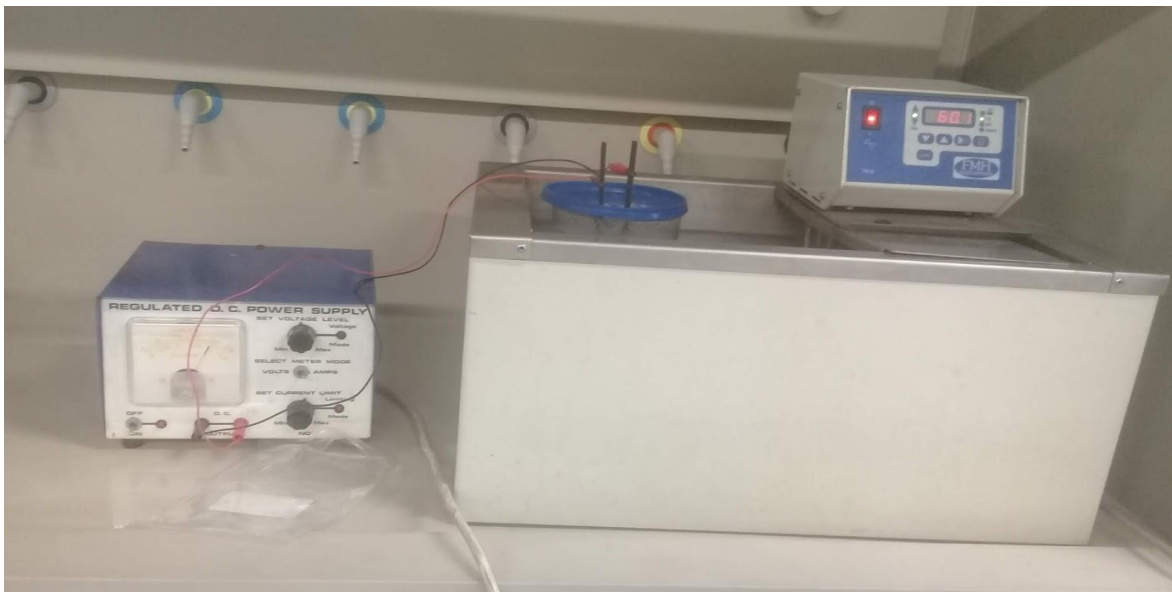
Photograph 3-2: Experimental setup for an EO process

3.2.3. Electrodes Preparation

Prior to each EC run, the aluminium and $Ti/IrO_2 - Ta_2O_5$ electrodes were rubbed with sandpaper and then cleaned with 1M HCl solution for at least 10 minutes to eliminate impurities from the

surface. They were then rinsed out with deionised water and left to dry. At the end of each run, the electrodes were washed thoroughly.
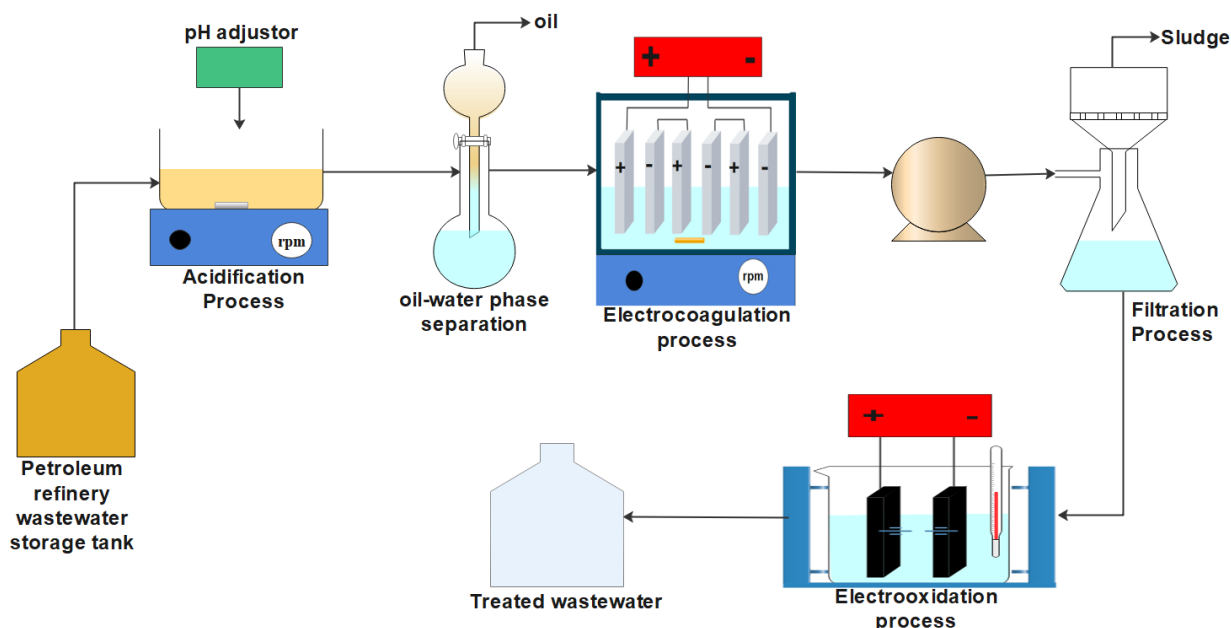
Figure 3-3: Experimental setup for petroleum refinery wastewater

3.3. Chemical Analysis

Conductivity, pH and turbidity were measured using , calibrated conductivity, pH and turbidity meters (Hanna Instruments), respectively. Petroleum refinery wastewater was characterized by a high concentration of Chemical Oxygen Demand (COD), oil & grease (O&G) and phenols. COD was measured by reactor digestion method using Hanna instrument. In brief, the measurement of parameters by Hanna instrument involves the addition of sample solution into a reagent containing vial, which is heated for a specified period, then cooled to room temperature. The concentration of the parameter sought is then measured using a Hanna's COD and multiparameter instrument. The range of the COD vials was 500 - 10000 mg/L, and a proper dilution factor was used to measure concentrations higher than this range. Hanna's COD and multiparameter instrument measured colour and COD concentration. Furthermore, FOG, COD, phenol and BTEX analysis were done off-site at an accredited analytical facility.

The instantaneous current efficiency (ICE) based on COD/phenol value was calculated using Equation 3-1 (Roopashree and Lokesh, 2014).

$$ICE = \frac{[(COD)_0 - (COD)_t]}{8It}FV$$

<div align="right">**Equation 3-1**</div>

Where, COD_0 and COD_t were the solutions COD values at time 0 and t, respectively (mg/l), V the solution volume (L), F the Faraday constant (96,485 C/mole), I was the applied current (A), and 8 the oxygen equivalent mass.

The electrical energy consumption (EEC) per unit volume of wastewater treated (kWh/m^3) was calculated from the following Equation 3-2 (Da Costa *et al.*, 2016).

$$EEC = \frac{\Delta E_c It}{1000\ V}$$

<div align="right">**Equation 3-2**</div>

Where ΔE_C is the average cell voltage.

3.4. Electrooxidation factorial trial

The experimental design of the EO process was carried out using the Box-Behnken Design (BBD) methodology. The BBD methodology was commonly used for the response surface methodology and is one of the most efficient designs, applicable (Ferreira *et al.*, 2007). In this study, NaCl concentration, temperature and current density were the variables used for optimisation. Design expert software version 10.0 (Stat-Ease Inc, Minneapolis, USA) was used to generate 16 experimental runs. The factors range and levels are presented in Tables 3-1.

Figure 3-4: Box Behnken design for the EO Process

Variables	Factor ranges and levels		
	-1	**0**	**1**
NaCl Concentration (g/l)	2	4	6
Temperature (°C)	20	40	60
Current Density (mA/cm^2)	5	7.5	10

A model that was determined to be an appropriate representation of the pollutant removal from the EO process is in the form highlighted in Equation 3.3.

$$y = \beta_0 + \sum \beta_i x_i + \sum \beta_{ii} x_i{}^2 + \sum \beta_{ij} x_i x_{jj}$$

<div align="right">**Equation 3-3**</div>

3.5. Research Apparatus

The following apparatus and equipment were used during the experiments to collect data and measure the removal of COD, FOG and BTEX from petroleum wastewater during acidification, electrocoagulation and electrooxidation processes.

3.5.1. Glassware

- 2-Litre bottles were used to store the wastewater samples after the EC process.
- Buchner Flask and funnel used to filter the wastewater after the EC process.
- 1-litre beakers were used as a reactor for the EO process.
- 1-litre bottles were used to store the wastewater sample after the EO process.
- The 6 litres round bottom flask was used for acidification.

3.5.2. Equipment

- Freed Electric magnetic heater/ stirrer was used for stirring at a constant rpm during acidification and the EC process. During the EO process, it was used as a heater to heat the wastewater to the desired temperature prior to the treatment.

Photograph 3-3: Magnetic heater/stirrer

- Hach pH meter was used to test the pH and the temperature of the wastewater

Photograph 3-4: benchtop pH meter

- FMH Water Bath bath was equipped with an immersion heating unit to keep the temperature at the desired temperature.

Photograph 3-5: Water bath

- A turbidity meter was used to measure the turbidity of the wastewater.

Photograph 3-6: Turbidity meter

- The Crison CM 35+ multimeter was used to test for the electrical conductivity, total dissolved solids and salinity.

Photograph 3-7: Crison CM 35+ multimeter

- HANNA HI83099-0_2 COD and multiparameter bench meter was used to test for colour and COD

Photograph 3-8: COD and multiparameter bench meter

- COD photometer was used to heat up the COD reagents to 150 °C for 2 hours.

Photograph 3-9: Hanna photometer

3.5.3. Materials

High-grade chemicals and reagents were used for this research. Sodium chloride (NaCl), sulphuric acid (H_2SO_4) and sodium hydroxide (NaOH) were purchased from Merck and COD. All solutions used in this study were prepared using water from an ultrapure Milli-Q purification system (MQ, Millipore) and for pH adjustment, 1M H_2SO_4 and/or 1M NaOH were used in all experiments.

3.6. Experimental Design

The RSM Box-Behnken design was applied to develop the appropriate experimental conditions. The BBD design indicated the random order of experimental runs to be followed. The kinetic and analytical test confirmed the design suitability when comparing the output and input of the experimental variables. Prediction and verification of the model were shown with the optimization of COD removal.

CHAPTER 4

Results and Discussion

.

Chapter 4: Results and discussion

4.1. Introduction

This chapter presents the results obtained with the removal of pollutants from industrial petroleum refinery wastewater (PRW) using laboratory bench scale integrated EC and EO process. The major pollutants were COD, FOG, Phenol and BTEX. The pollutant levels before and after degradation were used to evaluate how efficient the integrated process was. All experimental runs were conducted in randomized order and were repeated twice.

4.2. Petroleum Refinery Wastewater Characteristics

The industrial petroleum refinery wastewater used during this study was tested for specific characteristics. The average values are shown in Table 4.1. The COD, FOG and BTEX values are much higher than what is required by the City of Cape Town: Wastewater and Industrial Effluent By-law, 2013.

Table 4-1: Petroleum refinery wastewater characteristics

Parameters	Tested Values	CCT requirement
pH	6.52	5.5 - 12
TDS (mg/l)	7900	4000
Salinity (mg/l)	7480	None
Conductivity (µS/cm)	9670	5000 000
Turbidity (NTU)	514.8	None
Colour (PCU)	6952	
Benzene (µg/l)	1186.8	
Ethylbenzene (µg/l)	26.29	
mp – Xylene (µg/l)	122.4	
o – Xylene (µg/l)	122.5	
Toluene (µg/l)	141.6	
Oil and grease (mg/l)	37	
Phenol (mg/l)	763	
COD (mg/l)	4753	5000

4.3. Electrocoagulation (EC) of Petroleum refinery wastewater (PRW)

4.3.1. Effect of Current

In a batch EC process, the current is a crucial parameter since it is the only parameter that can be directly controlled. Holt, Barton, and Mitchell (2005) suggest that both coagulant dosage and bubble generation rate can be directly determined by current. Therefore, experiments were carried out to quantify the effect of operating current on COD, colour, and phenol when it is varied from 1.5 to 2.5, as shown in figure 4-1 to 4-3. The highest current allowed the highest removal. This observation is attributed to the fact that a high current generates a significant amount of oxidised aluminium, resulting in a higher amount of precipitate for the removal of colloidal particulates. Furthermore, Chen, Chen and Yue (2003) reported that the bubble density increases and decreases with increasing current, thus resulting in the best removal of pollutants and sludge flotation.

Therefore, an increase in current implies an increase in the amount of coagulant (Al^{3+}) generated by the electrochemical dissolution of the aluminium anode. Indeed, the amount of coagulant produced at a fixed time within the EC cell is related to the current flow, using Faraday's law. In the present investigation, a current of around 2.5 and pH 2 was found to be sufficient for better electrolytic flocculation and, consequently, a maximum removal efficiency (67.5% COD, 98.7% phenol, and 88.5% colour) as shown in figure 4-1.
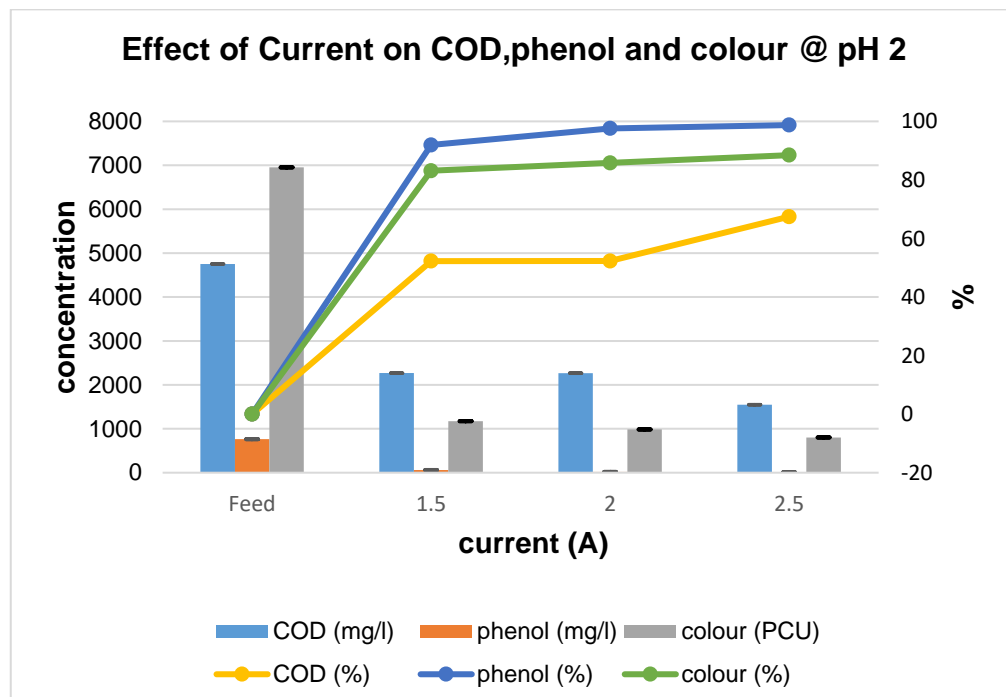
Figure 4-1: Effect of current on COD, phenol and colour @ pH 2
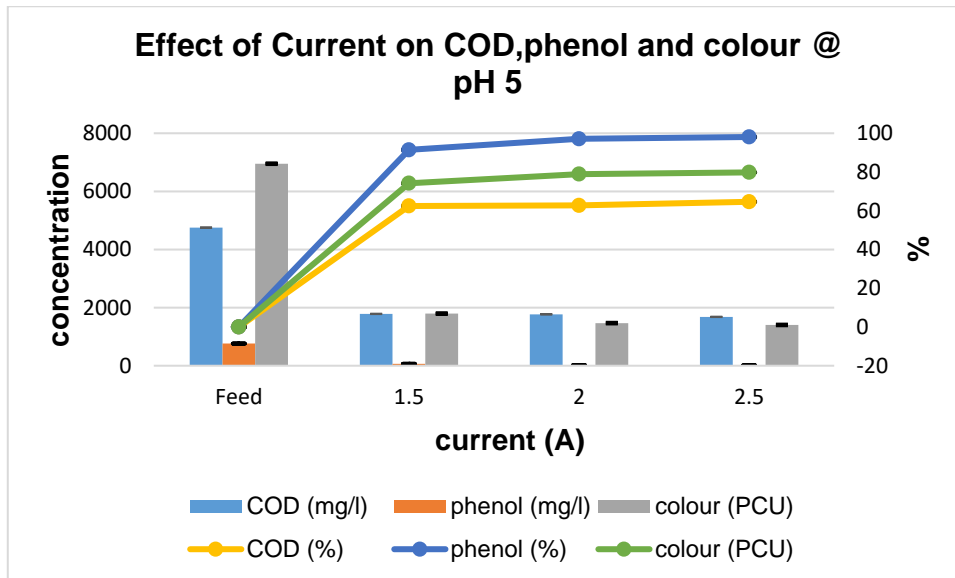
Figure 4-2: Effect of current on COD, phenol and colour @ pH 5
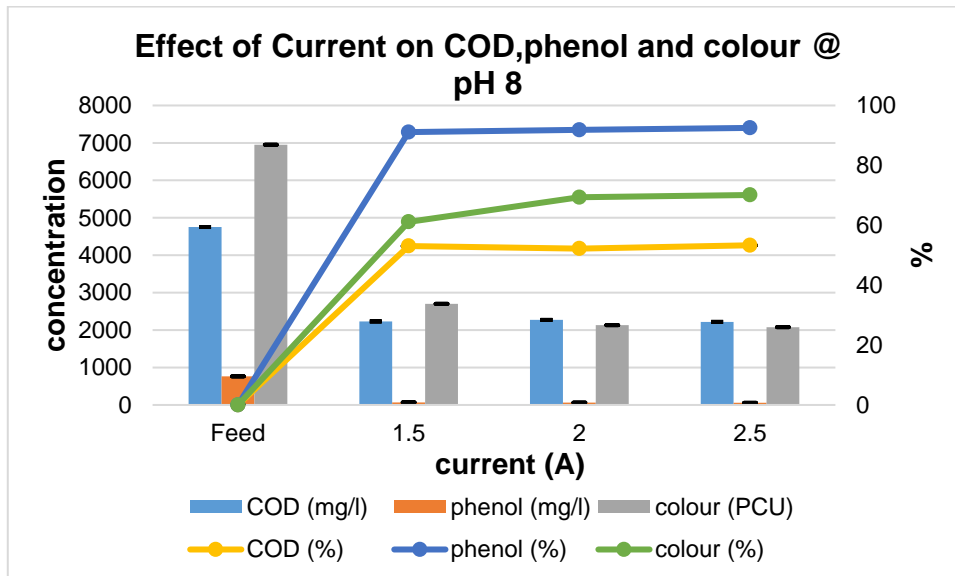
Figure 4-3: Effect of current on COD, phenol and colour @ pH 8

4.3.2. Effect of pH

Figure 4-4, 4-5 and 4-6 represent the removal efficiency of COD, phenol, and colour as a function of pH. The highest removals of COD, phenol and colour have been observed on acidic medium. In comparison, the removal efficiency decreased at pH 8, It can, therefore, be clarified that at pH 8 the aluminium hydroxide flocs are less reactive at this pH and the flocculation is less effective because of the small-sized flocks which cause the formation of a deposit on the anode and leads to an increase of the ohmic resistance of PRW (Miller and Chen, 2005).
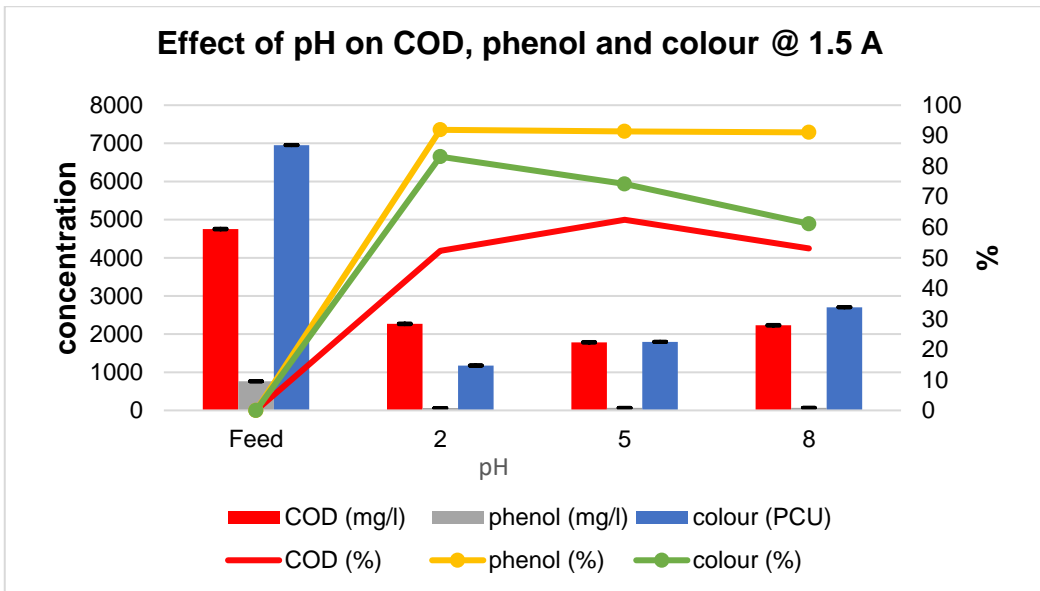
Figure 4-4: Effect of pH on COD, phenol and colour at 1.5A
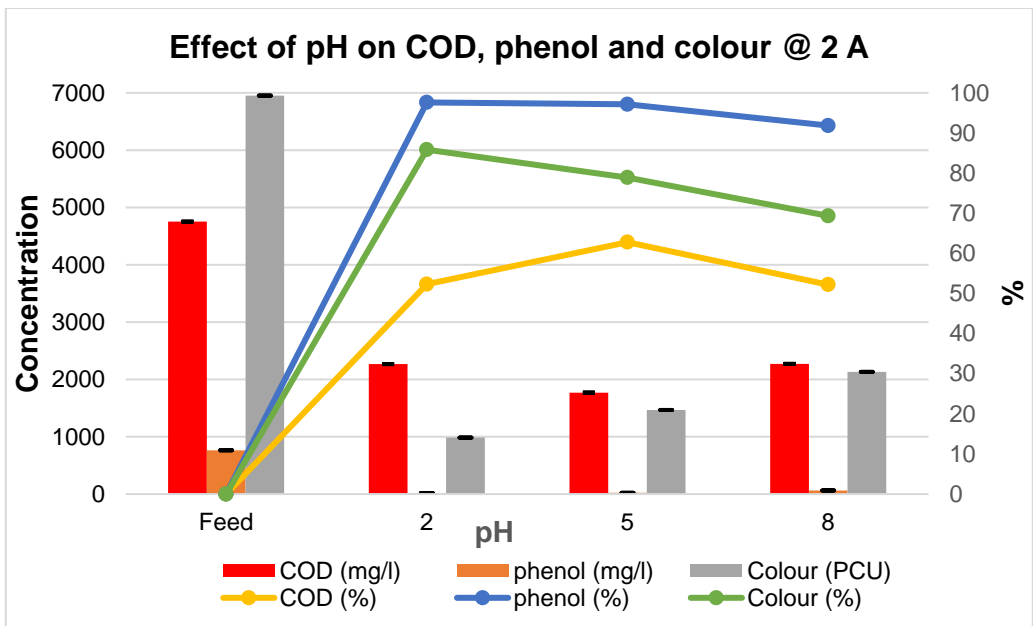
Figure 4-5: Effect of pH on COD, phenol and colour at 2A
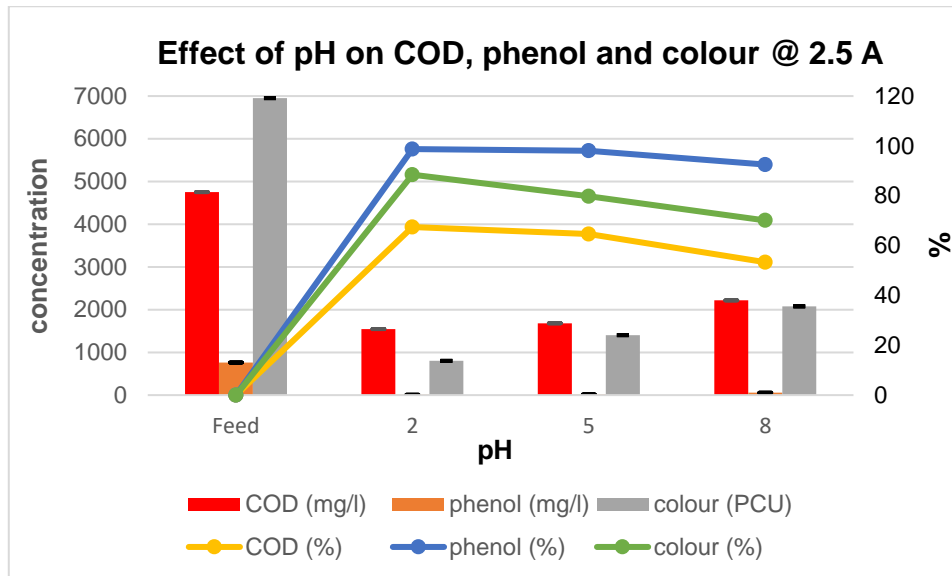
Figure 4-6: Effect of pH on COD, phenol and colour at 2.5A

It has been identified that the initial pH of the PRW is a critical parameter in the determination of the EC process efficiency. The effect of pH on COD, phenol, and colour degradation was varied from 2 to 8, as shown in the 4-4. During the process, the pH of the treated emulsion rises to the basic pH. Vik et al. (1984) attributed the pH rise in the cathode to the hydrogen evolution. Moreover, the rise in pH is due to the release of CO_2 from the wastewater owing to the H_2 bubbles. Also, the chemical dissolution of aluminium will consume hydrogen ions and give rise to the pH increase (Shen *et al.*, 2003).

4.4. Modelling electrocoagulation through adsorption isotherm

Since the pollutant removal is similar to the traditional adsorption, except for the generation of coagulants, the adsorption isotherm model can be extended to describe the experimental isotherm data and to identify the adsorption mechanism. Therefore, Isotherm models with two parameters have been considered to establish the relationship between the amounts of COD, phenol and colour adsorbed onto the aluminium hydroxides and its equilibrium concentration in PRW (Ouaissa *et al.*, 2014b). The removal of COD, phenol and colour was modelled by adsorption isotherm models of Freundlich, Langmuir, Temkin, and Dubinin–Radushkevich (D-R) at a constant pH of 5.

4.4.1. Freundlich adsorption isotherm

Freundlich's linearized model of adsorption isotherm was used to test the sorption data. K_F and n values were determined from the intercepts and slopes of the Freundlich plots and are shown in Table 4-2. According to Ganesan *et al.* (2013), n values between 1 - 10 represent beneficial adsorption, while values falling in the range of 0 and 10 indicate favourable adsorption. The values K_F and n also determine the steepness and curvature of the isotherm. Freundlich equation also offers a sufficient explanation of the adsorption data over a small concentration spectrum, even if it is not based on a theoretical context. K_F and n magnitude indicates a simple pollutant removal from wastewater and a high capacity for adsorption (Igwe and Abia, 2007). The value of n, which is related to the distribution of bonded ions on the adsorbent surface, was calculated to be less than 1 for the adsorption of COD, phenol and colour on the two adsorbent forms, which indicated favourable adsorption.
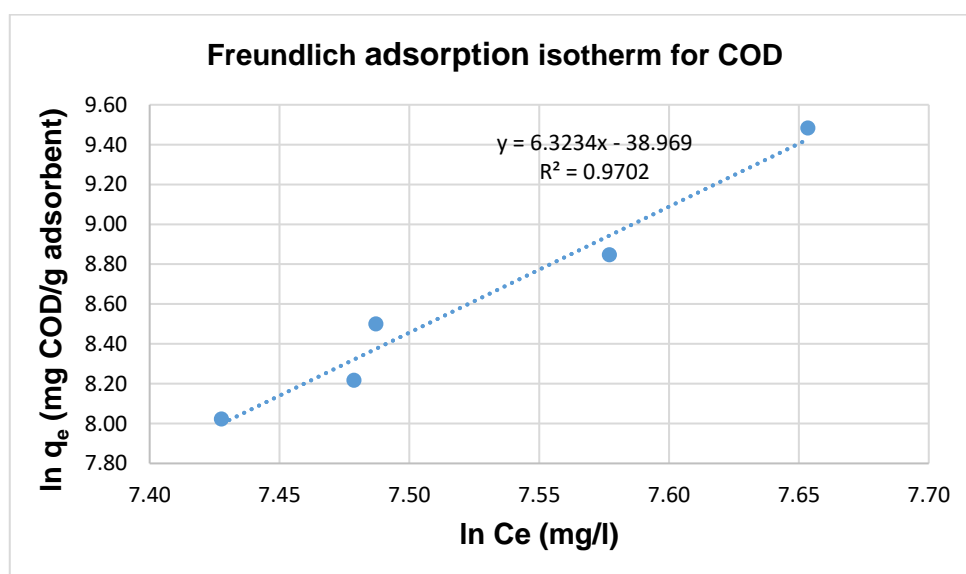
Figure 4-7: Freundlich plot for COD
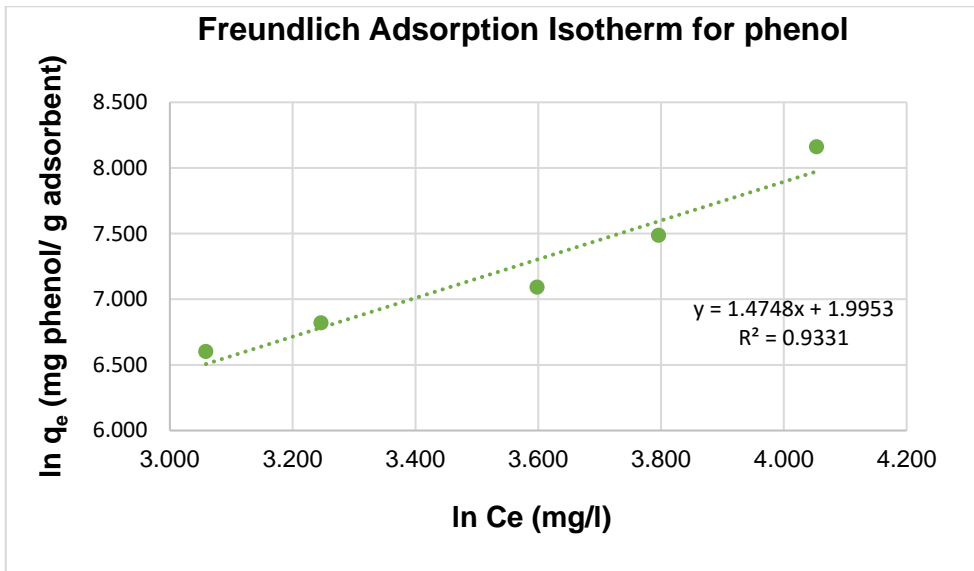
Figure 4-8: Freundlich plot for phenol
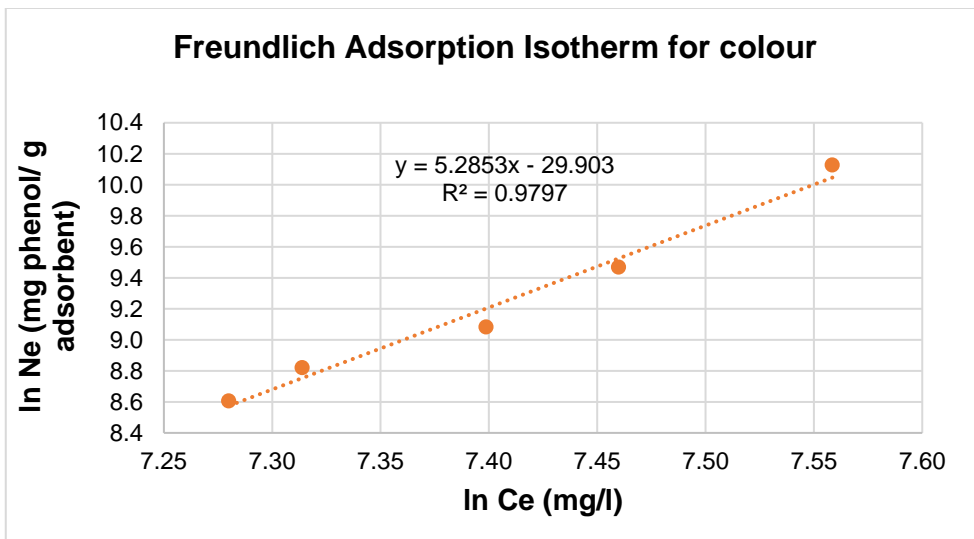
Figure 4-9: Freundlich plot for colour

4.4.2. Langmuir adsorption isotherm

Testing of the Langmuir isotherm from Equation (2-12), the $1/q_e$ plots for COD, phenol and colour adsorption as a function of $1/C_e$ are shown in Figure 4-10 to Figure 4-12. From the figures, linear regression equations for the Langmuir isotherm for the sorption process were obtained. From these regression equations and the linear plots, the values of monolayer capacity (q_{max}) and constant Langmuir (K_L) were calculated and are given in Table 4-2. The plots for COD and colour were found linear with strongly correlated coefficients (> 0.9) suggesting the Langmuir model applicability in these analyses. The correlation coefficient of phenol was found to be 0.716.
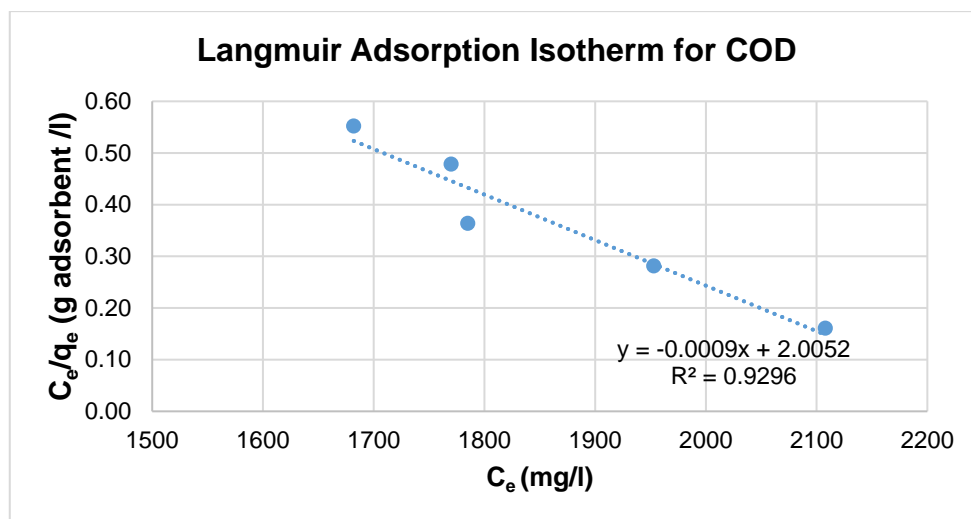
Figure 4-10: Langmuir plot for COD
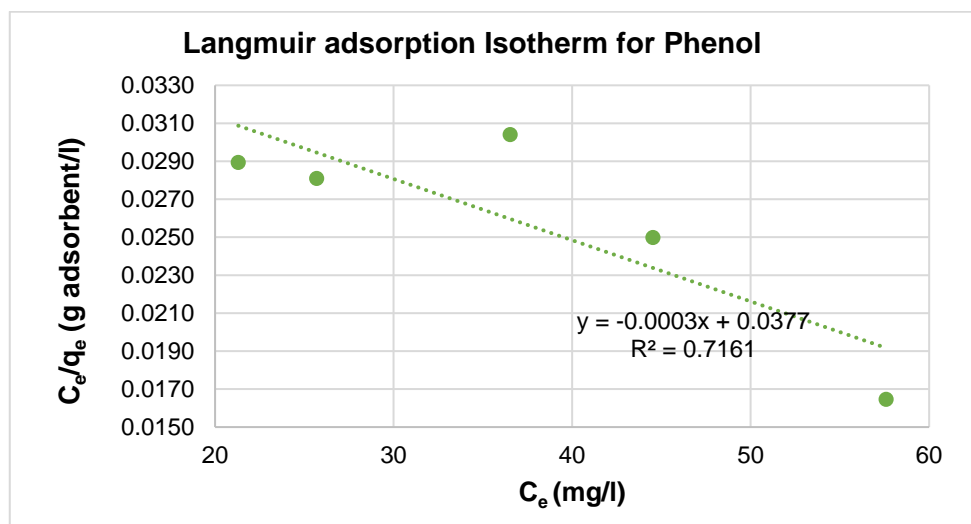
Figure 4-11: Langmuir plot for phenol
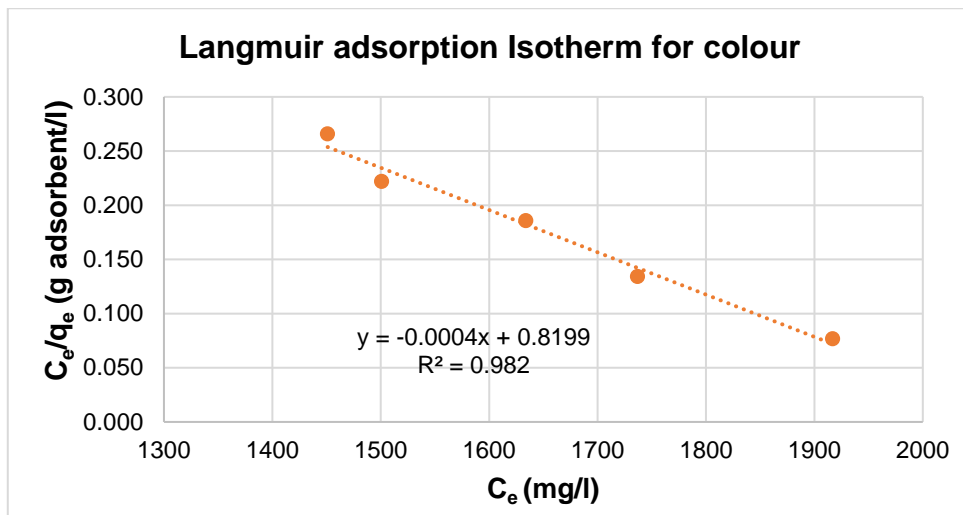
Figure 4-12: Langmuir plot for colour

4.4.3. Temkin adsorption isotherm

A plot of q versus ln C_e allowed for constants K_T and B to be calculated. Figure 4-13 to 4-15 shows that Temkin isotherm model simulations do not correlate satisfactorily with the experimental observation for phenol and colour.
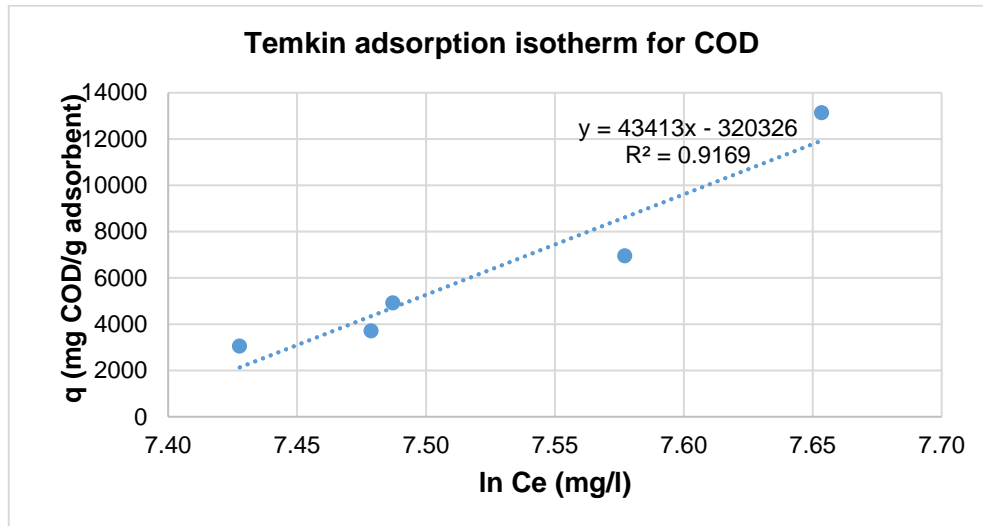
Figure 4-13: Temkin plot for COD
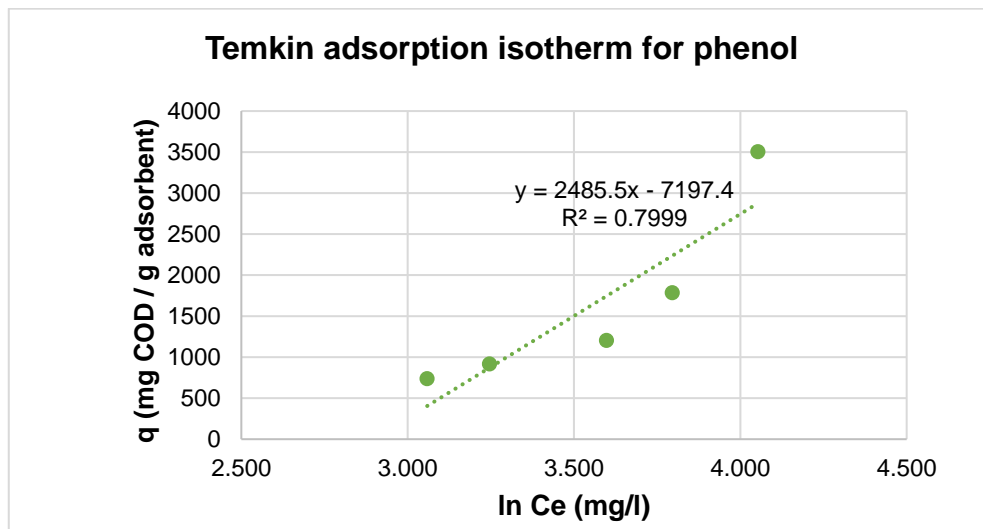
Figure 4-14: Temkin plot for phenol
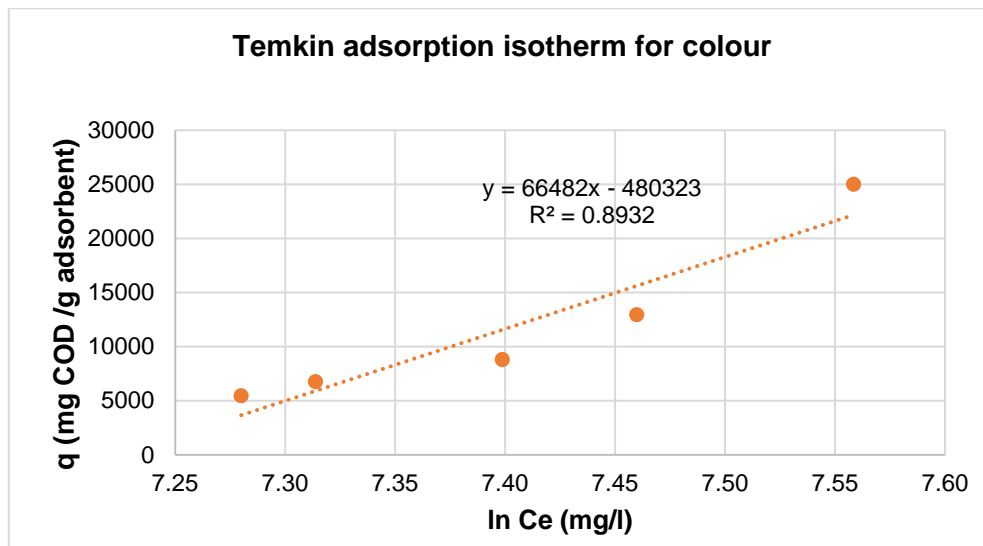
Figure 4-15: Temkin plot for colour

4.4.4. Dubinin-Radushkevich adsorption isotherm

The Dubinin-Radushkevich model, where the regression equation and R^2 values for COD, phenol and colour are shown in Figures 4-16 to 4-18. It was observed from these figures that this isotherm also gave an excellent description of the sorption process over the concentration range investigated. Table 4-1 displays the sorption energy (E_S) and the Dubinin-Radushkevich isotherm constants. The high X_m values show high sorption potential for COD, phenol and colour. The values of E_s often reflect the phase of physisorption. The positive E_S obtained indicated an endothermic sorption process that favours sorption at lower temperatures. This is similar to an earlier study by Horsfall et al. (2004). The Dubinin-Radushkevich isotherm, therefore, gives a perfect fit to the sorption cycle.
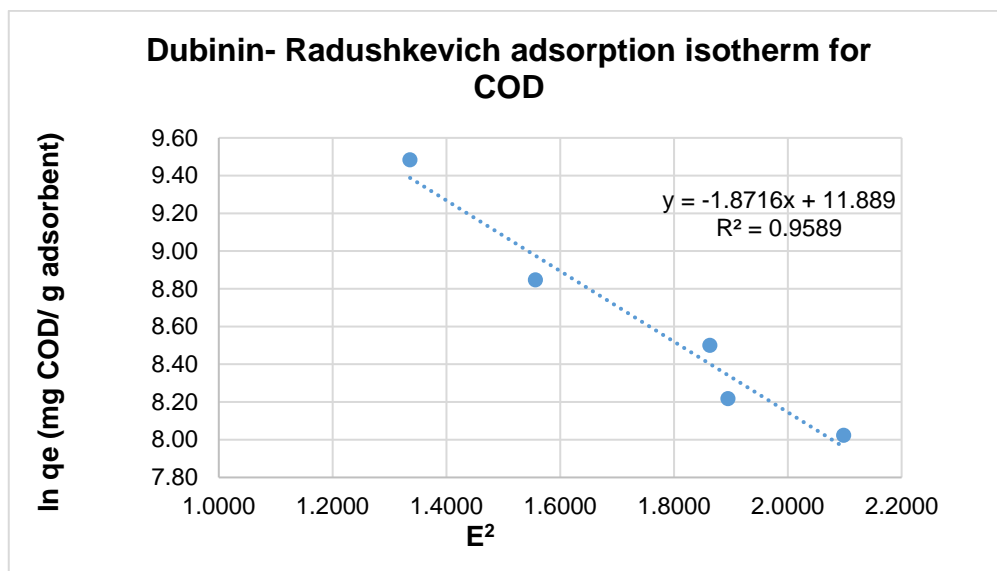
Figure 4-16: D-R isotherm model for COD
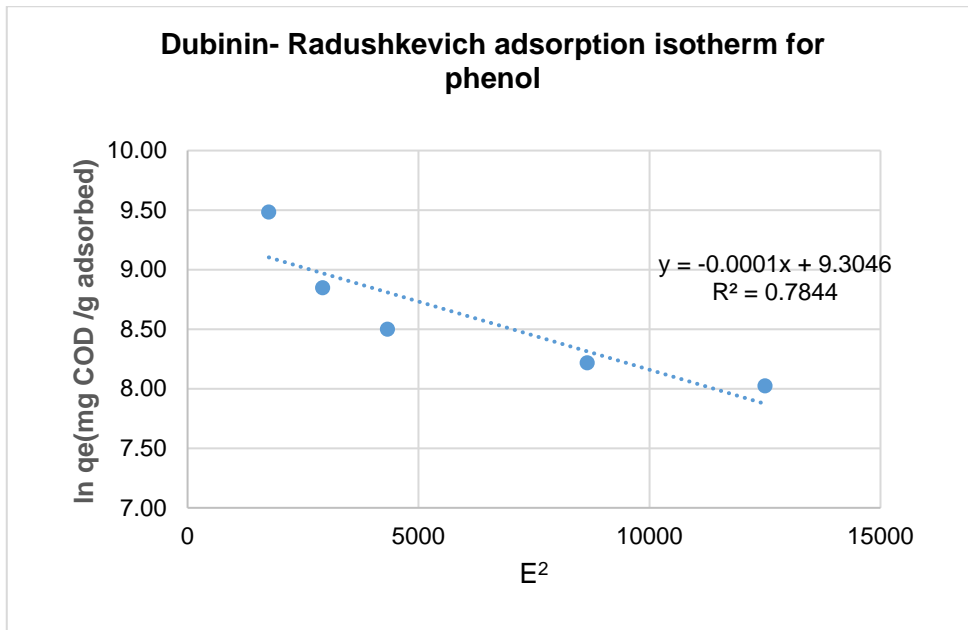
Figure 4-17: D-R isotherm model for phenol
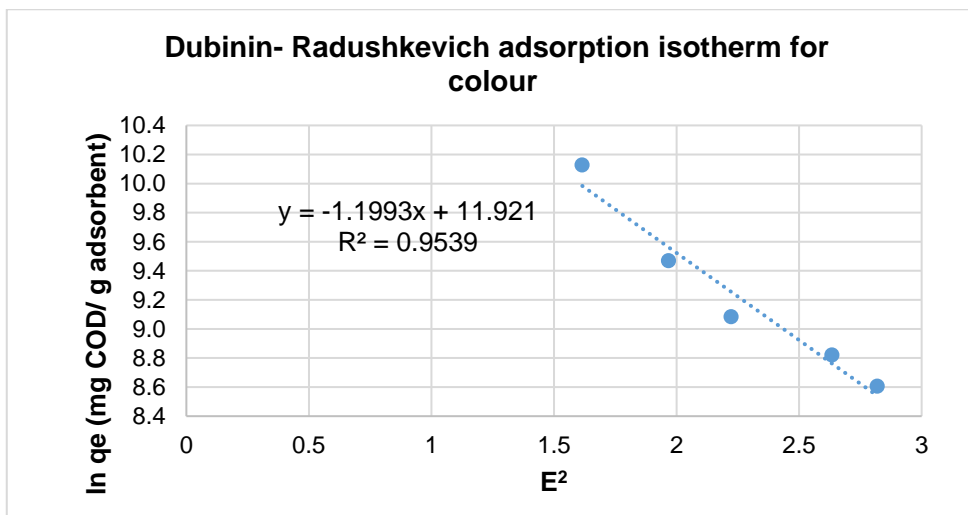
Figure 4-18: D-R isotherm model for colour

4.4.5. Comparisons of the isotherms

With the comparison of all the adsorption isotherms investigated, linear plots were obtained, which revealed the applicability of these isotherms on the ongoing adsorption process. Table 4-1 shows a summary comparison of the Regression Coefficient (R^2) for the four isotherm models. The acceptability and suitability of the isotherm equation to the equilibrium data are based on the correlation coefficients' values, where R^2 calculated at the least square fit statistics from linear regression. The R^2 values for the D-R isotherm are 0.7844, 0.9589 and 0.9539 for phenol, COD and colour, respectively. Over and above, the Freundlich isotherm was the best fit for COD and phenol while Langmuir was the best fit for colour. The values obtained for Temkin isotherms were 0.9169, 0.7999 and 0.8932 for COD, phenol and colour removal, respectively. These values were lower than the results obtained from the Freundlich, Langmuir and D-R isotherms, which suggests that the Temkin isotherm does not characterise well the equilibrium data of the adsorption of COD, phenol and colour onto aluminium electrodes. Therefore, the Temkin isotherm does not fit well with the sorption process. Therefore the results reveal that the adsorption isotherm models fitted the data in the order: Freundlich > D-R > Langmuir > Temkin.

Table 4-2: Isotherm constants for COD, phenol and colour adsorption.

Isotherm models	Parameters	COD	Phenol	Colour
Freundlich	n	0.158	0.68	0.19
	K_F (g^{-1})	1.19E-17	7.4	1.0E-13
	R^2	**0.9702**	**0.9331**	0.9797
Langmuir	q_{max} (mg/g)	-1111	-3333	-2500
	K_L (mg^{-1})	-0.00045	-0.00797	-0.0004879
	R^2	0.9296	0.7161	**0.982**
Temkin	B	43413	2485.5	66482
	K_T (g^{-1})	6.24E-04	0.0553	7.28E-04
	R^2	0.9169	0.7999	0.8932
Dubinin-Radushkevich	β (mg^{-1})	-1.87	-0.0001	-1.20
	X_m (mg/g)	145655.6	10988	150391.9
	E_s (kJ/mol	0.52	70.71	0.65
	R^2	0.9589	0.7844	0.9539

According to Gao *et al.* (2009), the major factors which affect the adsorption of metal species from the wastewater includes (i) pH value, (ii) surface area, (iii) initial concentration, (iv) the speciation of metal ions and (v) surface charge. As the particle size decreases, the surface area typically

increases, and as a result, the saturation capacity per unit mass of the adsorbent increases (Ören and Kaya, 2006). Therefore, this explains why the Freundlich isotherm model matches satisfactorily with the experimental observation.

4.5. Electrooxidation of Petroleum Refinery Wastewater

4.5.1. Effect of Current Density on COD and colour removal

COD and colour degradation was investigated at different current density levels at constant NaCl concentration and temperature conditions. All experimental runs were over a 12 hour electrolysis period a NaCl concentration of 4 g/l and the temperature at 40°C. In Figure 4-19, the current density from 5 to 7.5 mA/cm^2 shows an increase of COD and colour removal from 89.4 % to 91.2% and from 99.4 to 100%, respectively. However, no improvement in the removal of COD can be seen at 10 mA/cm^2.
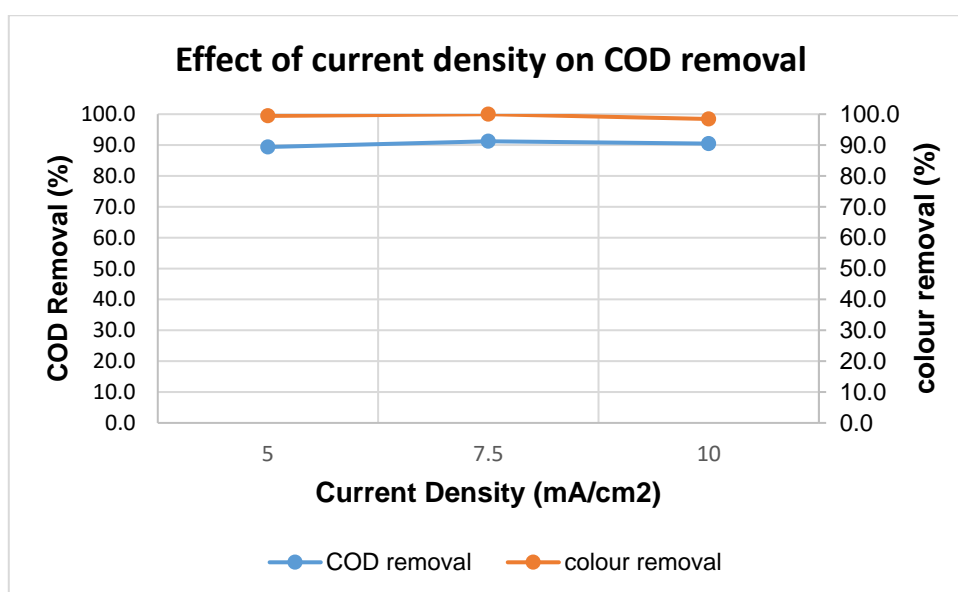
Figure 4-19: Effect of current density on electrooxidation

This observation could be due to the oxidation reaction mechanism that is under mass transfer control at high current density. If the current density is less than 20 mA/cm^2, insufficient organic compounds disperse from the middle solution to the vicinity of the Ti/IrO$_2$ – Ta$_2$O$_5$ anode, where the combination of organic compounds results in the degradation of organic pollutants (Wei *et al.*, 2013). Furthermore, Canizares *et al.* (2005) stated that high concentrations of contaminants in the wastewater support the current treatment efficiency, as the process is regulated by the generation of oxidizing species on the anode surface that interact with pollutants in the vicinity of the anode surface.

4.5.2. Effect of electrolysis time on COD removal

During the electrolysis run time, the degradation of COD at a current density of 7.5 mA/cm^2, NaCl concentration of 4 g/l and temperature of 40 °C is depicted in Figure 4-20. The COD removal percentage was highly dependent on the retention time of the operation. A steady removal percentage increase from 84,3% at the 2-hour to the highest peak of 91,5% at the 12-hour interval. Thereafter a continuous reduction of 2% to a percentage removal of 89,7% after 18 hours.
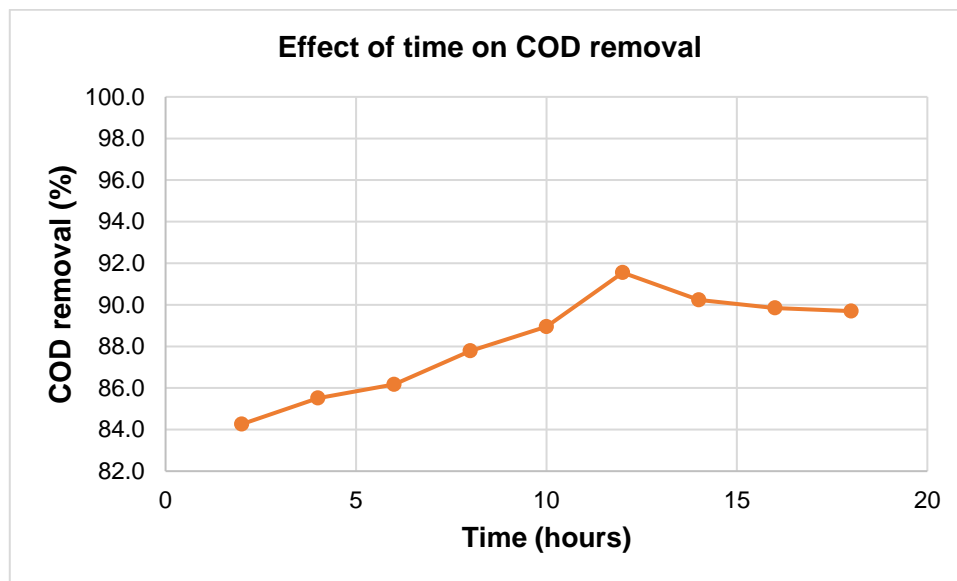
Figure 4-20: effect of time on electrooxidation

The above results clearly indicate that the greater the run time, the greater the degradation efficiency as the oxidation reaction has more time for the conversion of the pollutants. The results obtained from this study follow similar trends as it was also reported by (Nayır and Kara, 2018)

4.5.3. Effect of Temperature on COD removal

The influence of temperature was studied at 20, 40 and 60 °C for PRW treatment at a constant current density of 7.5 mA/cm². Figure 4-21 shows the effect of temperature on COD percentage removal as a function of time; it was observed that temperature greatly impacts the removal of COD because it was notably enhanced when the temperature was increased from 20 to 40 °C. An increase in temperature from 20 to 40 °C reduced the time required to remove COD from 94,6 to 95.5% after 12 hours. This observed behaviour is attributed to the fact that an increase in temperature affects the EO process via hydroxyl radicals (Da Silva *et al.*, 2013).

According to Solano *et al.* (2013), the electrolysis of wastewater produces active chlorine at the anode surface in an aqueous medium containing chloride ions. These potent oxidising agents can also oxidise organic materials quickly through a chemical reaction, the rate of which increases with temperature. In this case, the use of $Ti/IrO_2 - Ta_2O_5$ anode for electrooxidation of PRW enhances the production of chlorine gas, thus resulting in high COD removal at higher temperatures (Martínez-huitle *et al.*, 2012).
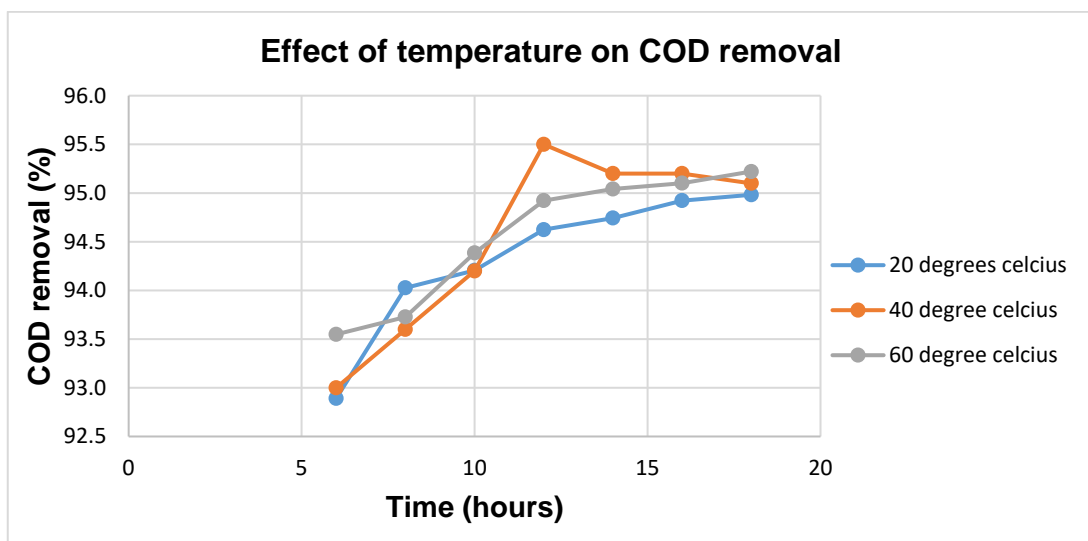
Figure 4-21: Effect of temperature on electrooxidation

From Figure 4-21, it is observed that increasing temperature to 60 °C reduces the removal. Therefore the optimal COD removal percentage can be obtained at a temperature of 40 °C. These findings are similar to the study reported in the literature by (Da Silva *et al.*, 2013)

4.5.4. Effect of electrolyte on COD and colour removal

NaCl was added as an electrolyte into the experimental sample at a constant current density of 7.5 mA/cm^2, as illustrated in Figure 4-22. The effect electrolyte concentrations between 2 and 6 g/l were significantly, visible. As the concentration of electrolytes increased, the removal efficiency of COD and colour increased from 85.7% to 91.2% and from 99.1% to 100%, respectively. The addition of NaCl increases the solution conductivity, thus resulting in lower power consumption. It was evident that the COD percentage removal also decreased proportionately as the concentration of Cl$^-$ ions decreases, which implies that the organic oxidation depends on the active chlorine released during electrolysis. The strong catalytic effect, in the presence of chloride ion (Esfandyari *et al.*, 2015).
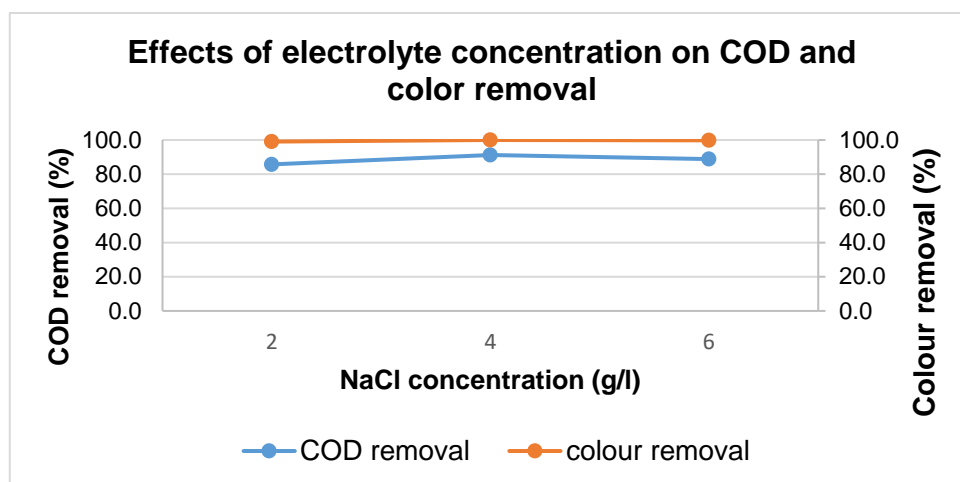
Figure 4-22: the effect of NaCl concentration on COD and colour removal

4.6. kinetics and thermodynamics studies of electrooxidation

4.6.1. Kinetic study

In the EO process, varieties of complex intermediates are formed, making it difficult to perform a detailed kinetic study of each reaction that happens during these processes. However, it is feasible to conduct a comparative kinetic study using the COD value to reflect the organic effluent contaminants' overall content (El-Ghenymy *et al.*, 2014). Therefore, this process's kinetic constants can be obtained through this method to reflect the effluent's mineralisation rate constant. The pseudo-first-order kinetic model was utilised using Equation 4-1 (Maljaei, Arami and Mohammad, 2009):

$$\frac{\ln COD_t}{\ln COD_0} = -kt$$

Equation 4-1

Where COD_0, COD_t, t and k are the initial COD concentration, COD concentration at t, t is the electrolysis time (hours), and k is the first order COD rate constant (hr^{-1}), respectively.

From this analysis, the linear fit between the ln (COD_t/COD_0) and electrolysis time can be approximated as first-order kinetics. The parameters k and R^2 (correlation coefficient) are summarised in Table 4-3, and the plot is presented in Figure 4-23 to 4-25. These data show that the highest k was 0.122 x 10^3 s^{-1} at 60 °C. This observation is similar to the work done by El-Ghenymy *et al.* (2014) on the degradation of the antibiotic sulphanilamide with Pt/carbon-felt and BDD/carbon-felt cells. The rapid increase in k with the temperature rise indicates the high degradation of COD by the hydroxyl radical formed. Ahmadi and Ghanbari, (2016), states that this may be due to the electrochemical conversion/combustion of organics on the oxide anode, MO_x (Ti/IrO$_2$ – Ta$_2$O$_5$) which can occur as follows:

- In the first step, PRW is adsorbed at the anode to produce hydroxyl radicals according to Equation 4-2:

$$MO_x + H_2O \rightarrow MO_x(\bullet OH) + H^+ + e^-$$

Equation 4-2

In the second step, the adsorbed hydroxyl radicals interact with the oxygen already present in the oxide anode:

$$MO_x(\bullet OH) \rightarrow MO_{x+1}(\bullet OH) + H^+ + e^-$$

Equation 4-3
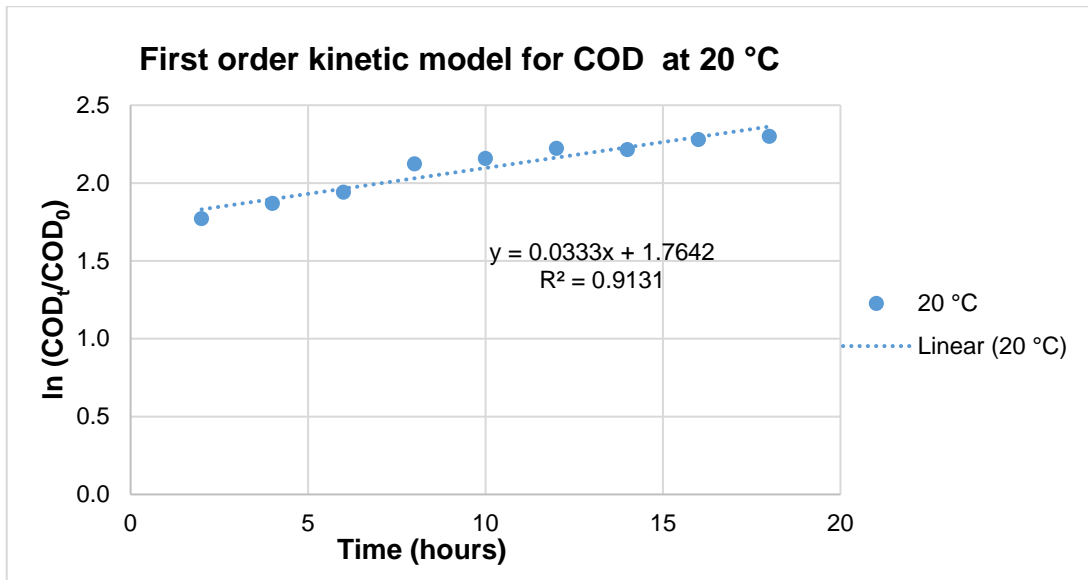
Figure 4-23: Effect of 20 °C on electrochemical degradation of COD at different time intervals
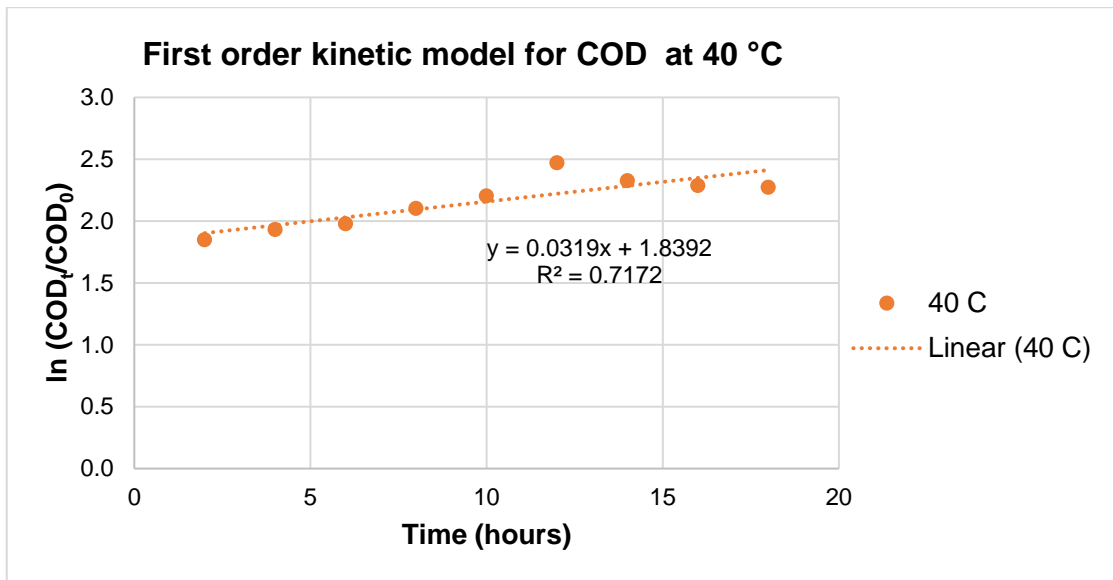
Figure 4-24: Effect of 40 °C on electrochemical degradation of COD at different time intervals

First order kinetic model for COD at 60 °C

y = 0.034x + 1.7928
$R^2 = 0.9099$
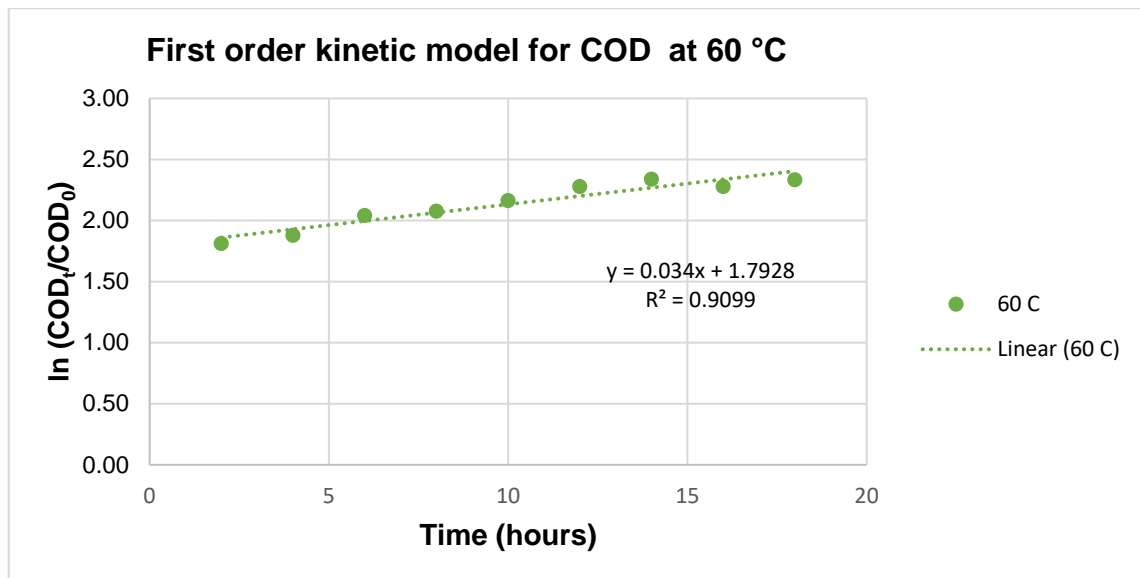
Figure 4-25: Effect of 60 °C on electrochemical degradation of COD at different time intervals

Table 4-3: Pseudo-first-order rate constant and square of the regression coefficient for COD removal under different temperatures

Temp (°C)	k (hr^{-1})	R^2
20	0.0333	0.9131
40	0.0319	0.7172
60	0.034	0.9099

4.6.2. Thermodynamic study

The thermodynamic parameters can be determined at different temperatures in order to understand the effect of temperature on the EO process. The Gibbs' energy COD can be determined by the constant of the first-order rate in Arrhenius form, as shown in Equation 4-5. (Ayawei, Ebelegi and Wankasi, 2017)

$$\Delta G = -RTlnK_c \qquad\qquad \textbf{Equation 4-4}$$

Where ΔG is the Gibbs free energy (kJ/mol), K_c is the equilibrium constant, R is the universal gas constant and T is the temperature (K). Therefore, entropy (ΔS) and enthalpy (ΔH) can be obtained by the following Equation 4-6 (Basu, 2010):

$$\ln K_c = \frac{\Delta S}{R} - \frac{\Delta H}{RT} \qquad\qquad \textbf{Equation 4-5}$$

The Gibbs free energy was obtained from equation 4-3 using the rate constants shown in Figure 4-27 to 4-28 above. The Gibbs free energy indicates the degree of the spontaneity of the EO process, and the higher negative value reflects a more energetically favourable nature (Abdolali *et al.*, 2016).

The values of K_c and ΔG are outlined in the table below. From the table, the positive values of ΔG are found to indicate the unfavourable nature of EO. The enthalpy change (ΔH = 2.765 and -1.6329 kJ/mol) and the entropy change (ΔS = -19.81 and -33.88 kJ/mol) in the van't Hoff linear plots of ln kc versus 1/T were obtained from the slope and intercept (Figure 4-26 and Equation 4-5). The negative value of ΔH indicates that the EO process is exothermic (Ganesan *et al.*, 2013), and the positive value ΔG show that the reaction is endergonic which indicates that Gibb's free energy increases during the EO process.
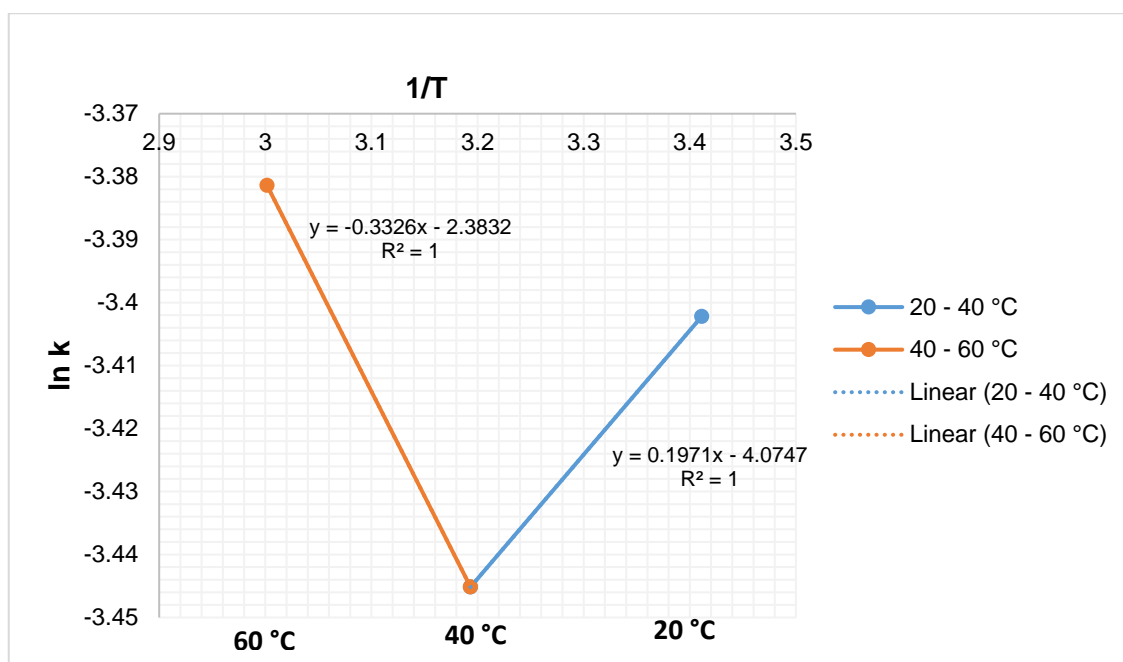
Figure 4-26: Arrhenius plot for the reaction between 30 to 50 °C

The decomposition rates (k) at different temperatures were used to calculate the activation energy (A_e) for the removal of COD using the Arrhenius equation and summarised in Table 4-4. The EO reaction exhibited two different kinetic regions. Two distinct A_e were obtained namely, between 20 – 40 °C region and between 40 – 60 °C. From Figure 4-26, the kinetic plot is linear with a negative slope which gives positive A_e of 2.77 kJ/mol within 40 – 60 °C. The negative A_e of -1.63 kJ/mol, obtained, indicates that the rate of COD degradation decrease with increasing temperature, this is due to the formation of very fine pores on the surface layer of the Ti/IrO$_2$ – Ta$_2$O$_5$ anode (Pang and Low, 2014).

Table 4-4: Thermodynamic parameters for the electrooxidation of COD

Temp (°C)	k (hr⁻¹)	A_e (kJ/mol)	ΔG (kJ/mol)	Δ°H (kJ/mol	Δ°S (kJ/mol)
20	0.0333	-1.63	8.29	2.765	-19.81
40	0.0319		8.97		
60	0.034	2.77	9.37	-1.639	-33.88

4.7. Combined EC-EO process

The combined treatment of PRW consisted of two consecutive treatment steps: (1) electrocoagulation (EC) using aluminium electrodes and (2) electrochemical oxidation (EO) using Ti/IrO$_2$–Ta$_2$O$_5$ anodes. The EC of PRW was investigated at the start in order to determine the operating conditions that would result in the maximum COD, phenol, colour; FOG and BTEX removal. The same methodology was applied to the EO process. The operating parameters of these two individual processes were established and pollutant removal confirmed. Thereafter they were combined as consecutive steps in order to remove COD, phenol, colour; FOG and BTEX from industrial PRW in an integrated process.

During the EC step at a constant electrolysis time of 3 hours, pH of 5 and at an applied current of 2.5 A, a % COD, phenol, colour and FOG removal of 64.6%, 98%, 79.8% and 100%, respectively was achieved. During the second step, EO with electrochemical oxidation process Ti/IrO2–Ta2O5 anodes taking place over 12 hours at a current density of 7.5 mA/cm², NaCl concentration of 4 g/l and temperature of 40 °C removed the % COD, phenol, colour and FOG to 91.3%, 100%, 100% and 100%, respectively. These individual processes and their respective COD, phenol and, colour and the FOG removal efficiencies are shown in Figure 4-27 and Table 4-5.
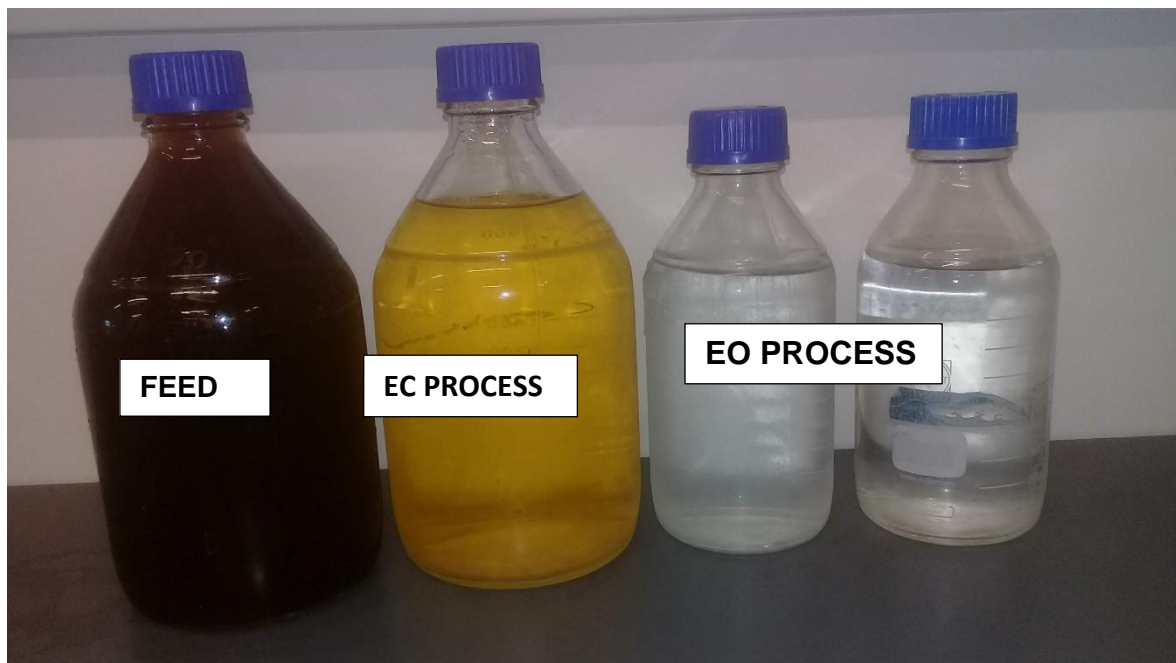
Photograph 4-1: Colour change of PRW

Photograph 4-1 shows the COD, phenol and, colour; the FOG and the BTEX concentration after each integrated step. A clear distinction can be seen between the untreated and treated wastewater when looking at the colour and clarity. There was a significant change in colour and clarity visible to the naked eye between the EC and EO effluents.
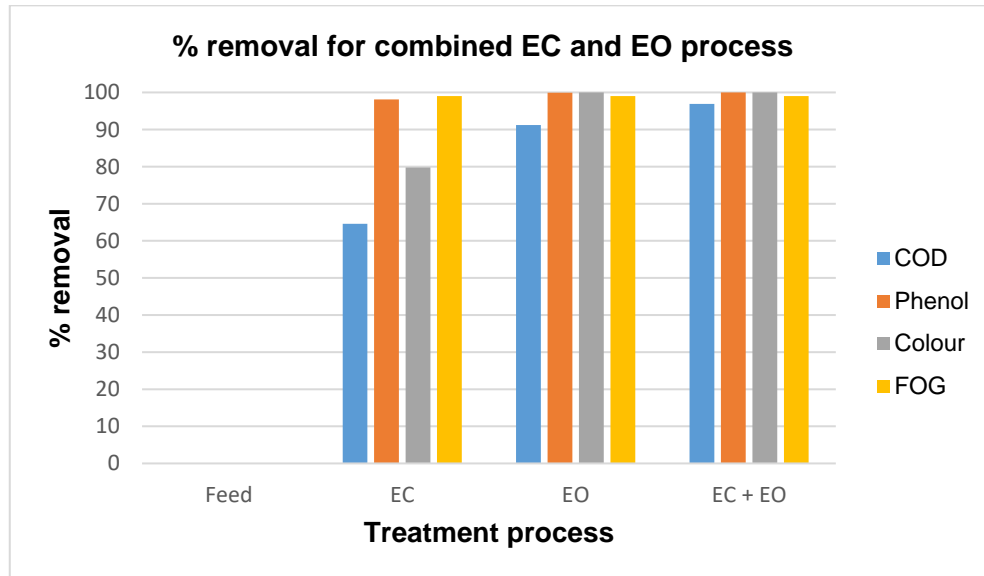
Figure 4-27: removal efficiency for combined EC and EO process

4.7.1. The effect of the combined EC-EO process on the removal of BTEX

Figure 4-28 shows the BTEX removal efficiency by using the EC, EO and combined EC-EO process at the optimal conditions of EC (2.5A applied current and initial pH of 5) and EO (7.5 mA/cm^2, 4 g/l supporting electrolyte, 40 °C temperature and 12 hours electrolysis time). The BTEX removal for the EC process was 99.15%, 94.7%, 100%, 94.76%, and 96.94% for Benzene, toluene, ethylbenzene, mp-xylene and o-xylene, respectively. It was observed that the EC process was able to remove over 90% BTEX, this due to the rather low BTEX initial concentrations. These findings are similar to the ones observed by Tawabini, Plakas and Karabelas (2020). The EO process was able to remove 100 % of BTEX. Overall, the integrated EC-EO system can efficiently remove BTEX
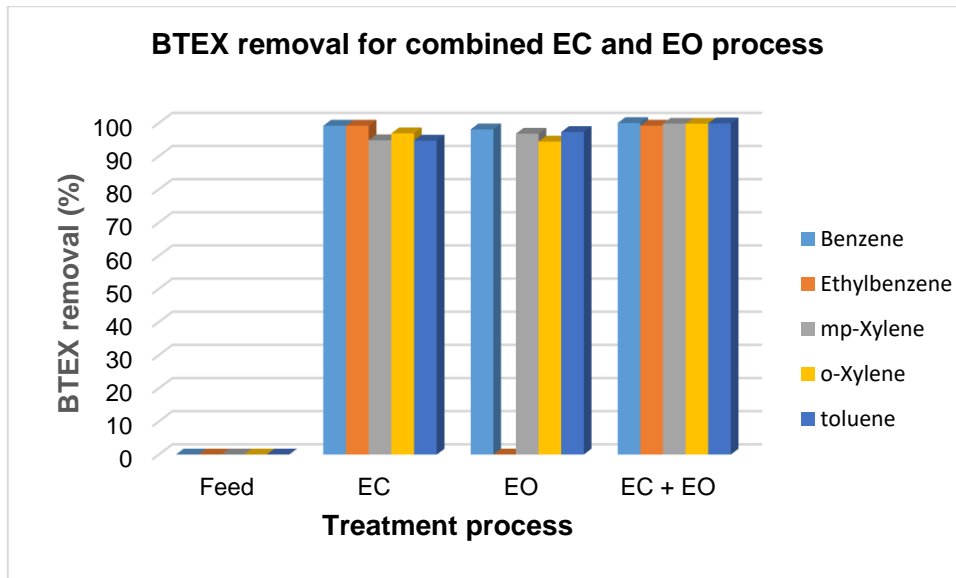
Figure 4-28: BTEX removal efficiency for combined EC and EO process

Table 4-5: Characteristics of the treated PRW

Parameters	Feed	EC	EO	EC + EO
COD (mg/l)	4753	1682	147	147
Phenol (mg/l)	763	14.75	<0.01	<0.01
Colour (mg/l)	6952	1404	0	0
FOG (mg/l)	43.5	<0.5	<0.5	<0.5
Benzene (µg/l)	1186.8	10.05	<0.2	<0.2
Ethylbenzene (µg/l)	26.29	<0.2	<0.2	<0.2
mp-Xylene (µg/l)	122.4	6.37	<0.2	<0.2
o-Xylene (µg/l)	122.5	3.75	<0.2	<0.2
Toluene (µg/l)	141.6	7.45	<0.2	<0.2

4.8. Process Economy

4.8.1. Operating Cost of Electrocoagulation process

One of the most important parameters which significantly affects the practical applicability of any treatment technology is the cost of the applied process (Khandegar and Saroha, 2013). For the EC process, the operational cost involves the material, primarily electrodes and electrical energy, as well as labour, maintenance, dewatering and disposal of sludge, and fixed costs. The following cost items rely mainly on the type of electrode material (Kobya *et al.*, 2013). In this study, energy and electrode material costs were considered as essential cost items in the estimation of operating costs (R/m^3). The operating cost of the EC at lab-scale was calculated by the following Equation 4-6 (Geraldino *et al.*, 2015):

$$\text{Operating cost} = aC_{energy} + bC_{electrode}$$

Equation 4-6

Where, C_{energy} (kWh/m^3), energy and $C_{electrode}$ ($kg\ Al/m^3$), the electrode consumption is obtained experimentally. "a" and "b" were energy consumption price (R 0.9001/kWh) and the electrode material price (R 45 /kg Al), respectively. The prices were provided in the South African Market in January 2020. The energy and electrode consumptions were calculated from Faraday's Law (Equation 4-7 and 4-8) (Kobya *et al.*, 2013).

$$C_{energy} = \frac{UIt_{EC}}{v}$$

Equation 4-7

and

$$C_{electrode} = \frac{It_{EC}M_w}{zFv}$$

Equation 4-8

Where U is cell voltage (V), I is current (A), t_{EC} is operating time (s), and v is PRW volume (m^3), Mw is the molecular mass of aluminium (26.98 g / mol), z is electron number transferred (zAl = 3), and F is a constant (96487 C / mol) of Faraday.

Figure 4-29 shows the effect of current on the operation cost of EC. It is observed that higher current results in higher operating cost within the range studied. Increasing the current from 0.5A to 2.5A increased the operating cost from $R12.95/m^3$ to $R64.77/m^3$. In this figure, most of the costs at the five investigated applied currents were due to the electrode consumption. However, this cost was almost identical for all the applied currents tested.
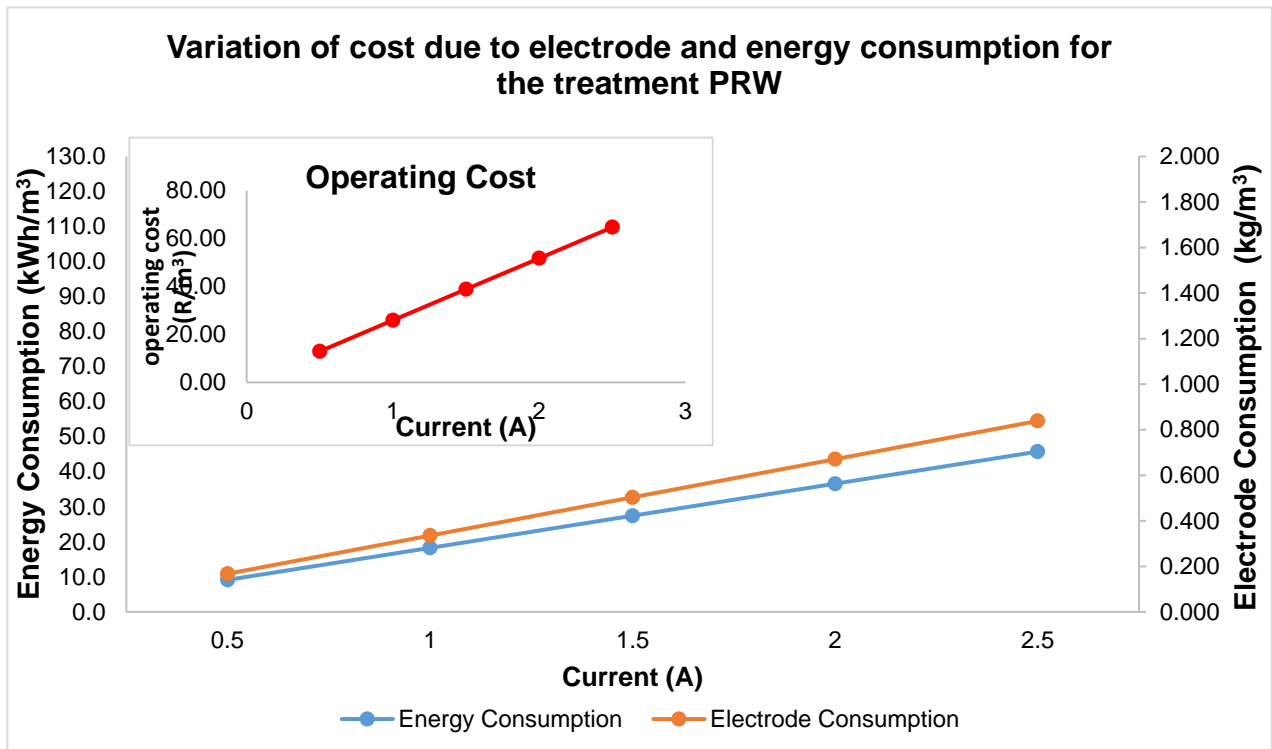
Figure 4-29: Variation of cost due to electrode and energy consumption for the treatment of PRW

The difference in the total operating cost was mainly due to energy consumption. The energy consumption contributed to more than 60% of the total operational cost. Furthermore, it was observed that both energy consumption and operating cost increased exponentially, while the electrode consumption increased linearly.

4.8.2. Operational cost for the EO process

EO was proven to be an efficient process; however, according to Güven *et al.* (2012), EO is an energy-intensive process. Therefore, its practical applicability is related to its operating cost rather than treatment efficiency. In this study, the operating cost of the EO process was calculated as the energy consumption. Figure 4-30 describes the effect of current on operating cost and energy consumption. As shown in this figure, an increase in applied current resulted in an increase in energy consumption and operating cost in the range studied at a constant electrolysis time of 12 hours. The energy consumption and operating cost increased with increasing applied current from 1.9 kWh/m^3 to 9.9 kWh/m^3 and R 1.73 per m^3 to R 8.91 per m^3, respectively. Therefore, the energy consumption at 2.5 A was 5.2 times the value at 1 A, indicating that a higher applied current lead to large amounts of energy consumption. According to Zou *et al.* (2017), as the applied current increases so does the energy consumption. The excess energy consumed is due to side reactions.
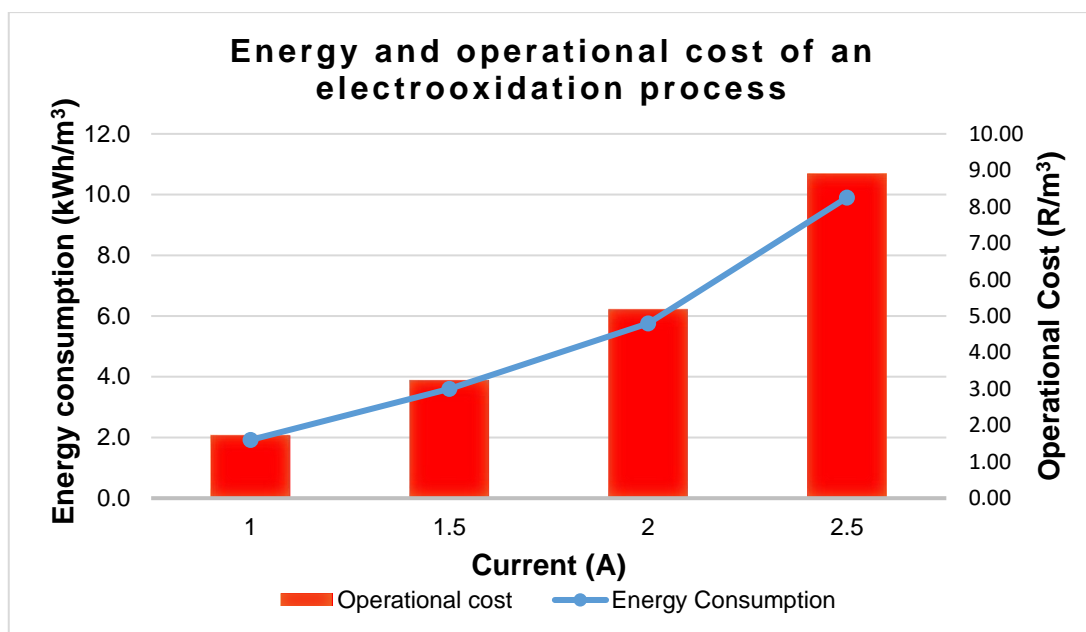
Figure 4-30: The relationship between energy consumption and operating cost

Increasing applied current from 1.5 A to 2.5 A did not enhance pollutant removal; therefore, 1.5 A was considered the optimum value for further experimental runs. Similar results were attained by Mussa, Othman and Abdullah, (2015); Körbahti and Turan, (2016).

CHAPTER 5

Optimisation using

Response Surface

Methodology (RSM)

Chapter 5: Optimisation using Response Surface Methodology (RSM)

5.1. Introduction

This chapter deals with the design of the experiment using the software package called Design Expert. Based on the dependant and independent variables and constraints identified, the model was selected to depict the outputs of the EO process. The aim was to predict the response of COD removal and to optimise the process to achieve the desired outcomes. The BBD model was applied considering the number of factors and levels at which these factors were required to be tested.

5.1.1. EO performance predicted using RSM and Box Behnken

The Box-Behnken design (BBD) was used in this study. It is a quadratic design approach which uses the midpoint, centre points and edges of the process. In this design, each factor can be tested on three levels, only. This design is advantages as it is sensitive to outliers and missing data. The BBD default setting reduces average prediction variances, resulting in the development of a robust model with outstanding prediction characteristics.

The model investigated the influence of temperature (A), NaCl concentration (B) and current density (C) on the EO process using COD removal. The experimental results in this study indicated that the removal of COD was significantly affected by these parameters. A second-order polynomial model equation was used to determine the relationship between the factors and the response, as shown in Equation 5-1. The design matrix indicating experimental run order and output data for the BDD can be seen in Table 5-1.

COD Removal % = 90.89 + 0.2A +1.32B + 0.72C + 0.56AB+0.068AC -0.16BC -2.19A^2 – 2.29B^2 – 0.74C^2 **Equation 5-1**

The positive sign of the coefficient in the regression equation depicts a synergistic effect, while the negative sign signifies an antagonistic effect on the response (Das and Mishra, 2017). From Equation 5-1, the value of the constant 90.89 was independent of any factor, while the interaction term BC and the quadratic terms A^2, B^2 and C^2 have a negative effect on the response. Thus, the response decreased as these terms increased, while the rest of terms A, B, C, AB and AC had a positive influence which indicated that the COD removal would increase with an increase of the magnitude of the parameters.

Table 5-1: Box-Behnken Design output results for COD removal

Run	Factors			COD removal (%)	
	A: Temperature (°C)	**B: NaCl concentration (g/l)**	**C: Current Density (mA/cm^2)**	**Experimental Value**	**Predicted Value**
1	40	2	7.5	87.00	87.28
2	40	4	7.5	91.70	90.89
3	40	6	7.5	90.20	89.92
4	60	2	10	84.90	84.95
5	20	4	7.5	88.20	88.50
6	20	6	10	86.20	86.73
7	40	4	10	90.60	90.87
8	20	2	10	85.90	85.52
9	40	4	5	89.10	89.43
10	20	2	5	83.70	83.90
11	20	6	5	86.00	85.75
12	60	6	10	89.10	88.38
13	40	6	10	89.70	89.74
14	60	2	5	83.40	83.05
15	60	4	7.5	88.50	88.90
16	60	6	5	86.70	87.12

The experimental and predicted values of COD removal is presented in Table 5-1. A total of 16 runs were investigated for this experiment. The results clearly indicated that a maximum COD removal of 91.7% was achieved at temperature, NaCl concentration and current density of 40 $^{\circ}$C, 4g/L and 7.5 mA/cm^2, respectively. This experimental run over a 12-hour electrolysis period with experimental run 2, compares well with the optimised, predicted COD removal. A close correlation between experimental and predicted values were found when a fair agreement was reached between the R^2 predicted

The ANOVA analysis for the Box-Behnken design experimental results output for the removal of COD where A is temperature, B the NaCl concentration and C the current density. This is summarised in Table 5-1, below. The analysis of variance was used to evaluate the determination coefficient, lack of fit and the importance of the linear, quadratic and interaction effects on the response of the independent variables. The p-value was used to determine the significance of the coefficient and the interaction strength of the combined factors. The respective variables indicated a highly significant model when the p-value is smaller and this is confirmed by Tahmouzi, et al (2014). According to Table 5-2, the p-value of the model is less than 0.0001, which indicates that the predicted quadratic model was significantly fitted. The independent variables of the temperature (A), NaCl (B) and current density and the interaction factor AB show the most significant effect on COD removal with $p < 0.05$. The interaction terms AC and BC were not significant. The p-value of the lack of fit was 0.0005, implying that the lack of fit was significant relative to the pure error of the model.

A close correlation in experimental and predicted values were found when there was a reasonable agreement between predicted R^2 (0.9564) and adjusted R^2 (0.9717), as shown in Table 5-2. The high value of the determination coefficient (R^2 = 0.9799) indicated sufficient mathematical model modification. This R^2 value showed that the model could describe variations of 97.99% in response to independent variables. A low coefficient of variance value of 0.46 indicated a reproducible and reliable model (Tian *et al.*, 2017). Hence, the regression model is significant.

Table 5-2: Analysis of variance (ANOVA) of the quadratic model for COD removal

Source	Sum of Squares	Different of square	Mean Square	F Value	p-value Prob > F	
Model	176.58	9	19.62	119.22	< 0.0001	significant
A-Temperature	0.80	1	0.80	4.86	0.0382	
B-NaCl concentration	37.02	1	37.02	224.96	< 0.0001	
C-Current Density	11.02	1	11.02	66.98	< 0.0001	
AB	4.95	1	4.95	30.08	< 0.0001	
AC	0.076	1	0.076	0.46	0.5049	
BC	0.45	1	0.45	2.75	0.1117	
A^2	29.58	1	29.58	179.74	< 0.0001	
B^2	28.09	1	28.09	170.66	< 0.0001	
C^2	2.92	1	2.92	17.76	0.0004	
Residual	3.62	22	0.16			
Lack of Fit	2.69	6	0.45	7.66	0.0005	significant
Pure Error	0.93	16	0.058			
Cor Total	180.20	31				
Standard Deviation	0.41				R-Squared	0.9799
Mean	87.56				Adj R-Squared	0.9717
Coefficient of variance %	0.46				Pred R-Squared	0.9564

5.1.2. Validation of Model

After the regression model was developed, the fitted model was tested to ensure that it provided an accurate approximation to the real system. Thangam, Suresh and Kannan (2014) states that if the model is not adequately fitted, optimising the fitted response surface is likely to produce inadequate or misleading performance. Three types of model diagnostics were used for verification, namely: the normal, residual and predicted vs experimental plot.

The comparison of the predicted and experimental values of COD removal is presented in Figure 5-1. It can be observed that the data scattered closer to the 45-degree line, resulting in a higher determination coefficient above 0.9 suggested that more than 90% of each dependent variable in this study through the modelling equation presented in Equation 5-1. Therefore, the agreement between the predicted and experimental values of COD removal is adequate and in accordance with the statistical significance of the quadratic model produced.
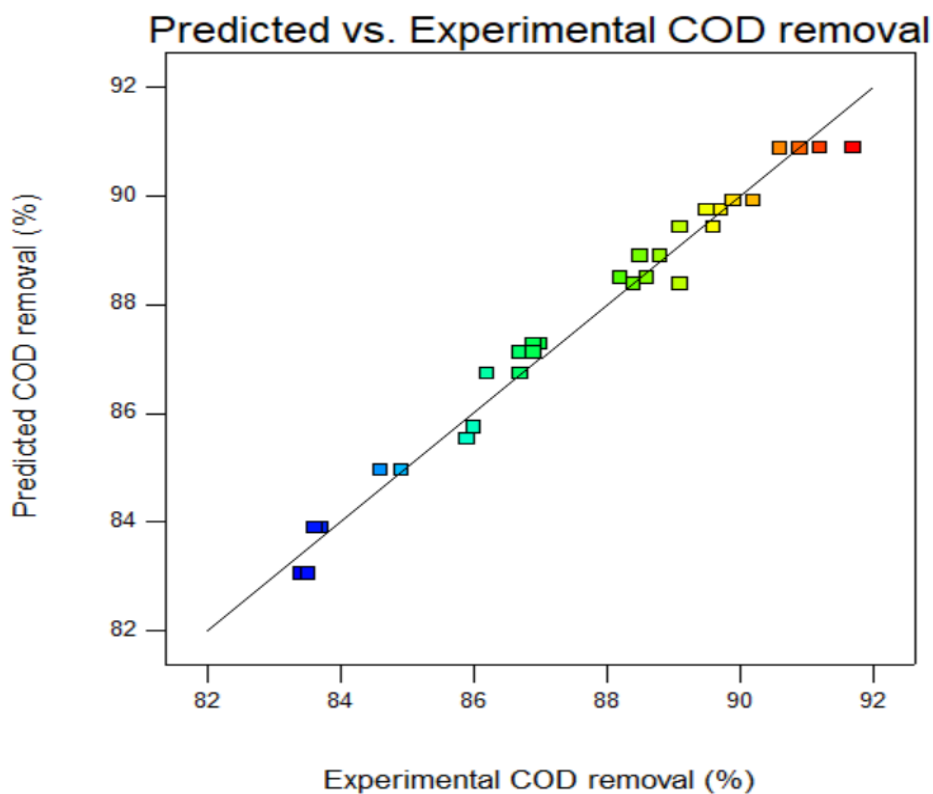
Figure 5-1: Predicted vs experimental COD removal values

The normality probability plot of the residual was constructed to investigate the independability of linear regression. The graph in Figure 5-2 displays the scatter of residuals in a linear format. Several points lie very close to and on the regression, line indicating a very good fit of the model compared to the data. The upper and lower normal percentage probabilities are also located close

to the line. This shows that the model has a perfect fit at the boundary points, as well. Thus, the normality percentage probability plot showed that the exact values provided sufficient estimation to the model. Furthermore, this confirms the accuracy of the Box-Behnken experimental design.
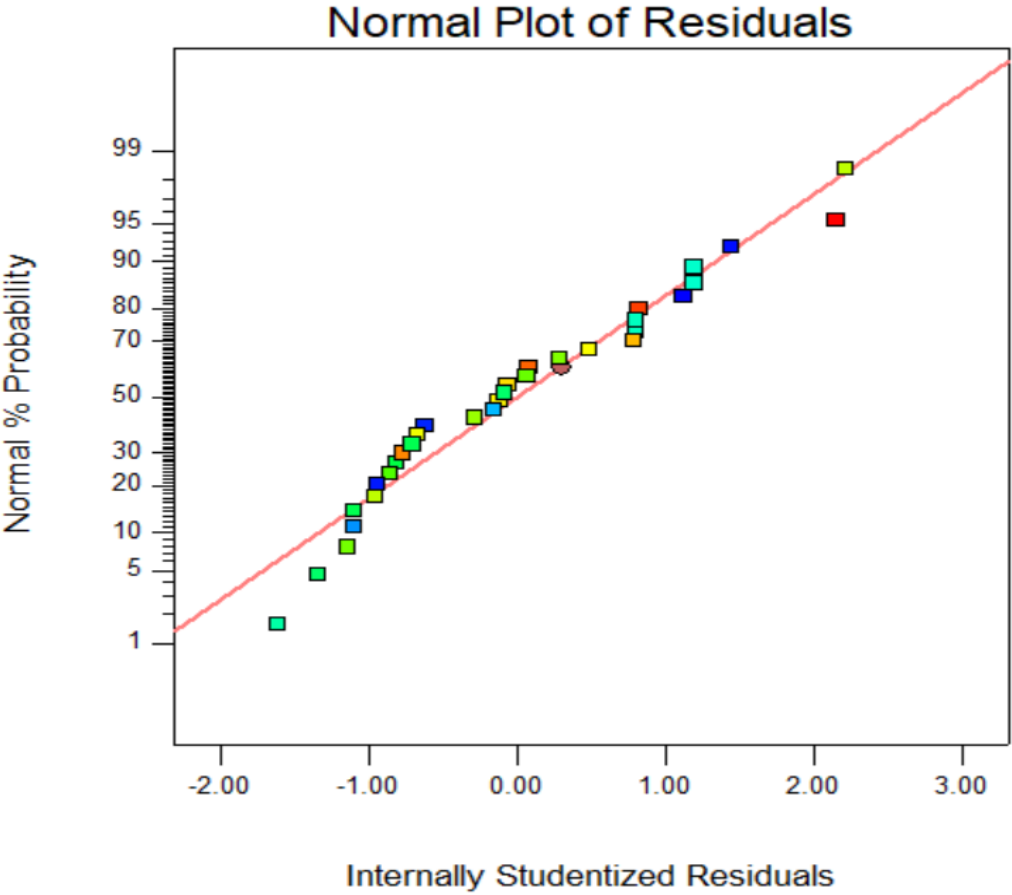
Figure 5-2: Plot of internally studentized residuals vs predicted response

The residuals from the least-squares are an essential tool for evaluating the adequacy of the model (Zhang *et al.*, 2012). Figure 5-3 shows the plot of residuals vs the predicted response. The model's residual plots are distributed randomly, without any trends. Thus, the results indicate good maximum response predictions along with constant variance and adequacy of the quadratic models.
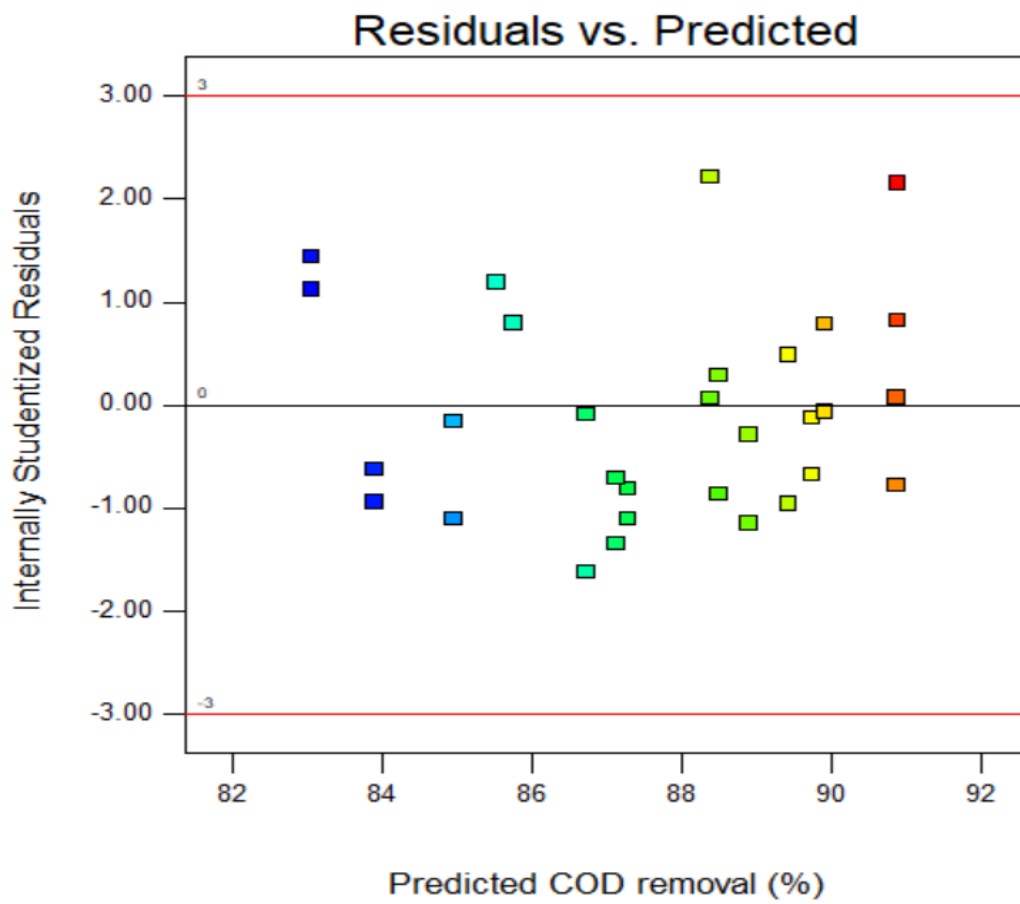
Figure 5-3: Plot of internally studentized residuals vs predicted response

5.2. Analysis of response

To further visualize and assess the influence of the independent variables, the three-dimension (3D) response surface plots and their corresponding two-dimensional (2D) contour maps for the modelled response were constructed as depicted in Figure 5-4. The 3D plot is very useful in evaluating the behaviour of the system within the experimental design (Sathian *et al.*, 2014). Furthermore, these plots endorsed the previously, presented, ANOVA study by identifying the relative contributions on the response of the operating parameters. The different single and interacting effects of parameters A, B and C on the removal of COD are displayed.

As it can be seen from Figure 5-4a, the plot illustrates an elliptical shape, while Figure 5-4b and 5-4c are circular. According to Sathian *et al.* (2014), the elliptical shape of the curve suggests a strong interaction between the two variables, and a circular shape indicates that there is no interaction between the variables. Therefore, the elliptical form of the contour in Figure 5-4a reflect the reciprocal interactions of temperature and NaCl concentration.

As can be seen in Figure 5-4a, the effects of temperature and NaCl concentration was determined when the current density was at its centre point (7.5 mA/cm^2). When the temperature and NaCl concentration was at a low level (20 °C and 5 mA/cm^2), the removal of COD was low. Therefore, a significant improvement in COD removal can be obtained by increasing the temperature and NaCl concentration to 42 °C and 4.5 g/l, respectively.

The interaction between temperature and current density and NaCl concentration and current density was statistically insignificant, as shown in Figure 5-4b and 5-4c.

a)

b)

115
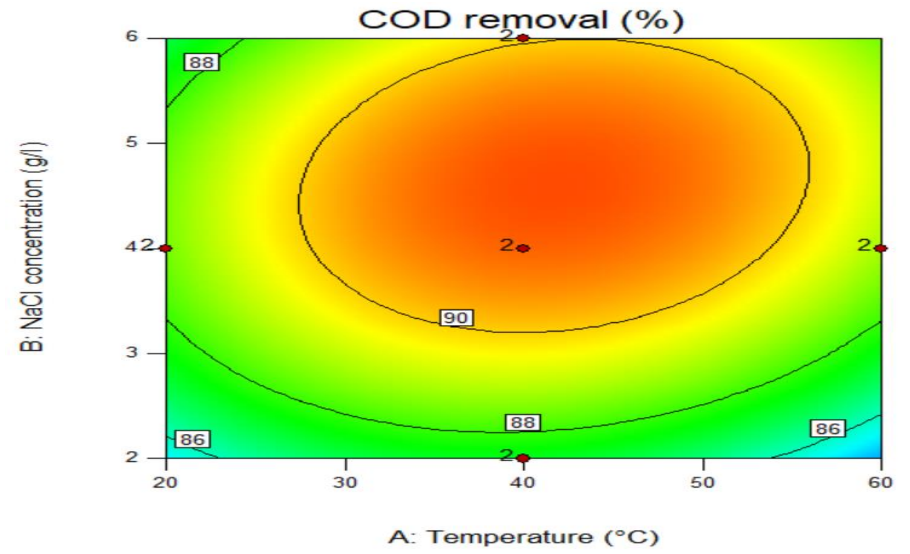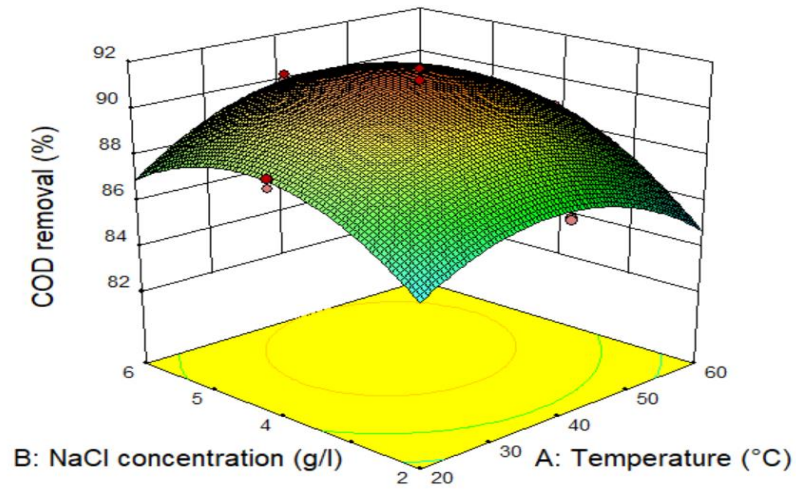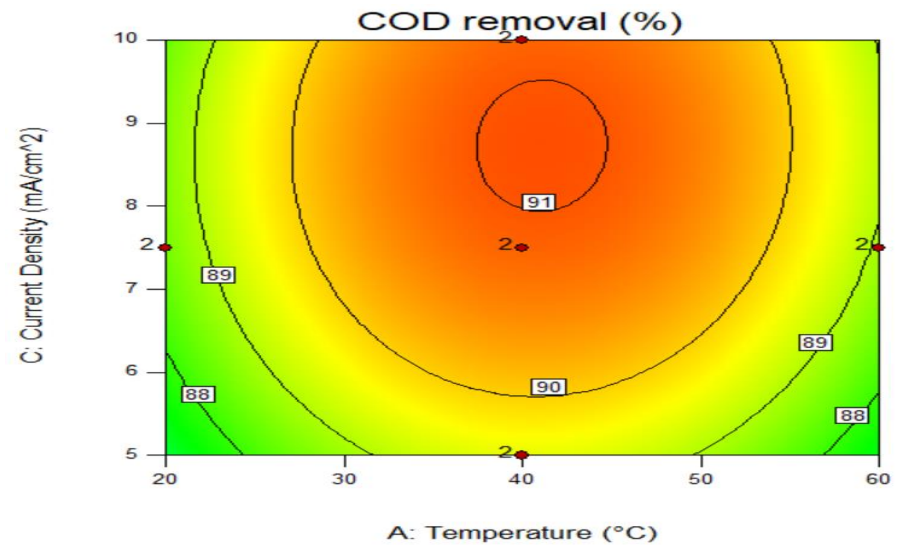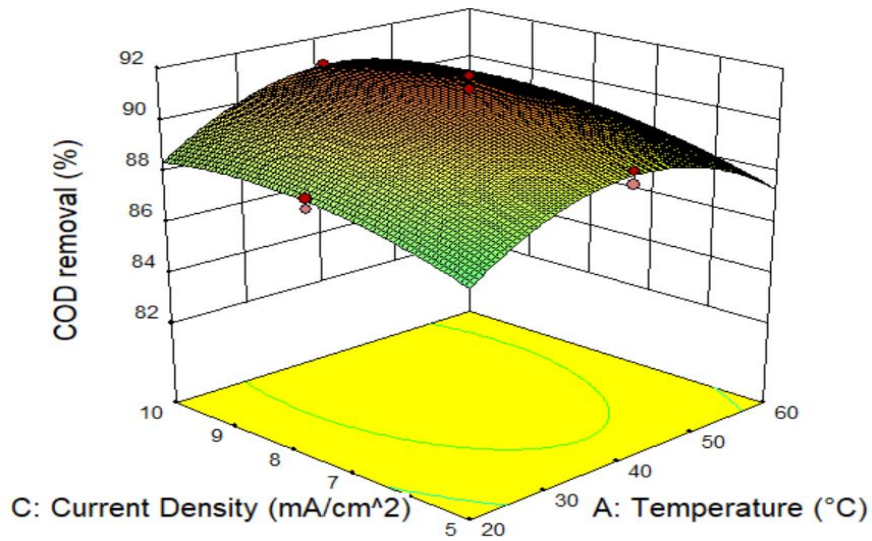
c)
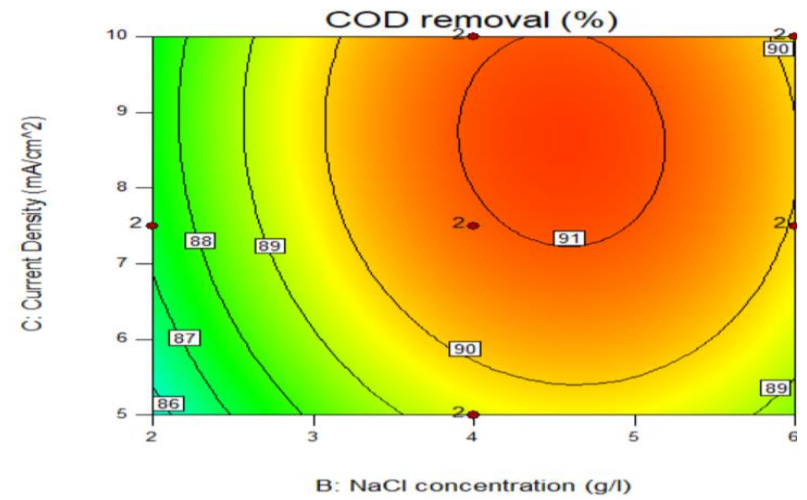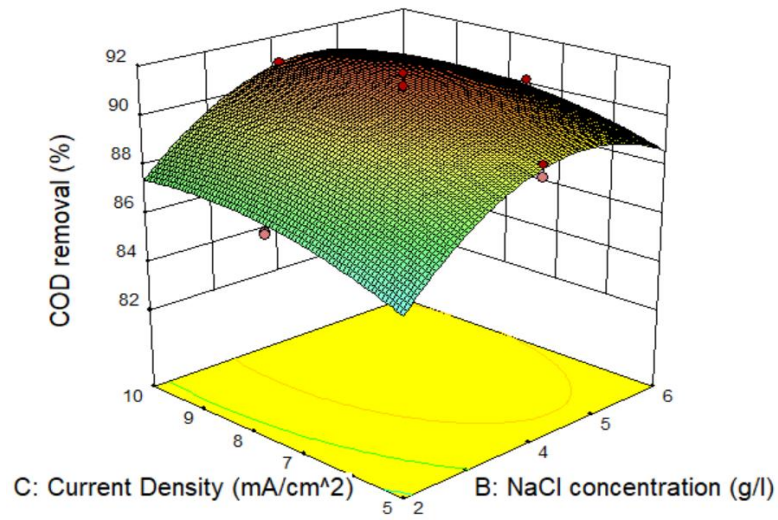
Figure 5-4: Effect of (a) Temperature and NaCl concentration, (b) Temperature and Current density and (c) NaCl concentration and Current density on COD removal
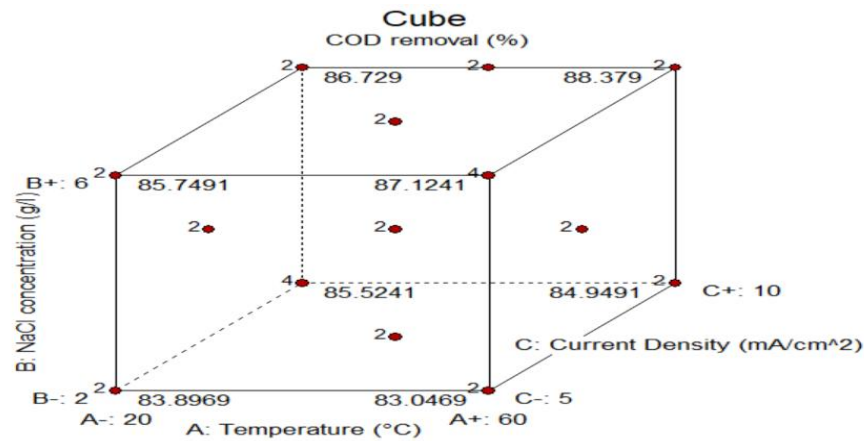
Figure 5-5: Cube plot for COD removal

116

CHAPTER 6

Conclusion and
Recommendation

Chapter 6: Conclusion and Recommendation

6.1. Conclusion

In this study, the treatment of petroleum refinery wastewater (PRW) consisted of two consecutive treatment steps: electrocoagulation (EC) using Aluminium electrodes and electrochemical oxidation (EO) using $Ti/IrO_2–Ta_2O_5$ anodes. The results obtained from this work include the removal efficiency, the kinetics and the energy consumption.

In the first step, PRW was treated using the EC process. The initial pH and applied current influenced the removal efficiency of COD, phenol, colour and FOG from PRW effluent during the EC process. An optimum value for COD, phenol and colour of 67.5%, 98.7% and 88.5%, respectively were observed under the experimental conditions of an initial pH of 5, applied current of 2.5A and electrolysis time of 3 hours. The energy consumption of the EC process was found to be 0.8 kWh/m^3. The Freundlich adsorption isotherm model matched the pollutant removal satisfactorily with the experimental observations.

For the second step, EO process, using a current density of 7.5 mA/cm2 supporting electrolyte (NaCl) concentration of 4 g/L, and temperature of 40°C, showed excellent removal efficiencies. These conditions could reduce COD, phenol, colour, FOG and BTEX by 91.3%, 100%, 100%, 100% and 100%, respectively. The energy consumption of 5.8 kWh/m^3 was estimated at these optimal values.

The optimisation of the EO process was conducted using the Box Behnken design. From the ANOVA results, it was observed that the P-value was less than 0.001 for the model developed, achieving an R^2 value of 0.98, when experimental and modelled results were compared. A quadratic equation obtained from the Box Behnken design was developed to predict the removal of COD from PRW. The optimum conditions were found to be 4.5 g/l NaCl, 42°C temperature and 7.5 mA/cm^2, to obtain a maximum COD removal of 92%.

The integrated treatment EC-EO process was able to reduce COD and other pollutant levels by 96% and 100%, respectively. This resulted in a treated effluent that complies with the discharge standards of the City of Cape Town. Therefore, the integrated process is a viable process for the treatment of PRW.

6.2. Recommendation

1. The characterisation of the sludge produced by the EC process must be evaluated to investigate the electrostatic characteristics of the Al sludge.

2. Pilot-scale experiments should be performed to check the applicability of the EC-EO system to large fluctuations in organic loading.

3. Membrane technology should be used as a polishing step to lower pollutant levels for recycling and reuse application during the EC-EO process.

References

References

Abbas, S. H. and Ali, W. H. (2018) 'Electrocoagulation Technique Used To Treat Wastewater: A Review', *American Journal of Engineering Research*, 7(10), pp. 74–88. Available at: www.ajer.org.

Abdelwahab, O. *et al.* (2013) 'Treatment of petrochemical wastewater containing phenolic compounds by electrocoagulation using a fixed bed electrochemical reactor', *International journal of Electrochemical Science*, 8, pp. 1534–1550.

Abdelwahab, O., Amin, N. K. and El-ashtoukhy, E. Z. (2008) 'Electrochemical removal of phenol from oil refinery wastewater', *Journal of Hazardous Materials*, 163(2009), pp. 711–716. doi: 10.1016/j.jhazmat.2008.07.016.

Abdolali, A. *et al.* (2016) 'A breakthrough biosorbent in removing heavy metals : Equilibrium , kinetic , thermodynamic and mechanism analyses in a lab-scale study', *Science of the Total Environment, The*. Elsevier B.V., 542, pp. 603–611. doi: 10.1016/j.scitotenv.2015.10.095.

Abou-Taleb, K. A. and Galal, G. F. (2018) 'A comparative study between one-factor-at-a-time and minimum runs resolution-IV methods for enhancing the production of polysaccharide by Stenotrophomonas daejeonensis and Pseudomonas geniculate', *Annals of Agricultural Sciences*. Faculty of Agriculture, Ain-Shams University, 63(2), pp. 173–180. doi: 10.1016/j.aoas.2018.11.002.

Ahmed, S. A. *et al.* (2019) 'Application of one –factor- at-a-time and statistical designs to enhance α-amylase production by a newly isolate Bacillus subtilis strain-MK1', *Biocatalysis and Agricultural Biotechnology*. Elsevier Ltd, 22(October), p. 101397. doi: 10.1016/j.bcab.2019.101397.

Akhter, M., Habib, G. and Qamar, S. U. (2018) 'Application of Electrodialysis in Waste Water Treatment and Impact of Fouling on Process Performance', *Journal of Membrane Science & Technology*, 08(02). doi: 10.4172/2155-9589.1000182.

Al-Amshawee, S. *et al.* (2020) 'Electrodialysis desalination for water and wastewater: A review', *Chemical Engineering Journal*, 380(July 2019). doi: 10.1016/j.cej.2019.122231.

Al-Malack, M. H. (2015) 'Performance of constant-flux immersed UF membrane treating petroleum refinery wastewater refinery wastewater', *Desalination and Water Treatment*, 57(19), pp. 1–11. doi: 10.1080/19443994.2015.1024753.

Albright, L. F. (2009) *Albright'S Chemical Engineering Handbook*. doi: 10.1201/9781420014389.ch6.

Aljuboury, D. A. D. A. *et al.* (2017) 'Treatment of petroleum wastewater by conventional and new technologies - A review', *Global NEST Journal*, 19(3), pp. 439–452.

Alvarado, L. and Chen, A. (2014) 'Electrodeionization: Principles, strategies and applications', *Electrochimica Acta*. Elsevier Ltd, 132, pp. 583–597. doi: 10.1016/j.electacta.2014.03.165.

AM, E. S., El Boraey, H. A. and HF, E. A. (2017) 'Chemical Treatment of Petroleum Wastewater and its Effect on the Corrosion Behavior of Steel Pipelines in Sewage Networks', *Journal of Chemical Engineering & Process Technology*, 08(01), pp. 1–9. doi: 10.4172/2157-7048.1000324.

Anderson, B. *et al.* (2010) *Awareness of Water Pollution as a Problem and the Decision to Treat Drinking Water among Rural African Households with Unclean Drinking Wate*, *Population Studies Center Research Report 10-701*.

Anderson, M. J. and Whitcomb, P. J. (2016) *RSM Simplified: Optimizing Processes Using Response Surface Methods for Design of Experiments, Second Edition*. 2nd Edition, *RSM Simplified*. 2nd Edition. New York: Productivity Press. doi: 10.1201/9781315382326.

Anglada, A., Urtiaga, A. and Ortiz, I. (2009) 'Contributions of electrochemical oxidation to waste-water treatment : fundamentals', *Journal of Chemical Technology and Biotechnology*, 84, pp. 1747–1755. doi: 10.1002/jctb.2214.

Araújo, C. S. T. *et al.* (2017) 'Elucidation of mechanism involved in adsorption of Pb(II) onto lobeira fruit (Solanum lycocarpum) using Langmuir, Freundlich and Temkin isotherms', *Microchemical Journal*. Elsevier B.V, (137), pp. 348–354. doi: 10.1016/j.microc.2017.11.009.

Arslan, G., Yazici, B. and Erbil, M. (2003) 'The effect of pH, temperature and concentration on electrooxidation of phenol', *Journal of Hazardous Materials*, 124, pp. 37–43. doi: 10.1016/j.jhazmat.2003.09.015.

Asghar, A., Abdul Raman, A. A. and Daud, W. M. A. W. (2014) 'A Comparison of Central Composite Design and Taguchi Method for Optimizing Fenton Process', *The Scientific World Journal*, 2014, pp. 1–14. doi: 10.1155/2014/869120.

Ayawei, N., Ebelegi, A. N. and Wankasi, D. (2017) 'Modelling and Interpretation of Adsorption Isotherms', *Journal of Chemistry*, 2017, pp. 1–11.

Babu, B. R. *et al.* (2014) 'Removal of pharmaceuticals from wastewater by electrochemical oxidation using cylindrical flow reactor and optimization of treatment conditions', pp. 37–41. doi: 10.1080/10934520902996880.

Babu, S. A. *et al.* (2011) 'Decolorisation of synthetic and real polluted water by indirect electrochemical oxidation process', *Water Environment*, 31(0257–8050), pp. 45–49.

Bagastyo, A. Y. *et al.* (2014) 'Electrochemical treatment of reverse osmosis concentrate on boron-doped electrodes in undivided and divided cell configurations', *Journal of Hazardous Materials*. Elsevier B.V., 279, pp. 111–116. doi: 10.1016/j.jhazmat.2014.06.060.

Bas, D. and Boyaci, I. H. (2007) 'Modeling and optimization I : Usability of response surface methodology', *Journal of Food Engineering*, 78, pp. 836–845. doi: 10.1016/j.jfoodeng.2005.11.024.

Basu, P. (2010) *Gasification Theory and Modeling of Gasifiers*. First Edit, *Biomass Gasification and Pyrolysis*. First Edit. © 2010 Elsevier Inc. doi: 10.1016/B978-0-12-374988-8.00005-2.

Bayar, S. *et al.* (2014) 'Pre-Treatment of Pistachio Processing Industry Wastewaters (PPIW) by Electrocoagulation using Al Plate Electrode', *Separation Science and Technology (Philadelphia)*, 49(7), pp. 1008–1018. doi: 10.1080/01496395.2013.878847.

Benalcazar, P., Krawczyk, M. and Kamiński, J. (2017) 'Forecasting global coal consumption: An artificial neural network approach', *Gospodarka Surowcami Mineralnymi / Mineral Resources Management*, 33(4), pp. 29–44. doi: 10.1515/gospo-2017-0042.

Bhagawan, D. *et al.* (2014) 'Treatment of the petroleum refinery wastewater using combined electrochemical methods', *Desalination and Water Treatment*, 7(8), pp. 3387–3394. doi: 10.1080/19443994.2014.987175.

Bi, J. *et al.* (2011) 'Removal of nitrate from groundwater using the technology of electrodialysis and electrodeionization', *Desalination and Water Treatment*, 34(1–3), pp. 394–401. doi: 10.5004/dwt.2011.2891.

Bingham, D. *et al.* (2008) 'Factorial designs with multiple levels of randomization', *Statistica Sinica*, 18(2), pp. 493–513.

'BP Statistical Review of World Energy' (2019) *BP Energy Economics*. 68th edn. London, pp. 1–62. doi: 10.1111/j.1468-0351.1993.tb00076.x.

Butler, E. *et al.* (2011) 'Electrocoagulation in Wastewater Treatment', *Water*, 3(4), pp. 495–525. doi: 10.3390/w3020495.

Bwapwa, J. K. (2018) 'Review on Main Issues Causing Deterioration of Water Quality and Water Scarcity : Case Study of South Africa', *Environmental Management and Sustainable Development*, 7(3), pp. 14–34. doi: 10.5296/emsd.v7i3.13156.

Calderón-Cárdenas, A. *et al.* (2020) 'Thorough Analysis of the Effect of Temperature on the Electro- Oxidation of Formic Acid', *The Journal of Physical Chemistry*, 124(44), pp. 24259–24270. doi: 10.1021/acs.jpcc.0c08059.

Calderón-cárdenas, A., Paredes-salazar, E. A. and Varela, H. (2020) 'Apparent Activation

Energy in Electrochemical Multistep Reactions : a Description via Sensitivies and Degrees of Rate Control Apparent Activation Energy in Electrochemical Multistep Reactions : a Description via Sensitivies and Degrees of Rate Control', *ACS Catalysi*, 10(16), pp. 9336–9345. doi: 10.1021/acscatal.0c02359.

Can, O. T. (2014) 'COD removal from fruit-juice production wastewater by electrooxidation electrocoagulation and electro-Fenton processes', *Desalination and Water Treatment*, 52(1–3), pp. 65–73. doi: 10.1080/19443994.2013.781545.

Canizares, P. *et al.* (2005) 'Electrochemical oxidation of phenolic wastes with boron-doped diamond anodes', *Water Research*, 39, pp. 2687–2703. doi: 10.1016/j.watres.2005.04.042.

Chatterjee, J., Rai, N. and Sar, S. K. (2014) 'Kinetic isotherm of amoxicillin antibiotic through adsorption and its removal by electrocoagulation', *Oriental Journal of Chemistry*, 30(2), pp. 775–784. doi: 10.13005/ojc/300251.

Chavalparit, O. and Ongwandee, M. (2009) 'Optimizing electrocoagulation process for the treatment of biodiesel wastewater using response surface methodology', *Journal of Environmental Sciences*. The Research Centre for Eco-Environmental Sciences, Chinese Academy of Sciences, 21(11), pp. 1491–1496. doi: 10.1016/S1001-0742(08)62445-6.

Chen, G. (2003) 'Electrochemical technologies in wastewater treatment', *Separation and Purification Technology*, 38, pp. 11–41. doi: 10.1016/j.seppur.2003.10.006.

Chen, X., Chen, G. and Yue, P. L. (2003) 'Anodic oxidation of dyes at novel Ti/B-diamond electrodes', *Chemical Engineering Science*, 58(3–6), pp. 995–1001. doi: 10.1016/S0009-2509(02)00640-1.

Chithra, K. and Balasubramanian, N. (2010) 'Modeling electrocoagulation through adsorption kinetics', *Journal of Modelling and Simulation of Systems*, 1(2), pp. 124–130.

Coelho, A. *et al.* (2006) 'Treatment of petroleum refinery sourwater by advanced oxidation processes', *Journal of Hazardous Materials*, 137, pp. 178–184. doi: 10.1016/j.jhazmat.2006.01.051.

Coelho, A., Castro, A. V and Jr, G. L. S. A. (2006) 'Treatment of petroleum refinery sourwater by advanced oxidation processes', *Journal of Hazardous Materials*, 137, pp. 178–184. doi: 10.1016/j.jhazmat.2006.01.051.

Comninellis, C. *et al.* (2008) 'Advanced oxidation processes for water treatment : advances and trends for R & D', *Journal of Chemical Technology and Biotechnology*, 83, pp. 769–776. doi: 10.1002/jctb.

Costa, A. S. *et al.* (2012) 'Environmental strategies to remove volatile aromatic fractions (BTEX) from petroleum industry wastewater using biomass', *Bioresource Technology*. Elsevier Ltd, 105,

pp. 31–39. doi: 10.1016/j.biortech.2011.11.096.

Da Costa, P. R. F. *et al.* (2016) 'Fuel station effluent treatment by electrochemical technology', *Journal of Electroanalytical Chemistry*. Elsevier B.V., 763, pp. 97–103. doi: 10.1016/j.jelechem.2015.12.038.

Cozmuta, L. M. *et al.* (2012) 'The influence of pH on the adsorption of lead by Na-clinoptilolite : Kinetic and equilibrium studies', *Water SA*, 38(2), pp. 269–278.

Czitrom, V. (1999) 'One-factor-at-a-time versus designed experiments', *American Statistician*, 53(2), pp. 126–131. doi: 10.1080/00031305.1999.10474445.

Das, S. and Mishra, S. (2017) 'Box-Behnken statistical design to optimize preparation of activated carbon from Limonia acidissima shell with desirability approach', *Journal of Environmental Chemical Engineering*. Elsevier B.V., 5(1), pp. 588–600. doi: 10.1016/j.jece.2016.12.034.

Daud, N. M. *et al.* (2014) 'Production of biodiesel and its wastewater treatment technologies : A review', *Process Safety and Environmental Protection*. Institution of Chemical Engineers, 94(October), pp. 487–508. doi: 10.1016/j.psep.2014.10.009.

Davarnejad, R., Mohammadi, M. and Fauzi, A. (2014) 'Journal of Water Process Engineering Petrochemical wastewater treatment by electro-Fenton process using aluminum and iron electrodes : Statistical comparison', *Journal of Water Process Engineering*. Elsevier Ltd, 3, pp. 18–25. doi: 10.1016/j.jwpe.2014.08.002.

Dehlert, G. W. (2010) *A First Course in Design and Analysis of Experiments*. Gary W. Dehlert.

Delgarm, N. *et al.* (2018) 'Sensitivity analysis of building energy performance: A simulation-based approach using OFAT and variance-based sensitivity analysis methods', *Journal of Building Engineering*. Elsevier Ltd, 15(December 2017), pp. 181–193. doi: 10.1016/j.jobe.2017.11.020.

Demirbas, A. (2015) 'Pyrolytic distillation of No. 4 Fuel Oil', *Petroleum Science and Technology*, 33(17–18), pp. 1611–1618. doi: 10.1080/10916466.2015.1079540.

Demirbas, A. and Bamufleh, H. S. (2017) 'Optimization of crude oil refining products to valuable fuel blends', *Petroleum Science and Technology*. Taylor & Francis, 35(4), pp. 406–412. doi: 10.1080/10916466.2016.1261162.

Department of Water and Environmental Affairs (2013) *Revision of general authorisations in terms of section 39 of the National Water Act, 1998 (Act NO. 36 of 1998) (The Act))*, *Government Gazette 36820*. Available at: https://cer.org.za/wp-content/uploads/2014/02/Revision-of-General-Authorisations-2013.pdf (Accessed: 18 October 2020).

Diya' uddeen, H. B., Daud, W. M. A. W. and Aziz, A. R. A. (2010) 'Treatment technologies for petroleum refinery effluents : A review', *Process Safety and Environmental Protection*, 89(2011), pp. 95–105. doi: 10.1016/j.psep.2010.11.003.

Diya'uddeen, B. H. *et al.* (2014) 'Journal of Industrial and Engineering Chemistry Hybrid of Fenton and sequencing batch reactor for petroleum refinery wastewater treatment', *Journal of Industrial and Engineering Chemistry*. The Korean Society of Industrial and Engineering Chemistry, 25, pp. 186–191. doi: 10.1016/j.jiec.2014.10.033.

Diya'uddeen, B. H., Daud, W. M. A. W. and Abdul Aziz, A. R. (2011) 'Treatment technologies for petroleum refinery effluents: A review', *Process Safety and Environmental Protection*, 89(2), pp. 95–105. doi: 10.1016/j.psep.2010.11.003.

Dohare, D. E. and Sisodia, T. (2014) 'Applications of Electrocoagulation in treatment of Industrial Wastewater : A Review', *INTERNATIONAL JOURNAL OF ENGINEERING SCIENCES & RESEARCH TECHNOLOGY*, 3(11), pp. 379–386.

El-Ghenymy, A. *et al.* (2014) 'Electro-Fenton degradation of the antibiotic sulfanilamide with Pt/carbon-felt and BDD/carbon-felt cells. Kinetics, reaction intermediates, and toxicity assessment', *Environmental Science and Pollution Research*, 21(14), pp. 8368–8378. doi: 10.1007/s11356-014-2773-3.

El-naas, M. H. *et al.* (2009) 'Assessment of electrocoagulation for the treatment of petroleum refinery wastewater', *Journal of Environmental Management*. Elsevier Ltd, 91(1), pp. 180–185. doi: 10.1016/j.jenvman.2009.08.003.

El-naas, M. H., Al-zuhair, S. and Al-lobaney, A. (2013) 'Treatment of Petroleum Refinery Wastewater by Continuous Electrocoagulation', *International Journal of Engineering Research and Technology*, 2(10), pp. 2144–2150.

El-naas, M. H., Al-zuhair, S. and Alhaija, M. A. (2009) 'Reduction of COD in refinery wastewater through adsorption on date-pit activated carbon', *Journal of Hazardous Materials*, 173(2010), pp. 750–757.

El-naas, M. H., Alhaija, M. A. and Al-zuhair, S. (2014) 'Evaluation of a three-step process for the treatment of petroleum refinery wastewater', *Journal of Environmental Chemical Engineering*. Elsevier B.V., 2(1), pp. 56–62. doi: 10.1016/j.jece.2013.11.024.

El-Naas, M. H., Surkatti, R. and Al-Zuhair, S. (2016) 'Petroleum refinery wastewater treatment: A pilot scale study', *Journal of Water Process Engineering*. Elsevier Ltd, 14, pp. 71–76. doi: 10.1016/j.jwpe.2016.10.005.

Emamjomeh, M. M. and Sivakumar, M. (2009) 'Review of pollutants removed by electrocoagulation and electrocoagulation / flotation processes', *Journal of Environmental*

Management. Elsevier Ltd, 90(5), pp. 1663–1679. doi: 10.1016/j.jenvman.2008.12.011.

EPA (2012) 'Guidlines for water reuse', *Guidelines for water reuse*, (September).

Esfandyari, Y. *et al.* (2015) 'Degradation and biodegradability improvement of the olive mill wastewater by peroxi-electrocoagulation / electrooxidation- electroflotation process with bipolar aluminum electrodes', *Environmental Science and Pollution Research*, 22, pp. 6288–6297. doi: 10.1007/s11356-014-3832-5.

Eslami, M., Zare, H. R. and Namazian, M. (2012) 'Thermodynamic Parameters of Electrochemical Oxidation of L-DOPA : Experimental and Theoretical Studies Thermodynamic Parameters of Electrochemical Oxidation of L-DOPA : Experimental and Theoretical Studies', *The Journal of Physical Chemistry*, 116(41), pp. 12552–12557.

Fayemiwo, O. M., Daramola, M. O. and Moothi, K. (2017) 'BTEX compounds in water – future trends and directions for water treatment', *Water SA*, 43(4), pp. 602–613. doi: 10.4314/wsa.v43i4.08.

Feng, Y. *et al.* (2016) 'Electrochemical technologies for wastewater treatment and resource reclamation', *Environmental Science: Water Research & Technology*. Royal Society of Chemistry, 2, pp. 800–831. doi: 10.1039/C5EW00289C.

Ferreira, S. L. C. *et al.* (2007) 'Box-Behnken design: An alternative for the optimization of analytical methods', *Analytica Chimica Acta*, 597(2), pp. 179–186. doi: 10.1016/j.aca.2007.07.011.

Frey, D. D. and Sudarsanam, N. (2008) 'An adaptive one-factor-at-a-time method for robust parameter design: Comparison with crossed arrays via case studies', *Journal of Mechanical Design, Transactions of the ASME*, 130(2), pp. 1–18. doi: 10.1115/1.2748450.

Fukuda, I. M. *et al.* (2018) 'Design of experiments (DoE) applied to pharmaceutical and analytical quality by design (QbD)', *Brazilian Journal of Pharmaceutical Sciences*, 54(Special Issue), pp. 1–16. doi: 10.1590/s2175-97902018000001006.

Ganesan, P. *et al.* (2013) 'Removal of manganese from water by electrocoagulation: Adsorption, kinetics and thermodynamic studies', *Canadian Journal of Chemical Engineering*, 91(3), pp. 448–458. doi: 10.1002/cjce.21709.

Gao, Z. *et al.* (2009) 'Investigation of factors affecting adsorption of transition metals on oxidized carbon nanotubes', *Journal of Hazardous Materials*, 167(1–3), pp. 357–365. doi: 10.1016/j.jhazmat.2009.01.050.

García, E. A. *et al.* (2014) 'Decentralised grey-water treatment combining adsorption and electrochemical oxidation Toilet flushing By adding granular activated carbon', 49(1), p. 11302.

Gargouri, B. *et al.* (2017) 'Chemosphere Chemical composition and direct electrochemical oxidation of table olive processing wastewater using high oxidation power anodes', 166. doi: 10.1016/j.chemosphere.2016.09.080.

Gasim, H. A. *et al.* (2012) 'Treatment of Petroleum Refinery Wastewater by using UASB Reactors', *International Journal of Chemical and Biological Engineering*, 6, pp. 174–177.

Gengec, E. *et al.* (2011) 'Optimization of baker's yeast wastewater using response surface methodology by electrocoagulation', *Desalination*, 286, pp. 200–209. doi: 10.1016/j.desal.2011.11.023.

Gengec, E. *et al.* (2012) 'Electrochemical treatment of Baker's yeast wastewater containing melanoidin: Optimization through response surface methodology', *Water Science and Technology*, 65(12), pp. 2183–2190. doi: 10.2166/wst.2012.130.

Geraldino, H. C. L. *et al.* (2015) 'Eficiência e custo operacional de um sistema de eletrofloculação aplicado ao tratamento de efluente da indústria de laticínio', *Acta Scientiarum - Technology*, 37(3), pp. 401–408. doi: 10.4025/actascitechnol.v37i3.26452.

Ghanim, A. N. and Ajjam, S. K. (2013a) 'Kinetic Modelling of Nitrate Removal from Aqueous Solution during Electrocoagulation', *Civil and Environmental Research*, 3(7), pp. 64–74.

Ghanim, A. N. and Ajjam, S. K. (2013b) 'Modeling of Textile Wastewater Electrocoagulation Via Adsorption isotherm kinetics', *The Iraqi Journal For Mechanical And Material Engineering*, 13(1), pp. 49–62.

Gherardini, L. *et al.* (2001) 'Electrochemical Oxidation of 4-Chlorophenol for Wastewater Treatment: Definition of Normalized Current Efficiency (φ)', *Journal of The Electrochemical Society*, 148(6), p. D78. doi: 10.1149/1.1368105.

Goupy, J. and Creighton, L. (2008) *Introduction to Design of Experiments*, *The American Statistician*. North Carolina: SAS. doi: 10.1198/tas.2008.s273.

Gudde, N. J. (2018) 'Adaptation of oil refineries to make modern fuels', in *Proceedings of the Institution of Mechanical Engineers, Part D: Journal of Automobile Engineering*, pp. 5–21. doi: 10.1177/0954407016680522.

Guo, S. *et al.* (2011) 'Improvement of acidification on dewaterability of oily sludge from flotation', *Chemical Engineering Journal*. Elsevier B.V., 168(2), pp. 746–751. doi: 10.1016/j.cej.2011.01.070.

Güven, G. *et al.* (2012) 'Specific energy consumption in electrochemical treatment of food industry wastewaters', *Journal of Chemical Technology and Biotechnology*, 87(4), pp. 513–522. doi: 10.1002/jctb.2739.

Hariz, I. Ben *et al.* (2013) 'Treatment of petroleum refinery sulfidic spent caustic wastes by electrocoagulation', *Separation and Purification Technology*, 107, pp. 150–157. doi: 10.1016/j.seppur.2013.01.051.

Hashemi, H. *et al.* (2015) 'Survey on electrode type effectiveness on electro coagulation process as a method for polluted water treatment in emergencies', pp. 185–188. doi: 10.4103/2347-9019.162548.

Havard, D. (2013) *Oil and Gas Production Handbook - An introduction to oil and gas production, transport, refining and petrochemical industry*. 3rd edn. Oslo: ABB.

Hayder, G. *et al.* (2014) 'Prediction model development for petroleum refinery wastewater treatment', *Journal of Water Process Engineering*. Elsevier Ltd, 4, pp. 1–5. doi: 10.1016/j.jwpe.2014.08.006.

Heidari, Z., Motevasel, M. and Jaafarzadeh, N. A. (2015) 'Application of Electro-Fenton (EF) Process to the Removal of Pentachlorophenol from Aqueous Solutions', *Iranian Journal of Oil & Gas Science and Technology*, 4(4), pp. 76–87.

Hinkelman, K. and Kempthorne, O. (2005) *Design and Analysis of Experiments -Volume 2 Advanced Experimental Design*. New Jersey: John Wiley & Sons, Inc.

Hinkelmann, K. and Kempthorne, O. (2005) *Design and Analysis of Experiments*, *Design and Analysis of Experiments*. New Jersey: John Wiley & Sons, Inc. doi: 10.1002/9781118147634.

Holt, P. K. *et al.* (2002) 'A quantitative comparison between chemical dosing and electrocoagulation', *Colloids and Surfaces A: Physicochemical and Engineering Aspects*, 211(2–3), pp. 233–248. doi: 10.1016/S0927-7757(02)00285-6.

Holt, P. K., Barton, G. W. and Mitchell, C. A. (2005) 'The future for electrocoagulation as a localised water treatment technology', *Chemosphere*, 59(3), pp. 355–367. doi: 10.1016/j.chemosphere.2004.10.023.

Ibrahim, D. S., Devi, S. P. and Balasubramanian, N. (2013) 'Electrochemical Oxidation Treatment of Petroleum Refinery Effluent', *International Journal of Scientific &Engineering Research*, 4(8), pp. 0–5. doi: 10.14299/00000.

Igwe, J. C. and Abia, A. A. (2007) 'Adsorption isotherm studies of Cd (II), Pb (II) and Zn (II) ions bioremediation from aqueous solution using unmodified and EDTA-modified maize cob', *Ecletica Quimica*. IEEE, 32(1), pp. 33–42. doi: 10.1109/SIIC.2013.6624206.

Islam, S. M. D.-U. (2019) 'Electrocoagulation (EC) technology for wastewater treatment and pollutants removal', *Sustainable Water Resources Management*. Springer International Publishing, 5(1), pp. 359–380. doi: 10.1007/s40899-017-0152-1.

Jamaly, S., Giwa, A. and Hasan, S. W. (2015) 'Recent improvements in oily wastewater treatment : progress, challenges , and future opportunities', *Journal of Environmental Sciences*, 37, pp. 15–30.

Jaruwat, P., Kongjao, S. and Hunsom, M. (2010) 'Management of biodiesel wastewater by the combined processes of chemical recovery and electrochemical treatment', *Energy Conversion and Management*. Elsevier Ltd, 51(3), pp. 531–537. doi: 10.1016/j.enconman.2009.10.018.

Jing, G. *et al.* (2017) 'A novel electro-catalytic degradation method of phenol wastewater with Ti/IrO2-Ta2O5 anodes in high-gravity fields', *Water Science and Technology*, 76, pp. 662–670. doi: 10.2166/wst.2017.262.

Juárez, H. R. *et al.* (2015) 'A Combined Electrocoagulation-Electrooxidation Process for Carwash Wastewater Reclamation', *International Journal of Electrochemical Science*, 10, pp. 6754–6767.

Kabdash, I. *et al.* (2012) 'Electrocoagulation applications for industrial wastewaters : a critical review', *Environmental Technology Reviews*, 1(1), pp. 2–45.

Karlsson, R. (2009) 'Experimental design', *Label-Free Biosensors*. Edited by M. A. Cooper. Cambridge: Cambridge University Press, pp. 29–47. doi: 10.1017/CBO9780511626531.004.

Keerthi, Vinduja, V. and Balasubramanian, N. (2013) 'Electrocoagulation-integrated hybrid membrane processes for the treatment of tannery wastewater', *Environmental Science and Pollution Research*, 20(10), pp. 7441–7449. doi: 10.1007/s11356-013-1766-y.

Khandegar, V. and Saroha, A. K. (2013) 'Electrocoagulation for the treatment of textile industry effluent - A review', *Journal of Environmental Management*. Elsevier Ltd, 128, pp. 949–963. doi: 10.1016/j.jenvman.2013.06.043.

Kobya, M. *et al.* (2013) 'Optimization of arsenic removal from drinking water by electrocoagulation batch process using response surface methodology', *Desalination and Water Treatment*, 51(34–36), pp. 6676–6687. doi: 10.1080/19443994.2013.769700.

Kolesnikov, V. A., Il'in, V. I. and Kolesnikov, A. V. (2019) 'Electroflotation in Wastewater Treatment from Oil Products, Dyes, Surfactants, Ligands, and Biological Pollutants: A Review', *Theoretical Foundations of Chemical Engineering*, 53(2), pp. 251–273. doi: 10.1134/S0040579519010093.

Körbahti, B. K. and Artut, K. (2010) 'Electrochemical oil / water demulsi fi cation and puri fi cation of bilge water using Pt / Ir electrodes', *Desalination*, 258, pp. 219–228. doi: 10.1016/j.desal.2010.03.008.

Körbahti, B. K. and Turan, K. M. (2016) 'Evaluation of Energy Consumption in Electrochemical Oxidation of Acid Violet 7 Textile Dye using Pt/Ir Electrodes', *Journal of the Turkish Chemical*

Society, Section A: Chemistry, 3(3), p. 75. doi: 10.18596/jotcsa.31804.

Koutsaftis, D., Polychronopoulou, E. and Chalarakis, L. (no date) 'TREATMENT OF INDUSTRIAL WASTEWATER USING THE ELECTROCOAGULATION – ELECTROFLOTATION TECHNOLOGY'.

Kumara, N. T. R. N. *et al.* (2014) 'Equilibrium Isotherm Studies of Adsorption of Pigments Extracted from Kuduk-kuduk (Melastoma malabathricum L.) Pulp onto TiO 2 Nanoparticles', *Journal of Chemistry*, 2014, pp. 1–6. doi: 10.1155/2014/468975.

Kuokkanen, V. *et al.* (2013) 'Recent Applications of Electrocoagulation in Treatment of Water and Wastewater — A Review', *Green and Sustainable Chemistry*, 3, pp. 89–121.

Li, Y. *et al.* (2009) 'Removal of Waterborne Particles by Electrofiltration: Pilot-Scale Testing Ying', *Envionmental Engineering Science*, 26(12), pp. 1795–1803.

Linares-Hernández, I. *et al.* (2010) 'A combined electrocoagulation-electrooxidation treatment for industrial wastewater', *Journal of Hazardous Materials*, 175(1–3), pp. 688–694. doi: 10.1016/j.jhazmat.2009.10.064.

Linares-hernández, I. and Barrera-díaz, C. E. (2009) 'A Combined Electrocoagulation – Electrooxidation Treatment for Industrial Wastewater', (October). doi: 10.1016/j.jhazmat.2009.10.064.

Lopez, A. M. *et al.* (2017) 'Potential of electrodialytic techniques in brackish desalination and recovery of industrial process water for reuse', *Desalination*. Elsevier B.V., 409, pp. 108–114. doi: 10.1016/j.desal.2017.01.010.

Lye, L. M. (2005) 'Tools and toys for teaching design of experiments methodology', *Proceedings, Annual Conference - Canadian Society for Civil Engineering*, 2005, pp. 1–9.

Maha Lakshmi, P. and Sivashanmugam, P. (2013) 'Treatment of oil tanning effluent by electrocoagulation: Influence of ultrasound and hybrid electrode on COD removal', *Separation and Purification Technology*. Elsevier B.V., 116, pp. 378–384. doi: 10.1016/j.seppur.2013.05.026.

Maljaei, A., Arami, M. and Mohammad, N. (2009) 'Decolorization and aromatic ring degradation of colored textile wastewater using indirect electrochemical oxidation method', *Desalination*. Elsevier B.V., 249(3), pp. 1074–1078. doi: 10.1016/j.desal.2009.05.016.

Mao, Z. and Campbell, C. T. (2019) 'Apparent Activation Energies in Complex Reaction Mechanisms : A Simple Relationship via Degrees of Rate Control Apparent Activation Energies in Complex Reaction Mechanisms : A Simple Relationship via Degrees of Rate Control', *ACS Catalysi*, 9(10), pp. 9465–9473. doi: 10.1021/acscatal.9b02761.

Martínez-huitle, C. A. *et al.* (2012) 'Applicability of diamond electrode / anode to the electrochemical treatment of a real textile effluent', *Journal of Electroanalytical Chemistry*, 674, pp. 103–107. doi: 10.1016/j.jelechem.2012.02.005.

Martínez-huitle, C. A., Moura, D. C. De and Ribeiro, D. (2014) 'Applicability of Electrochemical Oxidation Process to the Treatment of Petrochemical Effluents', 41, pp. 373–378. doi: 10.3303/CET1441063.

Martínez-huitle, C. A. and Rodrigo, M. A. (eds) (2018) *Electrochemical Water and Wastewater Treatment*. 2nd edn. Cambridge: Butterworth-Heinemann.

Martı, F., Sa, C. and Rodrigo, M. A. (2007) 'Study of the Electrocoagulation Process Using Aluminum and Iron Electrodes', pp. 6189–6195. doi: 10.1021/ie070059f.

Martınez-Huitle, C. A. and Ferro, S. (2006) 'Electrochemical oxidation of organic pollutants for the wastewater treatment : direct and indirect processes', *The Royal Society Reviews*, 35(12), pp. 1324–1340. doi: 10.1039/b517632h.

Mason, R. L., Gunst, R. F. and Hess, J. L. (2003) *Statistical Design and Analysis of Experiments With Applications to Engineering Science*. 2nd edn. New Jersey: John Wiley & Sons, Inc.

Mazzeo, D. E. C. *et al.* (2010) 'BTEX biodegradation by bacteria from effluents of petroleum refinery', *Science of the Total Environment*, 408(20), pp. 4334–4340. doi: 10.1016/j.scitotenv.2010.07.004.

Méndez, E. *et al.* (2012) 'Electrochimica Acta Effects of electrode material on the efficiency of hydrocarbon removal by an electrokinetic remediation process', *Electrochimica Acta*. Elsevier Ltd, 86, pp. 148–156. doi: 10.1016/j.electacta.2012.04.042.

Merlo, R. *et al.* (2011) 'Petroleum Refinery Stripped Sour Water Treatment Using the Activated Sludge Process', *Water Environment Research*, 83(11), pp. 2067–2078. doi: 10.2175/106143011x12989211841133.

Mollah, M. Y. A. *et al.* (2004) 'Fundamentals , present and future perspectives of electrocoagulation'. doi: 10.1016/j.jhazmat.2004.08.009.

Montgomery, D. C. (2013) *Design and Analysis of Experiments*. 8th edn. New Jersey: John Wiley & Sons, Inc. doi: 10.1002/9783527809080.cataz11063.

Mostafazadeh, A. K., Zolfaghari, M. and Drogui, P. (2016) 'Electrofiltration technique for water and wastewater treatment and bio-products management: A review', *Journal of Water Process Engineering*. Elsevier Ltd, 14(November), pp. 28–40. doi: 10.1016/j.jwpe.2016.10.003.

Moulai Mostefa, N. and Tir, M. (2004) 'Coupling flocculation with electroflotation for waste

oil/water emulsion treatment. Optimization of the operating conditions', *Desalination*, 161(2), pp. 115–121. doi: 10.1016/S0011-9164(04)90047-1.

Musingafi, M. C. C. and Tom, T. (2014) 'Fresh Water Sources Pollution: A Human Related Threat To Fresh Water Security in South Africa', *Journal of Public Policy & Governance*, 1(2), pp. 72–81.

Mussa, Z. H., Othman, M. R. and Abdullah, M. P. (2015) 'Electrochemical oxidation of landfill leachate: Investigation of operational parameters and kinetics using graphite-PVC composite electrode as anode', *Journal of the Brazilian Chemical Society*, 26(5), pp. 939–948. doi: 10.5935/0103-5053.20150055.

Myburgh, D. P. *et al.* (2019) 'Removal of COD from Industrial Biodiesel Wastewater Using an Integrated Process: Electrochemical-Oxidation with IrO2-Ta2O5/Ti Anodes and Chitosan Powder as an Adsorbent', *Environmental Processes.* Environmental Processes, 6(4), pp. 819–840. doi: 10.1007/s40710-019-00401-x.

Myers, R. H., Montgomery, D. C. and Anderson-Cook, C. M. (2016) *Response Suface Methodology: Process and Product Optimization Using Designed Experiments*. 4th edn. New Jersey: John Wiley & Sons, Inc.

Nair, A. T., Makwana, A. R. and Ahammed, M. M. (2014) 'The use of response surface methodology for modelling and analysis of water and wastewater treatment processes: a review', *Water Science and Technology*, 69(3), pp. 464–478. doi: 10.2166/wst.2013.733.

Nasution, M. A. *et al.* (2013) 'A Comparative Study Using Aluminum and Iron Electrodes for the Electrocoagulation of Palm Oil Mill Effluent to Reduce its Polluting Nature and Hydrogen Production Simultaneously', *Pakistan Journal*, 45(2), pp. 331–337.

Nayır, T. Y. and Kara, S. (2018) 'Container washing wastewater treatment by combined electrocoagulation – electrooxidation', *Separation Science and Technology*. Taylor & Francis, 53(10), pp. 1592–1603. doi: 10.1080/01496395.2017.1411365.

NER (National Environmental Regulations) (1999) *The National Environment (Standards for Discharge of Effluent into Water or on Land) Regulations, S.I*, *National Environment Act, Cap 153*. Available at: http://www.nemaug.org/regulations/effluent_discharge_regulations.pdf.

Nor, N. M. *et al.* (2017) 'Comparative analyses on medium optimization using one-factor-at-a-time, response surface methodology, and artificial neural network for lysine–methionine biosynthesis by Pediococcus pentosaceus RF-1', *Biotechnology and Biotechnological Equipment*. Taylor & Francis, 31(5), pp. 935–947. doi: 10.1080/13102818.2017.1335177.

Ören, A. H. and Kaya, A. (2006) 'Factors affecting adsorption characteristics of Zn2+ on two natural zeolites', *Journal of Hazardous Materials*, 131(1–3), pp. 59–65. doi:

10.1016/j.jhazmat.2005.09.027.

Ouaissa, Y. A. *et al.* (2014a) 'Removal of tetracycline by electrocoagulation: Kinetic and isotherm modeling through adsorption', *Journal of Environmental Chemical Engineering*. Elsevier Ltd, 2(1), pp. 177–184. doi: 10.1016/j.jece.2013.12.009.

Ouaissa, Y. A. *et al.* (2014b) 'Removal of tetracycline by electrocoagulation: Kinetic and isotherm modeling through adsorption', *Journal of Environmental Chemical Engineering*, 2(1), pp. 177–184. doi: 10.1016/j.jece.2013.12.009.

Pal, S. *et al.* (2016) 'Review of technologies for biotreatment of refinery wastewaters : progress, challenges and future opportunities', *Environmental Technology Reviews*, 5(1), pp. 12–38. doi: 10.1080/21622515.2016.1164252.

Palma-Goyes, R. E. *et al.* (2018) 'The effect of different operational parameters on the electrooxidation of indigo carmine on Ti/IrO2-SnO2-Sb2O3', *Journal of Environmental Chemical Engineering*, 6, pp. 3010–3017. doi: 10.1016/j.jece.2018.04.035.

Pang, W. K. and Low, I. M. (2014) *Understanding and improving the thermal stability of layered ternary carbides in ceramic matrix composites*, *Advances in Ceramic Matrix Composites*. Woodhead Publishing Limited. doi: 10.1533/9780857098825.2.340.

Pérez-Corona, M. *et al.* (2013) 'Evaluation of IrO2-Ta2O5/Ti electrodes employed during the electroremediation of hydrocarbon-contaminated soil', *Sustainable Environmental Research*, 23(4), pp. 279–284.

Permadi, A. and Wenten, I. G. (2010) 'Enzyme Separation and Purification Using', in *Prosiding Seminar Nasional Teknik Kimia "Kejuangan"*, pp. F03-10.

Pilat, B. (2001) 'Practice of water desalination by electrodialysis', *Desalination*, 139(1–3), pp. 385–392. doi: 10.1016/S0011-9164(01)00338-1.

Piñeiro, G. *et al.* (2008) 'How to evaluate models: Observed vs. predicted or predicted vs. observed?', *Ecological Modelling*, 216(3–4), pp. 316–322. doi: 10.1016/j.ecolmodel.2008.05.006.

Pitakpoolsil, W. and Hunsom, M. (2013) 'Adsorption of pollutants from biodiesel wastewater using chitosan flakes', *Journal of the Taiwan Institute of Chemical Engineers*. Taiwan Institute of Chemical Engineers, 44(6), pp. 963–971. doi: 10.1016/j.jtice.2013.02.009.

Pitakpoolsil, W. and Hunsom, M. (2014) 'Treatment of biodiesel wastewater by adsorption with commercial chitosan flakes: Parameter optimization and process kinetics', *Journal of Environmental Management*. Elsevier Ltd, 133, pp. 284–292. doi: 10.1016/j.jenvman.2013.12.019.

Rastegar, S. O. *et al.* (2011) 'Optimization of petroleum refinery effluent treatment in a UASB reactor using response surface methodology', *Journal of Hazardous Materials*. Elsevier B.V., 197, pp. 26–32. doi: 10.1016/j.jhazmat.2011.09.052.

Ratshomo, K. and Nembahe, R. (2018) *South african energy sector report*. Pretoria: Department of Energy.

Rocha, L. L. *et al.* (2007) 'Isolation and characterization of phenol-degrading yeasts from an oil refinery wastewater in Brazil', *Mycopathologia*, 164(4), pp. 183–188. doi: 10.1007/s11046-007-9043-6.

Roopashree, G. B. and Lokesh, K. S. (2014) 'Comparative study of electrode material (iron , aluminium and stainless steel) for treatment of textile industry wastewater', 4(4), pp. 519–531. doi: 10.6088/ijes.2014040400008.

Sadeghbeigi, R. (2000) 'Process Description', in *Fluid Catalytic Cracking Handbook*. Elsevier, pp. 1–39. doi: 10.1016/B978-088415289-7/50002-0.

Sahu, O., Mazumdar, B. and Chaudhari, P. K. (2014) 'Treatment of wastewater by electrocoagulation: A review', *Environmental Science and Pollution Research*, 21(4), pp. 2397–2413. doi: 10.1007/s11356-013-2208-6.

Samer, M. (2015) 'Biological and Chemical Wastewater Treatment Processes', in *Wastewater Treatment Engineering*. InTech, pp. 1–50. doi: 10.5772/61250.

Santo, C. E. *et al.* (2012) 'Optimization of coagulation – flocculation and flotation parameters for the treatment of a petroleum refinery effluent from a Portuguese plant', *Chemical Engineering Journal*. Elsevier B.V., 183, pp. 117–123. doi: 10.1016/j.cej.2011.12.041.

Santos, C. E. *et al.* (2015) 'Performance evaluation of the main units of a refinery wastewater treatment plant – A case study', *Journal of Environmental Chemical Engineering*. Elsevier B.V., 3, pp. 2095–2103. doi: 10.1016/j.jece.2015.07.011.

Dos Santos, E. V. *et al.* (2014a) 'Decontamination of produced water containing petroleum hydrocarbons by electrochemical methods : a minireview', *Environmental Science and Pollution Research*, 21(14), pp. 8432–8441. doi: 10.1007/s11356-014-2780-4.

Dos Santos, E. V. *et al.* (2014b) 'Decontamination of produced water containing petroleum hydrocarbons by electrochemical methods: A minireview', *Environmental Science and Pollution Research*, 21(14), pp. 8432–8441. doi: 10.1007/s11356-014-2780-4.

Santos, M. R. G. *et al.* (2006) 'The application of electrochemical technology to the remediation of oily wastewater', *Chemosphere*, 64, pp. 393–399. doi: 10.1016/j.chemosphere.2005.12.036.

Sathian, S. *et al.* (2014) 'Performance of SBR for the treatment of textile dye wastewater:

Optimization and kinetic studies', *Alexandria Engineering Journal*. Faculty of Engineering, Alexandria University, 53(2), pp. 417–426. doi: 10.1016/j.aej.2014.03.003.

Seader, J. D., Henley, E. J. and Roper, D. K. (2011) *Separtion Process Principles: Chemical and Biochemical Operations*. New Jersey: John Wiley & Sons, Inc.

Selvamuthu, D. and Das, D. (2018) *Introduction to Statistical Design of Experiments and Statistical Quality Control*. Singapore: Springer. doi: 10.1201/9781439819487-c1.

Shabir, G. *et al.* (2013) 'Treatment of Oil Refinery Wastewater Using Pilot Scale Fed Batch Reactor Followed by Coagulation and Sand Filtration', *American Journal of Environmental Protection*, 1(1), pp. 10–13. doi: 10.12691/env-1-1-2.

Shang, G., Zhang, G. and Gao, C. (2014) 'Treatment of simulated dilute Ni2+-containing wastewater by electrodeionisation with a bipolar membrane: Feasibility and current density distribution', *Desalination*. Elsevier B.V., 353, pp. 1–7. doi: 10.1016/j.desal.2014.09.003.

Sharma, S. and Simsek, H. (2019) 'Treatment of canola-oil refinery effluent using electrochemical methods: A comparison between combined electrocoagulation + electrooxidation and electrochemical peroxidation methods.', *Chemosphere*. Elsevier Ltd, 221, pp. 630–639. doi: 10.1016/j.chemosphere.2019.01.066.

Shen, F. *et al.* (2003) 'Electrochemical removal of fluoride ions from industrial wastewater', *Chemical Engineering Science*, 58(3–6), pp. 987–993. doi: 10.1016/S0009-2509(02)00639-5.

Shokrollahzadeh, S., Azizmohseni, F. and Golmohammad, F. (2008) 'Biodegradation potential and bacterial diversity of a petrochemical wastewater treatment plant in Iran', *Bioresource Technology*, 99, pp. 6127–6133. doi: 10.1016/j.biortech.2007.12.034.

Sillanpaa, M. and Shestakova, M. (2017) *Electrochemical Water Treatment Methods-Fundamentals, methods and full scale application*. Oxford: Butterworth-Heinemann. doi: 10.1016/B978-0-12-811462-9.01001-X.

Da Silva, A. J. C. *et al.* (2013) 'Electrochemical treatment of fresh , brine and saline produced water generated by petrochemical industry using Ti/IrO2 – Ta2O5 and BDD in flow reactor', *Chemical Engineering Journal*, 233, pp. 47–55. doi: 10.1016/j.cej.2013.08.023.

Simonin, J. P. (2016) 'On the comparison of pseudo-first order and pseudo-second order rate laws in the modeling of adsorption kinetics', *Chemical Engineering Journal*. Elsevier B.V., 300, pp. 254–263. doi: 10.1016/j.cej.2016.04.079.

Smith, B. and Hyde, B. (2000) 'Short-Bed Demineralization : An Alternative to Electrodeionization', in *Sixth International Conference on Cycle Chemistry in Fossil Plants (EPRI)*. Columbus, pp. 153–159.

Solano, A. M. S. *et al.* (2013) 'Decontamination of real textile industrial effluent by strong oxidant species electrogenerated on diamond electrode : Viability and disadvantages of this electrochemical technology', *Applied Catalysis B: Environmental.* Elsevier B.V., 130–131, pp. 112–120. doi: 10.1016/j.apcatb.2012.10.023.

Tahmouzi, S. (2014) 'Optimization of polysaccharides from Zagros oak leaf using RSM: Antioxidant and antimicrobial activities', *Carbohydrate Polymers.* Elsevier Ltd., 106(1), pp. 238–246. doi: 10.1016/j.carbpol.2014.02.028.

Tavares, M. G. *et al.* (2012) 'Electrochemical oxidation of Methyl Red using Ti / Ru 0 . 3 Ti 0 . 7 O 2 and Ti / Pt anodes', *Chemical Engineering Journal.* Elsevier B.V., 204–206, pp. 141–150. doi: 10.1016/j.cej.2012.07.056.

Tawabini, B. S., Plakas, K. V and Karabelas, A. J. (2020) 'A pilot study of BTEX removal from highly saline water by an advanced electrochemical process', *Journal of Water Process Engineering.* Elsevier, 37(April), p. 101427. doi: 10.1016/j.jwpe.2020.101427.

Taylor, P. *et al.* (2010) 'Separation Science and Technology Comparative Study of Electrocoagulation and Electrooxidation Processes for the Degradation of Ellagic Acid From Aqueous Solution Comparative Study of Electrocoagulation and Electrooxidation Processes for the Degradation o', (October 2014), pp. 37–41. doi: 10.1080/01496395.2010.505224.

Tezcan, U., Koparal, A. S. and Bakir, U. (2009) 'Electrocoagulation of vegetable oil refinery wastewater using aluminum electrodes', *Journal of Environmental Management.* Elsevier Ltd, 90(1), pp. 428–433. doi: 10.1016/j.jenvman.2007.11.007.

Thangam, R., Suresh, V. and Kannan, S. (2014) 'Optimized extraction of polysaccharides from Cymbopogon citratus and its biological activities', *International Journal of Biological Macromolecules.* Elsevier B.V., 65, pp. 415–423. doi: 10.1016/j.ijbiomac.2014.01.033.

Tian, S. *et al.* (2017) 'Optimization conditions for extracting polysaccharide from Angelica sinensis and its antioxidant activities', *Journal of Food and Drug Analysis.* Elsevier Ltd, 25(4), pp. 766–775. doi: 10.1016/j.jfda.2016.08.012.

Tien, T. T. *et al.* (2017) 'Electrochemical Water Treatment Technology in Viet Nam : Achievement & Future Development', *Science Journal of Chemistry*, 5(6), pp. 87–94. doi: 10.11648/j.sjc.20170506.13.

Tir, M. and Moulai-Mostefa, N. (2008) 'Optimization of oil removal from oily wastewater by electrocoagulation using response surface method', *Journal of Hazardous Materials*, 158(1), pp. 107–115. doi: 10.1016/j.jhazmat.2008.01.051.

Tony, M. A. *et al.* (2015) 'Kinetic Modeling Of Diesel Oil Wastewater Degradation Using Photo-Fenton Process', *Environmental Engineering and Management Journal*, 15(1), pp. 11–16.

Ugurlu, M. *et al.* (2007) 'The removal of lignin and phenol from paper mill effluents by electrocoagulation', *Journal of Environmental Management*, 87, pp. 420–428. doi: 10.1016/j.jenvman.2007.01.007.

Vaez, M., Zarringhalam Moghaddam, A. and Alijani, S. (2012) 'Optimization and modeling of photocatalytic degradation of azo dye using a response surface methodology (RSM) based on the central composite design with immobilized Titania nanoparticles', *Industrial and Engineering Chemistry Research*, 51(11), pp. 4199–4207. doi: 10.1021/ie202809w.

Vafajoo, L., Ghanaat, F. and Ghalebi, A. (2014) 'An Investigation of a Petrochemical Wastewater Treatment utilizing GAC : A Study of Adsorption Kinetics', *Procedia - Social and Behavioral Sciences*. Elsevier B.V., 10, pp. 131–135. doi: 10.1016/j.apcbee.2014.10.030.

Vasudevan, S. (2016) 'Can Electrochemistry Make the Worlds Water Clean? – A Systematic and Comprehensive Overview', *International Journal of Waste Resources*, 6(2), pp. 1–5. doi: 10.4172/2252-5211.1000210.

Vasudevan, S., Lakshmi, J. and Sozhan, G. (2012) 'Optimization of electrocoagulation process for the simultaneous removal of mercury, lead, and nickel from contaminated water', *Environmental Science and Pollution Research*, 19(7), pp. 2734–2744. doi: 10.1007/s11356-012-0773-8.

Vasudevan, S. and Oturan, M. A. (2014) 'Electrochemistry : as cause and cure in water pollution — an overview', pp. 97–108. doi: 10.1007/s10311-013-0434-2.

Verlicchi, P. and Grillini, V. (2020) 'Surface Water and Groundwater Quality in South Africa and Mozambique—Analysis of the Most Critical Pollutants for Drinking Purposes and Challenges in Water Treatment Selection', *Water*, 12(1), pp. 1–21. doi: 10.3390/w12010305.

Vik, E. A. *et al.* (1984) 'Electrocoagulation of potable water', *Water Research*, 18(11), pp. 1355–1360. doi: 10.1016/0043-1354(84)90003-4.

Wahid, Z. and Nadir, N. (2013) 'Improvement of one factor at a time through design of experiments', *World Applied Sciences Journal*, 21(SPECIAL ISSUE1), pp. 56–61. doi: 10.5829/idosi.wasj.2013.21.mae.99919.

Wang, B. *et al.* (2016) 'Effect of Organic Matter Removal during Combined Adsorption-Coagulation Treatment of Petroleum Refinery Effluent Effect of Organic Matter Removal during Combined Adsorption-Coagulation Treatment of Petroleum Refinery Effluent', 3330(June). doi: 10.1080/09593330.2016.1197319.

Wang, C.-T., Chou, W. and Kuo, Y. (2009) 'Removal of COD from laundry wastewater by electrocoagulation / electroflotation', *Journal of Hazardous Materials*, 164, pp. 81–86. doi: 10.1016/j.jhazmat.2008.07.122.

Wang, H. *et al.* (2014) 'Phenolic wastewater treatment by an electrocatalytic membrane reactor', *Catalysis Today*. Elsevier B.V., 236, pp. 121–126. doi: 10.1016/j.cattod.2014.05.003.

Wei, J. J. *et al.* (2013) 'Energy consumption of electrooxidation systems with boron-doped diamond electrodes in the pulse current mode', *International Journal of Minerals, Metallurgy and Materials*, 20(1), pp. 106–112. doi: 10.1007/s12613-013-0700-0.

Wei, L. *et al.* (2010) 'Electrochimica Acta Electrochemical pretreatment of heavy oil refinery wastewater using a three-dimensional electrode reactor', *Electrochimica Acta*. Elsevier Ltd, 55(28), pp. 8615–8620. doi: 10.1016/j.electacta.2010.08.011.

Wenyu, X. I. E., Li, Z. and Jianjun, C. (2007) 'Treatment of Slightly Polluted Wastewater in an Oil Refinery Using a Biological Aerated Filter Process', *Wuhan University Journal of Natural Sciences*, 12(6), pp. 1094–1098. doi: 10.1007/s11859-007-0080-2.

Wijeyekoon, S. L. J. *et al.* (2007) 'Effective Process Conditions and Reactor Design Parameters for Oil Separation by Electrocoagulation', *Engineer*, XXXX(4), pp. 175–184.

Yan, Z. and Meng, H. (2011) 'Electrochemical investigation of the IrO2-Ta2O5 coated anode with different heat treatment processes of the Titanium substrates', *Electrochemical and Solid-State Letters*, 14(10), pp. C16–C19. doi: 10.1149/1.3611016.

Yang, G. C. C. and Li, C.-J. (2007) 'Electrofiltration of silica nanoparticle-containing wastewater using tubular ceramic membranes', *Separation and Purification Technology*, 58(1), pp. 159–165. doi: 10.1016/j.seppur.2007.07.019.

Yavuz, Y., Koparal, A. S. and Bak, Ü. (2010a) 'Treatment of petroleum refinery wastewater by electrochemical methods', *Desalination*, 258, pp. 201–205. doi: 10.1016/j.desal.2010.03.013.

Yavuz, Y., Koparal, A. S. and Bak, Ü. (2010b) 'Treatment of petroleum refinery wastewater by electrochemical methods', *Desalination*, 258(1–3), pp. 201–205. doi: 10.1016/j.desal.2010.03.013.

Ye, S. and Li, N. (2016) 'Comparison of Electrochemical Treatment of Petroleum Refinery Effluents Using Electrooxidation , Electrocoagulation and Electrophenton Process', *International journal of Electrochemical Science*, 11, pp. 6173–6182. doi: 10.20964/2016.07.20.

Yu, L., Han, M. and He, F. (2017) 'A review of treating oily wastewater', *Arabian Journal of Chemistry*, 10, pp. S1913–S1922. doi: 10.1016/j.arabjc.2013.07.020.

Zhang, M. hui *et al.* (2019) 'A review on Fenton process for organic wastewater treatment based on optimization perspective', *Science of the Total Environment*. Elsevier B.V., 670, pp. 110–121. doi: 10.1016/j.scitotenv.2019.03.180.

Zhang, M. Q. *et al.* (2012) 'Water ' s Dependence on Energy : Analysis of Embodied Energy in

Water and Wastewater Systems by Weiwei Mo A dissertation submitted in partial fulfillment of the requirements for the degree of Doctor of Philosophy Department of Civil and Environmental Engi'.

Zheng, X. *et al.* (2015) 'Overview of membrane technology applications for industrial wastewater treatment in China to increase water supply', *Resources, Conservation and Recycling*. Elsevier B.V., 105, pp. 1–10. doi: 10.1016/j.resconrec.2015.09.012.

Zhuwakinyu, M. (2012) *Water 2012 - A review of the South Africa's water sector*, *Powertech*.

Zou, J. *et al.* (2017) 'Electrochemical oxidation of COD from real textile wastewaters : Kinetic study and energy consumption', *Chemosphere*. Elsevier Ltd, 171, pp. 332–338. doi: 10.1016/j.chemosphere.2016.12.065.

Appendices

Appendix A

Experimental Data

Appendix A: Experimental Data

1. Raw data for electrocoagulation

Table A- 1: Kinetic Data for COD for electrocoagulation

			COD			
Run	pH	Current	Run	Duplicate	Average	STDV
Feed					4753	
1	8	1.5	2238	2224	**2231**	**9.9**
2	2	2.5	1541	1553	**1547**	**8.5**
3	2	2	2273	2261	**2267**	**8.5**
4	8	2	2253	2290	**2272**	**26.2**
5	5	2	1778	1761	**1770**	**12.0**
6	2	1.5	2262	2275	**2269**	**9.2**
7	5	2.5	1674	1689	**1682**	**10.6**
8	5	1.5	1794	1775	**1785**	**13.4**
9	8	2.5	2224	2214	**2219**	**7.1**

Table A-2: Kinetic Data for phenol for electrocoagulation

			Phenol			
Run	pH	Current	Runs	Average	STDV	STDV
Feed					763	
1	8	1.5	68.5	67.3	**67.9**	**0.8**
2	2	2.5	8.8	10.5	**9.65**	**1.2**
3	2	2	17.3	19.2	**18.25**	**1.3**
4	8	2	55.2	69.3	**62.25**	**10.0**
5	5	2	28.5	15	**21.75**	**9.5**
6	2	1.5	61	62.1	**61.55**	**0.8**
7	5	2.5	14.2	15.3	**14.75**	**0.8**
8	5	1.5	65.2	65.8	**65.5**	**0.4**
9	8	2.5	69.3	45	**57.15**	**17.2**

Table A-3: Kinetic Data for colour for electrocoagulation

			Colour			
Run	pH	Current	Runs	Average	STDV	STDEV
Feed					6952	
1	8	1.5	2706	2697	**2701.5**	6.4
2	2	2.5	801	804	**802.5**	2.1
3	2	2	981	989	**985**	5.7
4	8	2	2133	2130	**2131.5**	2.1
5	5	2	1471	1463	**1467**	5.7
6	2	1.5	1176	1170	**1173**	4.2
7	5	2.5	1396	1412	**1404**	11.3
8	5	1.5	1786	1802	**1794**	11.3
9	8	2.5	2067	2089	**2078**	15.6

2. Raw data for Electrooxidation

Table A-4: Effect of time on EO at 20°C

Time (hrs)	Time (s)	COD (mg/l) at 20 °C			
		Run		Average	Standard deviation
2	7200	289	281	285	**5.7**
4	14400	259	258	259	**0.7**
6	21600	238	243	241	**3.5**
8	28800	200	201	201	**0.7**
10	36000	194	193	194	**0.7**
12	43200	180	183	182	**2.1**
14	50400	176	190	183	**9.9**
16	57600	170	173	172	**2.1**
18	64800	168	168	168	**0.0**

Table A-5: Effect of time on EO at 40°C

Time (hrs)	Time (s)	COD (mg/l) at 40 °C			
		Run		Average	Standard deviation
2	7200	265	262	264	**2.1**
4	14400	247	238	243	**6.4**
6	21600	234	229	232	**3.5**
8	28800	208	201	205	**4.9**
10	36000	187	183	185	**2.8**
12	43200	142	141	142	**0.7**
14	50400	161	166	164	**3.5**
16	57600	169	171	170	**1.4**
18	64800	175	170	173	**3.5**

Table A-6: Effect of time on EO at 60°C

Time (hrs)	Time (s)	COD (mg/l) at 60 °C			
		Run		Average	Standard deviation
2	7200	271	276	274	**3.5**
4	14400	253	259	256	**4.2**
6	21600	216	219	218	**2.1**
8	28800	210	210	210	**0.0**
10	36000	188	197	193	**6.4**
12	43200	170	173	172	**2.1**
14	50400	166	157	162	**6.4**
16	57600	164	179	172	**10.6**
18	64800	160	165	163	**3.5**

Table A-7: COD Data for electrooxidation

Run	Parameters			COD			
	Temp	NaCl (g/l)	C.D (mA/cm^2)	Run		average	STDEV
1	40	2	7.5	234	244	239	7.07
2	40	4	7.5	152	142	147	7.07
3	40	6	7.5	183	190	186.5	4.95
4	60	2	10	416	446	431	21.21
5	20	4	7.5	183	186	184.5	2.12
6	20	6	10	206	214	210	5.66
7	40	4	10	158	162	160	2.83
8	20	2	10	218	274	246	39.60
9	40	4	5	182	174	178	5.66
10	20	2	5	268	282	275	9.90
11	20	6	5	234	234	234	0.00
12	60	6	10	182	194	188	8.49
13	40	6	10	150	154	152	2.83
14	60	2	5	422	414	418	5.66
15	60	4	7.5	170	178	174	5.66
16	60	6	5	222	232	227	7.07

Table A-8: Colour data for electrooxidation

Run	Parameters			Colour			
	Temp	NaCl (g/l)	C.D (mA/cm^2)	Run		average	STDEV
1	40	2	7.5	8	7	7.5	0.707107
2	40	4	7.5	0	0	0	0
3	40	6	7.5	2	1	1.5	0.707107
4	60	2	10	54	59	56.5	3.535534
5	20	4	7.5	20	18	19	1.414214
6	20	6	10	13	13	13	0
7	40	4	10	14	11	12.5	2.12132
8	20	2	10	24	32	28	5.656854
9	40	4	5	7	2	4.5	3.535534
10	20	2	5	15	12	13.5	2.12132
11	20	6	5	13	18	15.5	3.535534
12	60	6	10	11	9	10	1.414214
13	40	6	10	0	0	0	0
14	60	2	5	28	31	29.5	2.12132
15	60	4	7.5	4	5	4.5	0.707107
16	60	6	5	12	13	12.5	0.707107

Appendix B

Sample Calculations

Appendix B: Sample Calculations

1. **Adsorption isotherms**

- **Adsorption Capacity**

Electrode consumption was estimated according to Faraday's law

$$W_{ad} = \frac{DtM}{zF}$$

$$W_{ad} = \frac{0.000372 \times 3 \times 27}{3 \times 96500}$$

$$= 0.000375 \text{ g/cm}^2$$

$$\therefore W = 1344 * 0.000375$$

$$= 0.504 \text{ g}$$

$$N_e = \frac{V(C_0 - C_e)}{W}$$

$$= \frac{2.5(4753 - 2108)}{0.504}$$

$$\therefore N_e = 13\ 130 \ mg/g$$

- **Freundlich isotherm**

K_F and n was determined from a linearized form of Equation 2-11

$$\ln q = \ln K_F + \frac{1}{n} \ln C_e$$

The equation of the linearized plot of the Freundlich isotherm has a slope 1/n and an intercept (lnq).
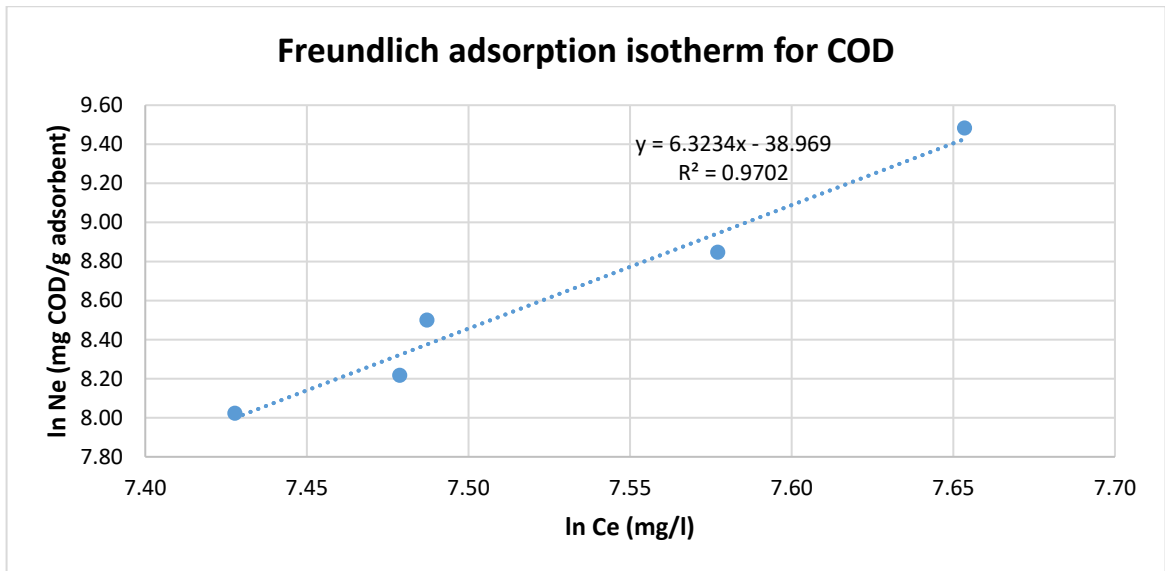
Figure B- 1: Freundlich adsorption isotherm

$$y = 6.3234x - 38.969$$

$$\therefore \frac{1}{n} = 6.3234$$

$$\therefore n = \frac{1}{6.3234}$$

$$\therefore n = 0.158$$

and $\ln q = -38.969$

$$\therefore q = e^{-38.969}$$

$$= 1.19 \times 10^{-17} \, g^{-1}$$

- **Langmuir isotherm**

$$\frac{C_e}{q_e} = \frac{1}{q_{max}K_L} + \frac{C_e}{q_{max}}$$

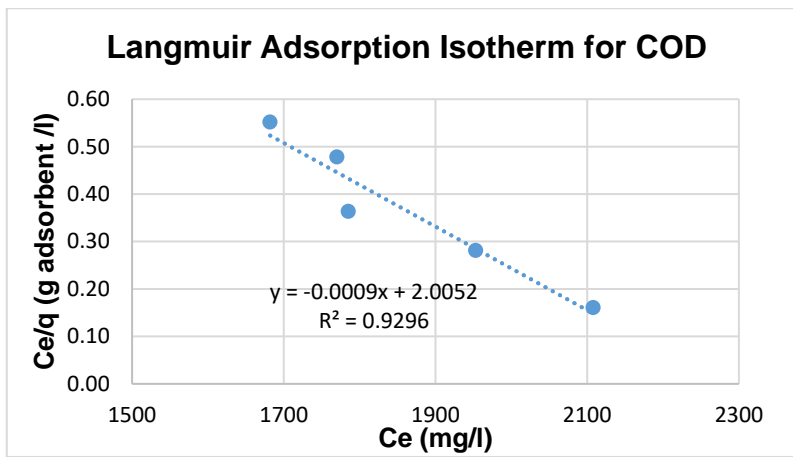Where the slope of the equation is $1/q_{max}$, and the intercept is $1/K_Lq_{max}$

Figure B-2: Langmuir adsorption isotherm for COD

$y = -0.0009x + 2.0052$

$\dfrac{1}{q_{max}} = -0.0009$

$\therefore q_{max} = \dfrac{1}{-0.0009}$

$\therefore q_{max} = -1111 \text{ mg/g}$

and $\dfrac{1}{q_{max}K_L} = 2.0052$

$\therefore K_L = \dfrac{\mathbf{1}}{2.0052 \times \boldsymbol{q_{max}}}$

$\therefore K_L = \dfrac{1}{2.002 \times -1111}$

$\quad = -0.00045 \text{ mg}^{-1}$
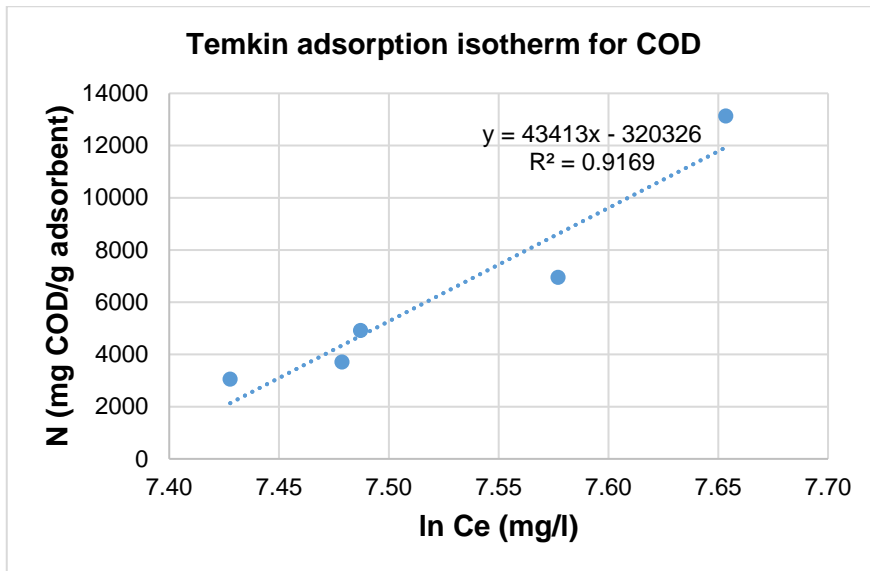
- **Temkin isotherm**

$q = B \ln K_T + B \ln C_e$

Figure B-3: Temkin adsorption isotherm for COD

$$y = 43413x - 320326$$

$$\therefore B = 43\,413$$

$$and\ BlnK_T = -320326$$

$$\therefore \ln K_T = \frac{-320326}{43413}$$

$$\therefore K_T = e^{-7.379}$$

$$\therefore K_T = 0.00062\ g^{-1}$$

- **Dubinin-Raduschkevich isotherm**

Equation 2-14 was used to fit data to the Dubinin-Raduschkevich isotherm. The Polanyi potential (E) (J/mol) was calculated with Equation 2-15.

$$\ln q_e = \ln X_m + \beta E^2$$
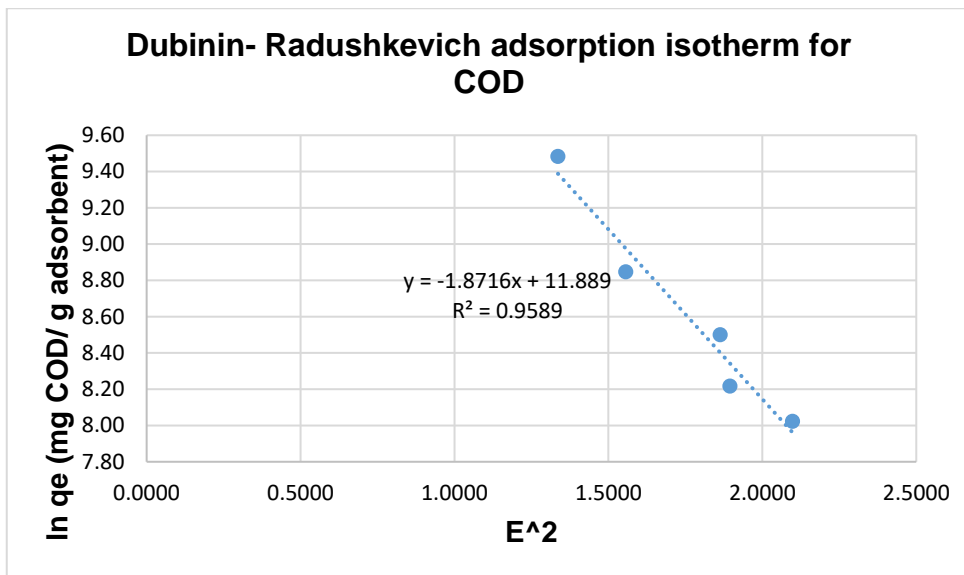
$$E_s = \frac{1}{\sqrt{-2\beta}}$$

Figure B- 4: Dubinin – Radushkevich adsorption isotherm for COD

$$Y = -1.8716x + 11.889$$

$$\ln X_m = 11.889$$

$$\therefore X_m = e^{11.889}$$

$$\therefore X_m = 145\ 656 \text{ mg/g}$$

$$\beta = -1.8716 \text{ mg}^{-1}$$

$$E_s = (-2\beta)^{-1/2}$$

$$\quad = [-2(-1.9716)]^{-1/2}$$

$$\therefore E_s = 0.52 \text{ kJ/mol}$$

Appendix C

Sample Preparation and

Analytical Procedures

Appendix C: Sample Preparation and Analytical Procedures

All methods were followed as prescribed by Hanna Instruments.

1. Determination of COD

High Range COD reagents (HI93754C-25) were used to determine the COD in the wastewater. This method requires a blank reagent correction once. For improved accuracy measurement, run a blank for each set of measurements and always use the same lot of reagents for blank and samples.

Procedure

- Add 0.2 mL of deionized water to the first vial (#1) and 0.2 mL of sample to the second vial (#2) while keeping the vials at a 45-degree angle. Replace the caps and invert several times to mix
- Insert the vials into the reactor and heat them for 2 hours at 150 °C.
- Switch off the reactor at the end of the heating period. Wait 20 minutes to allow the vials to cool to about 120 °C.
- Invert each vial several times while still warm, then place them in the test tube rack. And then leave the vials in the tube rack to cool to room temperature.
- Select the COD HR on the COD and multiparameter photometer method
- Insert the blank vial (#1) into the holder, and then press Zero. The display will show -0.0- when the meter is zeroed and ready for measurement.
- Remove the vial.
- Insert the sample vial (#2) into the holder and press Read to start the reading. The instrument displays the results in mg/L of oxygen (O_2).

2. Determination of Colour

MEASUREMENT PROCEDURE

- Fill one cuvette up to the mark with deionized water and replace the cap. This is the blank.
- Select the Colour of Water method on the COD and multiparameter photometer
- Place the blank into the holder and close the lid.
- Press the Zero key. The meter will show "-0.0-" when the meter is zeroed and ready for measurement.
- Remove the blank
- Fill the second cuvette up to the mark with the unfiltered sample and replace the cap. This is the apparent colour.
- Filter 10 mL of the sample through a filter with a 0.45 µm membrane into the third cuvette. This is the true colour.
- Insert the apparent colour cuvette into the instrument and close the lid.
- Press Read to start the reading.
- The meter displays the value of apparent colour in PCU
- Remove the cuvette, insert the true colour cuvette into the instrument and ensure that the notch on the cap is positioned securely into the groove. • Press Read to start the reading. The meter displays the value of true colour in PCU